FUTURISTIC AIR COMPRESSOR SYSTEM DESIGN AND OPERATION BY USING ARTIFICIAL INTELLIGENCE

A Thesis

Submitted to the Faculty

of

Purdue University

by

Babak Bahrami Asl

In Partial Fulfillment of the

Requirements for the Degree

of

Master of Science in Mechanical Engineering

December 2018

Purdue University

Indianapolis, Indiana

THE PURDUE UNIVERSITY GRADUATE SCHOOL
STATEMENT OF COMMITTEE APPROVAL

Dr. Ali Razban

Department of Mechanical and Energy Engineering

Dr. Jie Chen

Department of Mechanical and Energy Engineering

Dr. David W. Goodman

Department of Electrical and Computer Engineering Technology

Approved by:

Dr. Jie Chen

Head of the Graduate Program

To my parents, Habib and Nadereh who love me for who I am, and have supported me through all the ups and downs and every hard decision that I have faced. They've inspired me to follow my dreams. Without them, this work would not be possible.

ACKNOWLEDGMENTS

I would like to express my sincerest gratitude to my supervisors Dr. Ali Razban and Dr. Jie Chen for their financial and academic support. Under their guidance, I learned the key principles of research, and was able to grow in my knowledge of engineering, both in theory and practice. Without their support and supervision this journey would never have been possible. Also, my special thanks to Dr. David Goodman for his role on my advisory committee, as well as his input throughout this research. His guidance, assistance, and friendship are appreciated.

I have been fortunate to be part of the Industrial Assessment Center (IAC) on our campus. This enabled me to gain invaluable experience by providing the opportunity to do real-world problem solving for various manufacturing facilities. This work would not have been possible without the facilities and resources provided for researchers at IAC. Therefore, I would like to thank the US Department of Energy (DOE) for supporting this center, and giving us the opportunity not only to study, but also to advance research that is making the world more energy efficient.

Also, I would like to thank Electro-Spec Incorporation, Citizens Energy Group and Eiteljorg Museum for giving me the opportunity to use their facilities as my case studies. Their cooperation is very much appreciated.

Finally, I would like to thank my dear friend and colleague Allen Da-Chun Wu, who assisted me with various aspects of this project, especially the load prediction section. His endless support and help throughout this work is truly appreciated. I would like to acknowledge my dear childhood friend Mahmood Hosseini for his help debugging and testing the Python program. His help during the final section of this research is really appreciated.

TABLE OF CONTENTS

Page

Page

LIST OF TABLES

LIST OF FIGURES

SYMBOLS

w	weight matrix
θ	bias Vector
u	bias Vector
x	neural network input, sample sequence
X	actual measured value
$\bar{X}$	mean of the measured sample
y	neural network output
Y	predicted value by model
u	weight matrix
m	median value from moving window, mass
W	set of numbers within a moving window
K	sliding window half-width
S_i	median absolute deviation (MAD)
n_σ	threshold parameter
n	number of input neurons, number of predictions
m	number of hidden layer neurons
R^2	coefficient of determination
F	fuel, function
Q	flow rate
Q_g	flow rate generated
Q_L	flow rate consumption
Q_S	flow rate stored
t	time
η	efficiency

V	volume
V_g	generated compressed air volume at the required pressure
V_L	consumed compressed air volume at the required pressure
V_L	stored compressed air volume at the required pressure
V_{max}	volumetric amount of stored mass at the line pressure
P	pressure
R	specific gas constant
T	temperature, time set to turn off the system after running unloaded
T'	time the compressor is loaded
a	fitted line coefficient value
c	inequality constraint
ceq	equality constraint
ub	upper boundary
lb	lower boundary
c	inequality constraint
ceq	equality constraint
A	inequality constraint
b	inequality constraint
Aeq	equality constraint
beq	equality constraint
α	constant
S	storage size
FI	fractional power consumption increase

ABBREVIATIONS

AI	Artificial Intelligence
ANN	Artificial Neural Network
PRV	Pressure Regulator Valve
FRL	Filter Regulator Lubricant
HP	Horse Power
VSD	Variable Speed Drive
VFD	Variable Frequency Drive
FSD	Fixed Speed Drive
STLF	Short Term Load Forecasting
MTLF	Medium Term Load Forecasting
LTLF	Long Term Load Forecasting
ANFIS	Adaptive Neuro-Fuzzy Inference System
RBFN	Radial Basis Function Network
FFNN	Feed Forward Neural Network
LSTM	Long Short-Term Memory Networks
GRNN	General Regression Neural Network
RGRNN	Rotated General Regression Neural Network
RBFN	Radial Basis Function Network
MLP	Multilayer Perceptron
PLS	Partial Least Squares
RNN	Recurrent Neural Networks
HMI	Human Machine Interface
RPM	Revolutions Per Minute
PID	Proportional Integral Derivative

CAGI	Compressed Air and Gas Institute
SEU	Significant Energy User
FP	Fraction Full Load Power
FC	Fraction Rated Capacity
PT	Pressure Transducer
PS	Pressure Switch
SPSS	Statistical Package for the Social Science
MAD	Median Absolute Deviation
RMSE	Root Mean Squared Error

ABSTRACT

Bahrami Asl, Babak. M.S.M.E., Purdue University, December 2018. Futuristic Air Compressor System Design and Operation by Using Artificial Intelligence. Major Professor: Ali Razban.

The compressed air system is widely used throughout the industry. Air compressors are one of the most costly systems to operate in industrial plants in terms of energy consumption. Therefore, it becomes one of the primary targets when it comes to electrical energy and load management practices. Load forecasting is the first step in developing energy management systems both on the supply and user side. A comprehensive literature review has been conducted, and there was a need to study if predicting compressed air systems load is a possibility.

Systems load profile will be valuable to the industry practitioners as well as related software providers in developing better practice and tools for load management and look-ahead scheduling programs. Feed forward neural networks (FFNN) and long short-term memory (LSTM) techniques have been used to perform 15 minutes ahead prediction. Three cases of different sizes and control methods have been studied. The results proved the possibility of the forecast. In this study two control methods have been developed by using the prediction. The first control method is designed for variable speed driven air compressors. The goal was to decrease the maximum electrical load for the air compressor by using the system's full operational capabilities and the air receiver tank. This goal has been achieved by optimizing the system operation and developing a practical control method. The results can be used to decrease the maximum electrical load consumed by the system as well as assuring the sufficient air for the users during the peak compressed air demand by users. This method can also prevent backup or secondary systems from running during the peak

compressed air demand which can result in more energy and demand savings. Load management plays a pivotal role and developing maximum load reduction methods by users can result in more sustainability as well as the cost reduction for developing sustainable energy production sources. The last part of this research is concentrated on reducing the energy consumed by load/unload controlled air compressors. Two novel control methods have been introduced. One method uses the prediction as input, and the other one doesn't require prediction. Both of them resulted in energy consumption reduction by increasing the off period with the same compressed air output or in other words without sacrificing the required compressed air needed for production.

1. INTRODUCTION

The compressed air system is commonly used in almost all industries. Due to the high-energy loss of this system during the energy conversion process, compressed air is considered the most expensive form of energy. Because of the sufficiently large electrical load, compressors are recognized as one of the best electrical energy saving candidates for industrial facilities as well as demand side management [1]. This section intends to introduce the air compressor system and the current system control methods as well as giving a brief definition of the technical terms related to the power engineering which have used throughout this research such as electrical demand, energy and load profile.

1.1 Definitions and System Overview

Electricity cost for industrial facilities mainly consists of energy charge and demand charge. In this section, the definitions of energy, demand, maximum demand and load profile have been provided.

1.1.1 Electrical Energy

The U.S. Energy Information Administration (EIA) defined electrical energy as "the ability of an electric current to produce work, heat, light, or other forms of energy. It is measured in kilowatt-hours [2]." Price per kilowatt-hour varies significantly between different locations due to tariffs, such as the price of power generation, government subsidies, local weather patterns, transmission and distribution infrastructure, and industry regulation. Therefore, this study is focused on the actual kilowatt-hour saving rather than cost saving.

1.1.2 Electrical Demand

Consumers usually think of their electricity as consumed energy (in kilowatt-hours) over the billing period. However, utility system operators and designers' cares more about power (in kilowatts or megawatts, measuring the instantaneous rate of energy flow) demanded at any time. Therefore, the term demand refers to a physical quantity of power, not energy. Having that immediate demand under various circumstances is the primary challenge in power systems design and operation, and the one that commands for the majority of investment and effort [3]. Electric power distribution handbook defines demand as "the load average over a specified time period, often 15, 20, or 30 min. Demand can be used to characterize real power, reactive power, total power, or current" [4] which is how utilities measure demand to charge consumers, and it contradicts with the actual supplied real-time electrical demand defined as the instantaneous rate of energy flow (power).

1.1.3 Load Profile and Maximum Electrical Demand (Peak Demand)

Peak demand over the billing period for each user is the most common interest among all utility providers. Each provider has its method to calculate the peak demand and cost associated. Therefore, there is no generic way of calculating peak demand. Below are the two methods that are most common in the industry.

Fixed Window (Block Window): The maximum demand calculation during a defined interval (usually every 15 minutes). Once the data is obtained, the value is stored and it makes a reset to start a new calculation for the next 15 minutes. These 4 registers will be measured every hour [5, 6].

Sliding Window: The maximum demand calculation during a defined interval (usually every 15 minutes). Once the data is received, it will wait one minute to start a new 15 minutes calculation (this time may vary depending on the re-

gion). Every minute it will register one maximum demand value from the last 15-minute period. These 60 registers will be measured every hour [5].

Load profile represents instantaneous demand over the time. Data collection can be at any level, from an individual electricity user to an entire grid. The maximum can be termed as the peak demand, peak load or peak [3]. Figure 1.1 shows the effect of a 350 HP air compressor on the entire plant electrical demand. The data is logged from a metal casting plant which operates 24/7 during the weekdays. The data has been logged from the beginning of the week for two days. The plant started the operation on 6:30:00 in the morning and the air compressor has kicked in before other equipment. Due to the large size of the air compressor, its effect on the load profile of the factory is considerable. The logged peak demand for this 48 hours was 1689.6 kW, and the air compressor was responsible for 14.2% (240.586 kW). After start up the factory, demand fluctuates from 1689.6 kW to 1075.2 kW, and the air compressor demand varies from 249.2 kW to 116.7 kW. The maximum possible air compressor effect on the overall demand is 21.56% (132.5 kW) which makes it one of the best choices for demand management.

Calculating how much each subsystem such as air compressor system contributes to this maximum demand is a complicated task. Different techniques and calculations are required based on the location, utility provider and the size of the facility. U.S. national renewable energy lab presented numerous techniques such as utilizing different engineering methods, hourly simulation modeling, billing data analysis, load monitoring and end-use metered data analysis [7]. Reducing the maximum load on each subsystem can eventually reduce the maximum load and save money. Due to the complicated nature of calculating the impact of instantaneous load on the maximum billed demand, the study is focused on the air compressor load profile.

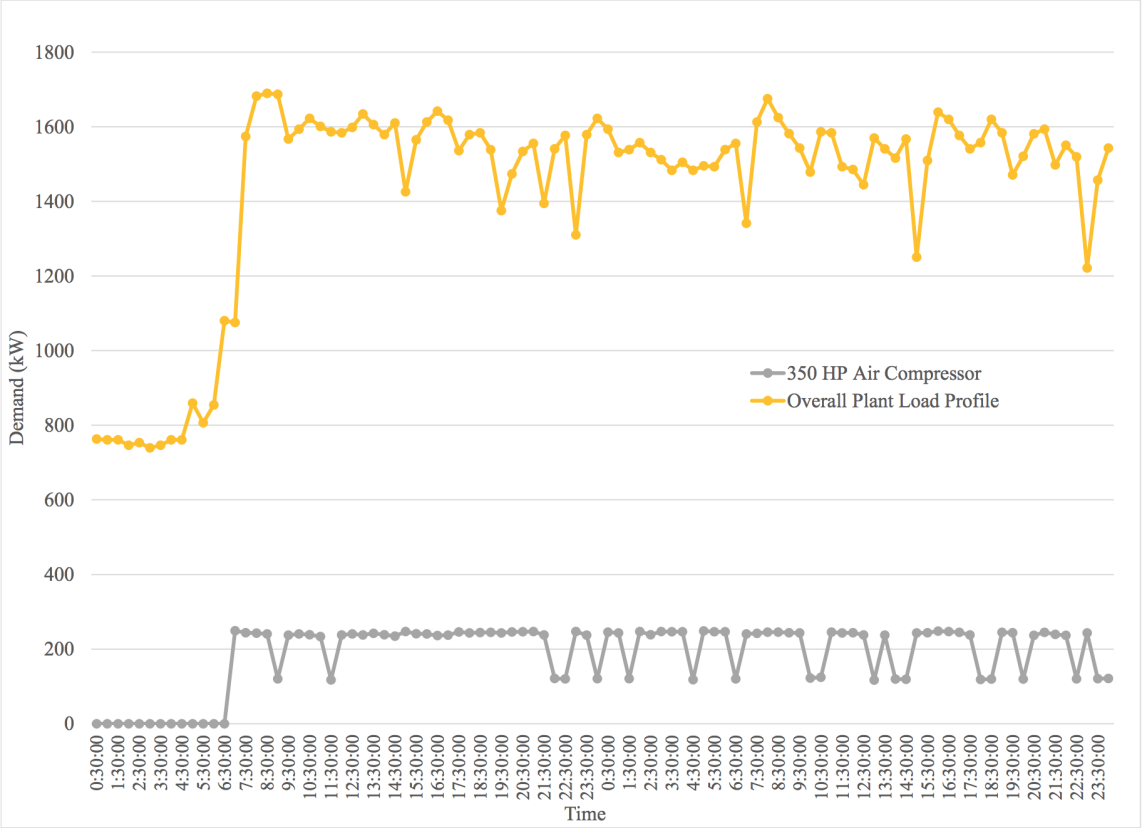

Fig. 1.1. Air Compressor Effect on Demand.

1.2 Air Compressor System

This section aims to give an overview of the air compressor system architecture. Considering electricity, natural gas, and water as three most crucial utilities, compressed air is considered as the fourth utility in almost every industry. While pneumatic tools are usually less energy efficient than electric tools, they are popular since they weigh less than electrical and hydraulic tools resulting in less physical stress and injuries on workers. They are mainly used in manufacturing facilities for applications such as automation equipment, packing, injection molding, sandblasting, process operations such as aeration, etc. Due to the simplicity of design, safety, flexibility,

broad control capability, lighter weight, and lower operation and maintenance cost pneumatic systems are favorable in industry [8, 9].

Compressed air systems have two crucial design aspect. Both of which have many sub-systems and sub-components. Supply side, incorporates compressors and air treatment components, and the demand side includes distribution and storage systems and end users. Figure 1.2 shows a typical industrial compressed air system and its components. All of the subsystems before the PRV (pressure regulator valve) is considered as supply side, and anything after is regarded as demand or distribution side [9, 10]. The mechanical device that takes in the filtered ambient air and raises

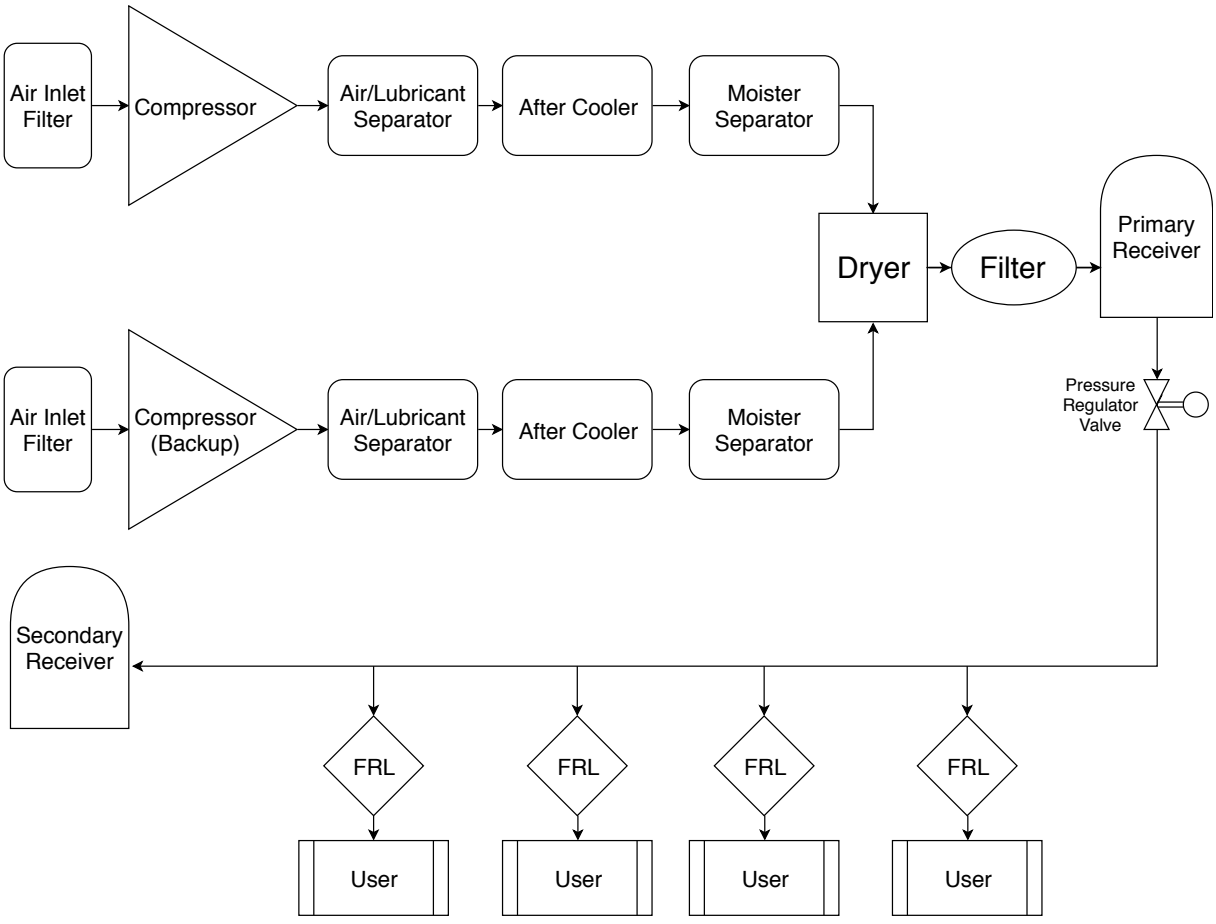

Fig. 1.2. Typical Air Compressor System.

its pressure is called the compressor. Usually an electrically driven motor powers the compressor. There are two types of air compressors:

Positive Displacement: A given volume of air or gas is trapped in a compression chamber, and the occupied volume is mechanically reduced, producing a rise in pressure before discharge.

Dynamic: Kinetic energy is converted into pressure energy in order to compress the air. Impellers and the discharge volutes (diffusers) rotate at very high speeds. The shape of the impeller blades defines the air flow and the pressure (or head) made in the centrifugal-type dynamic compressors.

Figure 1.3 presents the compressor type tree. Rotary screw compressors have become more popular during recent decades. In these compressors, two rotors trap air and increase the pressure along the rotors by reducing the volume. Helical twin screw compressor is one of the most common types. Rotary screw compressors can be found as lubricated or dry (without oil) types. Air/lubricant separator separates the lubricant and recirculates it back to the compressor to prevent lubricant contamination with water in the after-cooler after compressing the air in lubricated compressors. After-coolers are responsible for reducing the increased air temperature due to compression. This temperature reduction will condensate the water vapor. Therefore, a separator is needed to remove moisture from the system. After separator, air usually becomes saturated. This air can condensate through the distribution system by exposing to colder temperatures and cause corrosion and many other issues. This problem can be solved by utilizing air dryers. Figure 1.4 shows different air dryer technologies. Refrigerant and desiccant dryers are two major types. Absorption and adsorption separate vapor water in desiccant dryers. Refrigerant dryers use a refrigeration cycle to decrease the temperature and discard the water. Depending on the application and requirements proper air dryers can be selected. Energy waste can occur by running air dryers beyond required pressure dew point [8–12]. After air dryers, filters are used to purify the air from particulates, condensate, and lubricant. Choosing the right

filters can reduce the pressure drop and save energy [13]. Filtered air destination is primary receivers. They are intended to help the system to meet peak demand and help control system pressure by monitoring the rate of pressure change in the system. Air receivers can assist with wide air usage variation, reducing compressor size and increasing the efficiency. Air receivers play a pivotal role in the system due to the following tasks [8–12].

- Acting as a damper for reciprocating air compressors.
- Water and lubricant-free compressed air storage.
- Reducing air compressor running by satisfying peak demands with stored air.
- Helping screw compressors to run more efficiently and decrease motor starts by Reducing load/unload or start/stop cycle frequencies. Screw compressors are intended to run no more than 4,6 starts per hour.
- Better and more stable system control is possible by slowing system pressure changes.

Pressure regulator valve or flow controllers after air receivers differentiate the supply side from the demand side. Their primary function is stabilizing the system. Compressors are not controlled directly with them. On the demand side, the distribution system consisting of main headers, branches, hoses, and valves connects the various air compressor users to the supply side with minimum pressure loss. Proper line sizing with considering future expansion, a looped system with sloped piping and condensate drainage points are the best design practices. Depending on the user requirements Filter Regulator Lubricator (FRL) system is used. Regulator reduces the line pressure to the user's desire. The lubricator is used to lubricate the tools and filters are used to make sure that pure air is going into the user. Some of the users require a high volume of air in a short amount of time. Dimensioning the whole system based on this temporary load is not economically feasible. Therefore, a secondary air receiver is used to supply this user during the peak [8–12, 14].

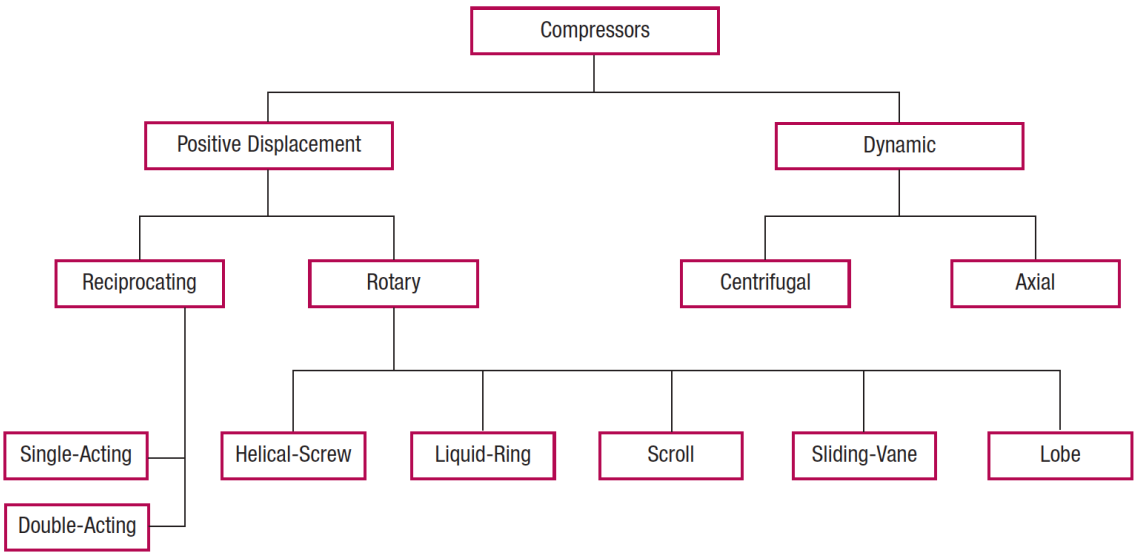

Fig. 1.3. Compressor types [11].

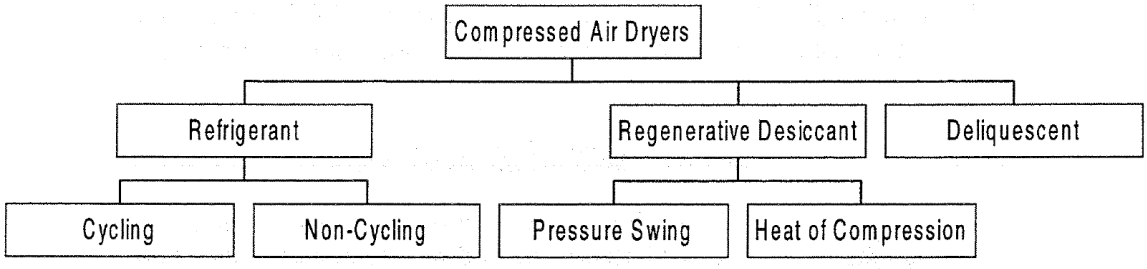

Fig. 1.4. Air dryer types [9].

1.3 Air Compressor System Control Methods

Air compressors normally do not operate at full-load during the operation hours. Control system is vital to minimize the energy usage and efficiency of the system. System control schematic is developed based on the compressor type and air usage profile. Multiple compressors with varying users' demand need a custom tailored strategy. This research intends to study simple systems with one compressor involved.

However, the novelty of the proposed algorithms can be adopted for these systems to save more energy as well. Following are the developed control strategies by the air compressor manufacturers so far [8–12, 14].

Start/Stop: Start/stop control is the most straightforward and most energy efficient control strategy. Commonly, a signal received from a pressure switch which triggers by discharge pressure is used to turn the motor on or off. This strategy is used for reciprocating or rotary screw compressors less than 30 HP with low duty cycle. Using this methodology with high duty cycle can damage the compressor and increase the maintenance cost. During the off time, the stored air in the receiver is being used.

Load/Unload: Online/offline control and constant speed control are other names for this method. In this scheme, the motor runs continuously. Air compressor inlet is controlled with a solenoid valve which can fully open or close the inlet. There is nothing in between. Unloaded rotary screw compressor can consume 15-35% less energy while there is no work is being delivered.

Modulating Controls: Modulating or throttling inlet controls the compressor output by changing the inlet air valve position. This method is more common to use in the centrifugal type of air compressors. It is not applicable for reciprocating and oil-free rotary screw compressors. By utilizing inlet guide vanes on centrifugal compressors' impeller inlet, better results can be achieved however the possibility of surge reduces the lowest throttling capability. Lubricant injected rotary compressors can be controlled by modulating the inlet with a regulating valve. A signal from the system or discharge pressure depending on the system setpoint can reduce the compressor inlet pressure and mass flow rate accordingly. Modulation range is typically between 100% to 40%. The air compressor will run as fully unloaded at 40%.

Dual-Control/Auto-Dual: This control method allows the user to switch between constant speed control (load/unload) and start/stop for reciprocating compres-

sors. A timer is used to stop the motor after running unload for the pre-set time in oil-injected rotary screw compressors.

Variable Displacement: It is a control method with the capability of operating between loaded and unloaded or similarly start and stop. This control scheme has designed for reciprocating compressors to allow them to have three step control meaning 0%-50%-100% or five-step control meaning 0%-25%-50%-75%-100%. The goal is to load the motor to the required air production to save more energy. For rotary screw compressor, this technique uses capacity control valves such as sliding, poppet or spiral valves to modify the compressor output in combination with modulating the inlet air valve. The intention is to meet the air production demand by changing compressor output pressure. Usually, this method is very efficient above 60% of load and is equal to unloading the compressor below 40% of capacity.

Variable Speed Drives(VSD) or Variable Frequency Drive(VFD): This control method can keep the system pressure constant with +/-1 psi among an extensive range of load. This method uses VFD technology which is modifying the frequency of the electric power lines to the motor to change the speed and torque of electric motors. Rotary screw compressors can be stopped in a determined number of times in a given time. This method can operate the compressor in the exact required demand. It worth mentioning that this method works well on positive displacement compressors since the displacement and rotational speed have a linear relationship. However, for dynamic compressors, this method can be inefficient since the efficiency of the compressor can fall at the lower speed and will require higher torque and energy usage.

Capacity Controls for Centrifugal Type Compressors: Inlet air density and the interstage water cooling system make centrifugal compressors complicated to control. The goal is to avoid air compressor surge and choke. Surging is caused by back flow during low air demand and will damage the compressor.

Choking is caused by reaching the inlet air speed to 1 Mach at the inlet due to high demand. Decreasing inlet pressure can avoid both by closing the inlet throttle valve.

Several compressors feeding a combined system needs a more complex control system based on the air demand profile and system architecture. Standard techniques are listed as follows [8–12].

- Cascaded Pressure Band Control
- Network Control
- Single Master (Sequencing) Controls
- Multi-Master (Network) Controls

Nowadays, machine learning and its capabilities such as automatically obtaining profound insights, recognizing unknown patterns, and creating high performing predictive models are well known. Artificial Intelligence (AI) became one of the hottest topics in this century because of its vast skills to use in different systems and applications. This study intends to use AI to load forecast the air compressor system and use the outcome to design a novel control algorithm to operate a compressed air system with respect to demand and energy perspective without sacrificing the user needs which in this case is the required air for production. Overall, the skeleton of this study can be seen below.

Power Consumption Prediction: The output can be used as an input to control systems which can be for air compressor itself to operate more efficiently or to use as an input for building or factory energy management systems to reduce the overall electrical demand by modifying other systems operation during the peak.

Air Compressor Maximum Electrical Load Reduction: Reducing air compressor effect on electrical demand as well as operating the system more smoothly and robustly to increase the lifetime by using the prediction outcome.

Air Compressor Energy Usage Reduction: Using the prediction outcome to develop a new load/unload control algorithm to further reduce energy consumption.

All in all, the thesis is divided into five chapters. Chapter 1, defines some of the terms that have been used in electric systems and talks about the air compressor system and its control methods. Chapter 2, introduces electrical load forecasting methods as well as presenting and proposes a neural network time series and long short-term memory networks for air compressor load forecast. The section will discuss the details of the case studies and the outcome results and their accuracy. Chapter 3 uses the results to propose a novel algorithm to operate the system in real time with a lower maximum electrical load. Chapter 4 covers the usage of the prediction to develop a new load/unload with auto shut off control algorithm to maximize the energy saving. Chapter 5 concludes the research and presents the future work that can be done to continue this research.

2. AIR COMPRESSOR LOAD FORECAST

2.1 Introduction

By the passage of time, energy management and its importance are getting higher attention due to the shortage of fossil fuels, stricter environmental law restrictions, new supply and demand policies and the increasing of utility prices. In the past decades, energy costs were viewed as overhead instead of an important cost function. This behavior has changed during the last decade. As a result, we can see more companies and organizations have energy management plans and they have more concerns about energy efficiency [15]. Data mining plays a pivotal role in energy management plans. In 2012, White House asked utility companies to provide customers energy data in an easy and secure way. Due to this request, US department of energy started Green Button program which is an industry-led initiative to provide energy usage data from utility providers to the customers to help them manage energy use and save on their bills [16]. Also, some of the major utility providers started their portal to provide same information by using smart metering devices. This data can help both users and electricity providers as power grids are designed to meet users energy usage and demand at the same time. This essential duty has become more challenging for high fluctuation in electricity demand. There are two different perspectives on demand-side management. On the grid side, the utility provider wants to keep the grid stable and ready to meet peak demands by building the sufficient infrastructure. On the other hand, the users' primary goal is clearly decreasing the costs [17]. For reducing the demand cost, users need to maintain the demand as flat as possible. For reducing the energy cost, they need to utilize more energy efficient equipment or production methods. Future load prediction plays a pivotal role for both

utility providers and users. Decisions such as power system operation, maintenance and planning can be performed with an accurate load forecasting method [18].

Predicting compressed air systems load profile will be valuable to the industry practitioners as well as related software providers in developing better practice and tools for load management and look-ahead scheduling programs. It will also provide the foundation for our control methods in chapter 3 and 4. The main burden in this kind of prediction is that there are lots of parameters (minute, hour, day of week, line pressure, intake temperature, compressed air flow rate and power) that need to be taken into consideration as well as high fluctuation in some air compressor demand patterns.

The objective of this chapter is to Feed-Forward Neural Network (FFNN) with time delays, and Long Short-Term Memory (LSTM) recurrent neural network techniques to predict the air compressor load profile. A brief overview of the load forecasting techniques and NN technique usage in compressors as a form of literature survey is given. Later, a brief overview of Neural Networks have been given. Afterward, experimental setups description for our case studies and the results are presented. Three different type of air compressors of different sizes and control methods have been studied.

2.2 Electrical Load Forecasting

The goal of the second chapter of this thesis is to use AI to predict the air compressor load profile. Therefore, this section will start with a review of load forecasting techniques. Load forecasting or demand forecasting is vital for managing the operation and maintenance of power systems [19]. It is defined as providing future energy usage based on the historical data in order to prepare the adequate volume of energy for the usage time. Based on the needed time ahead for decision making, there are different categories of load forecasting. Namely, short-term load forecasting (STLF) with a range of a few minutes ahead up to a day ahead [20, 21], medium-term load

forecasting (MTLF) with a range of one week to a year ahead [22] and long-term load forecasting (LTLF) from one year to decades [23]. Different authors have various definitions for the range of these forecasting methods. This research is concentrated on the short-term load forecasting of a compressed air system since it can have more impact on the efficiency and load management of the system and the whole facility.

Various methodologies have been utilized for STLF which can be divided into two classifications: statistical methods and artificial intelligence methods (AI). Numerous statistical methods have been proposed including regression models [24], autoregressive integrated moving average (ARIMA) models [25, 26], support vector regression (SVR) [27]. Artificial neural network (ANN) with combined algorithms are considered in the AI category. ANN has been combined with fuzzy logic algorithm [28], genetic algorithm [29], and particle swarm optimization [30] and etc. Khosravi et al. has a comprehensive literature review regarding the AI based load demand forecasting techniques and presents a performance evaluation of AI techniques and their current potential [31]. Demand forecasting techniques are applicable in various scales. From hourly energy usage prediction of a residential house [32,33] to an entire nation. Kadir Kavaklioglu conducted a study to predict Turkey's electricity consumption [34]. Forecasting techniques also used to predict the annual energy usage of different sectors in a nation such as the Spanish banking sector [35] and United States residential sector [36].

ANN can map the inputs of the model to outputs without using complicated mathematical models. Thus, it has a better performance than statistical techniques [37]. It is also more reliable under uncertainty scenarios and does not demand human expertise. For forecasting problems due to dynamically changing interconnected weight values, ANN methods show better performance in comparison with statistical methods. Faster convergence speed of network, lower computational complexity, lower the training period, better generalization and enhancing the performance of the network can be gained by increasing correlation impact, pre-processing the training data, utilizing optimal network structure and better learning algorithms [38]. Therefore, this

study is utilizing ANN to predict the air compressor power consumption. The next section gives a brief introduction to ANN technique usage on compressors.

2.3 ANN Technique Usage on Compressors

Designing and improving compressors are always the main goal of designers. Compressor performance maps have a great importance for simulation and design purposes. Experimental values at various operating conditions are being used to draw these maps. These experiments are time consuming, costly and cannot cover the entire range of operation. Therefore, many researchers have used machine learning techniques to predict these curves for different operating conditions. Fei et al. used a novel artificial neural network integrating feed-forward back-propagation neural network with Gaussian kernel function [39]. Yu et al. applied a three-layer back-propagation neural-network with LevenbergMarquardt algorithm to predict stage-by-stage axial-compressor performance [40]. General regression neural network (GRNN), rotated general regression neural network (RGRNN), radial basis function network (RBFN) and multilayer perceptron (MLP) network are applied by Ghorbanian and Gholamrezaei to predict the compressor performance [41]. Hybrid ANN with Partial least squares (PLS) model is used by Tian et al. to predict the thermodynamic performance of a scroll compressor [42]. A variable speed reciprocating compressor have been studied to predict mass flow rate, power consumption and discharge temperature at different operating conditions by using ANN in [43].

In summary compressor performance prediction have been studied widely. There was a need to study the possibility of time series prediction of the air compressors electrical load profile. Two-Layer Feed-Forward Neural Network (FFNN) with time delays and Long Short-Term Memory (LSTM) recurrent neural network are two types of ANNs which we used in this study. The next section provides a brief introduction to neural networks.

2.4 Neural Networks

This section will provide a brief overview of Neural Networks. NNs are a part of machine learning tools which process the data similar to the human brain. They are basically made of artificial neurons similar to the Figure 2.1. There are several kinds of neural networks such as Radial basis function networks (RBFN), Adaptive neuro-fuzzy inference system (ANFIS) [44], Kohonen self-organizing networks, and recurrent networks. Our concentration in this research is on feed forward neural networks (FFNNs) because the FFNN is one of the most commonly used NNs for energy forecasting [45]. The main task of these networks is to approximate unknown relationships between input and output. The output is the product of processing the input data which is four data in Figure 2.1. Typically, two steps are required for processing. First step is combining the input data. The second step is using the first step outcome as an input to a nonlinear activation function. The combination exercises the weights associated to each link and a fixed bias term θ [46]. The activation function must be an increasing function whose derivative exists. The most popular type of activation functions are the followings.

- Identity Function $y = x$
- Bounded Sigmoid $y = \frac{1}{1+e^{-x}}$

A three-layer FFNN is shown in Figure 2.2. Information flows the input layer through the hidden layer to the output in one direction. There are no connections exist between neurons in the same layer. The number of input neurons depends on the number of inputs, and the number of output neurons depends on the number of outputs layer is equal to the number of outputs. The user chooses the number of hidden layers and the number of neurons in each hidden layer. The number of hidden layer neurons is recommended by the following relationship as $m = 2n+1$, where m is the number of hidden layer neurons and n is the number of input neurons [47]. In the example network shown in Figure 2.2 the weight matrices are $W_{i,j}$ and $u_{j,k}$ connecting

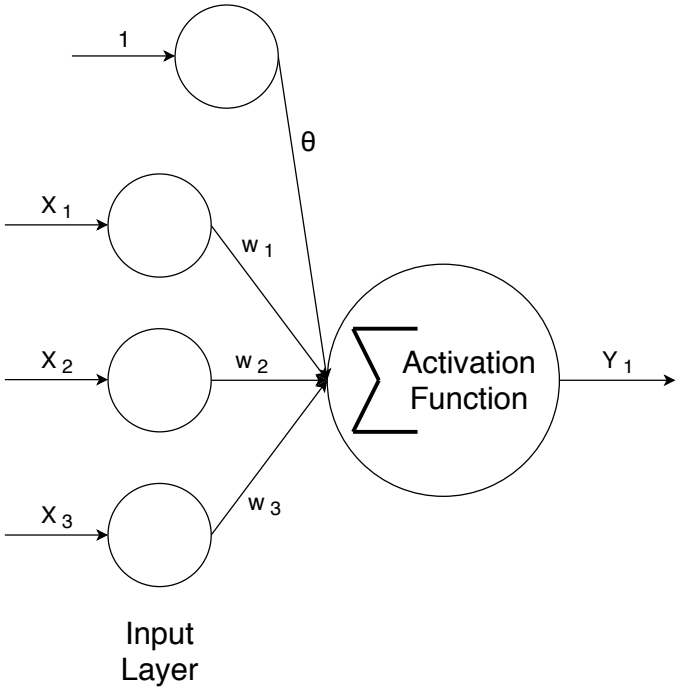

Fig. 2.1. An Artificial Neuron.

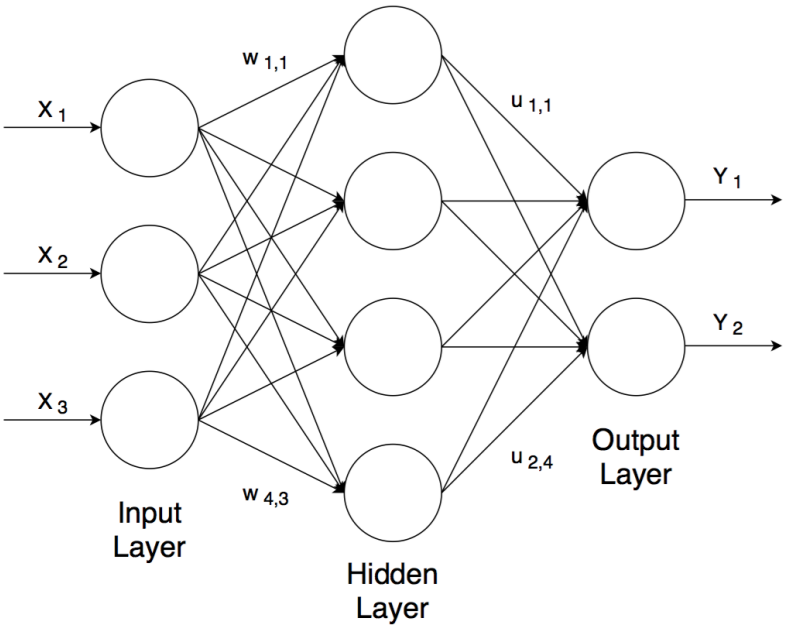

Fig. 2.2. A Three Layer Feed Forward Neural Network.

the input i to neuron j. The bias vector which can be applied to input or output or both is annotated with θ. The bias vector helps the network to converge better and give a better outcome. By using bounded sigmoid functions for the activation of the hidden layer and the linear functions for the output layer, the network output will be as follows [46, 48].

$$y_k = \sum_{j=1}^{4}(u_{jk}.\frac{1}{1+exp(-\sum_{i=1}^{3} w_{ij}.x_i + \theta_j)}) + \theta_k \tag{2.1}$$

According to the formula mentioned above the output computation of a simple network, can become complicated. FFNN weights are estimated during the training phase by using trial and error to reach the output. Many optimization algorithms such as back-propagation with gradient descent optimization have been developed for this phase. Back-propagation utilizes the steepest-descent technique based on the calculation of the gradient of the loss function for the network. Learning process starts with assigning random numbers to the weights. Afterward, the calculated output based on the input will be used to compare the network output to the actual output and adjust the weights accordingly until we have a network that has an output with an acceptable predefined error threshold [46, 48]. The forecasting capability of the FFNN has been widely tested on many time series problems [49–52]. The robustness of these networks depends on the application, input and outputs relationship. FFNN can have different outputs depending on the training and chosen input data. While the FFNN has limitations, the LSTM can solve many time series tasks unsolvable by feed-forward networks [53]. LSTM is a special type of recurrent neural networks (RNN). A typical LSTM unit is made of a cell, an input gate, an output gate and a forget gate. The cell remembers values over arbitrary time intervals and the three gates regulate the flow of information into and out of the cell. Being capable of lagging of unknown duration between important events in a time series makes LSTM networks are capable of organizing, processing and making predictions based on time series data [54].

2.5 Case Studies

2.5.1 50 HP Rotary Screw VFD Air Compressor

The first air compressor for our case study is located in a $50,000 ft^2$ facility which does electroplating and surface finishing for different products. Compressed air in this company is mainly used for driving pneumatic double diaphragm pumps, automation actuators, press tools, and air nozzles for cleaning purposes. Overall, the system is composed of: a 50 HP rotary screw compressor, a filter, an air dryer, and an air receiver. Figure 2.3 shows the described system.

Fig. 2.3. 50 HP Air Compressor System. From Left to Right: Air Receiver, Air Dryer and Air Compressor.

The installation is set up to control the volumetric flow and maintain the line pressure by controlling the rotation speed of the compressor by utilizing a VFD. Additionally, the compression system includes several devices to measure: line pressure, discharge pressure, volumetric flow rate, inlet air temperature and discharge temperature. Also, an inductive sensor is used to measure the rotation speed of the compressor. The compressor connection to the motor is through a shaft. The logic of the control system is to maintain the air receiver tank pressure at 8.27 bar (120 psi)

which is considered as the line pressure. A PID controller is utilized to implement this logic by driving the VFD. Our data acquisition system consists of a three-phase energy logger from Fluke connected to the compressor power source, 100 Amp split-core AC current sensor from ONSET connected to the air dryer power source, 200-psi gauge pressure sensor from ONSET connected to the compressed air pipe before air dryer and after air receiver tank and a temperature sensor with the range of $-40°C$ $(-40°F)$ to $50°C$ $(122°F)$ from ONSET to measure intake air temperature. We also used the air compressor HMI (Human Machine Interface) to collect volumetric flow rate, discharge pressure, and temperature. Table 2.1 presents the specifications of the studied system. Table 2.2 provides information about the sensors used to monitor the operation of the air compressor system. This table also includes the uncertainty for each sensor. Minutely data were collected for 38 days under normal plant operating conditions to later analyze the compressor load forecast using ANNs.

Table 2.1.
50 HP air compressor system specifications.

Parameter	**Value**	**Units**
Compressor Motor Capacity	37	kW
Maximum Motor Speed	3600	RPM
Full Load Current	71	A
Maximum Discharge Pressure	13	bar
Air Dryer Compressor	1.86	kW
Air Dryer Fan	0.124	kW

Table 2.2.
Measured parameters and their uncertainty on 50 HP air compressor.

Parameter	**Instrument**	**Uncertainty**
Temperature	Thermocouple	$\pm 0.25°C$
Pressure	Pressure transducers	$\pm 1\%$
Mass Flow Rate	Human Machine Interface	$\pm 0.5\%$
Current	Split-core 100 Amp AC current Sensor	$\pm 5\%$
Rotation Speed	Inductive sensor	$\pm 1\%$
Compressor Energy Logger	Fluke Power Logger 1730	$\pm 1\%$

2.5.2 100 HP Rotary Screw Load/Unload Air Compressor

The Second air compressor for our case study is located in a $2,000,000 ft^2$ facility which is a waste water treatment plant. Compressed air in this facility is mainly used for driving pneumatic actuators and pneumatic solenoid valves.

Table 2.3.
100 HP air compressor system specifications.

Parameter	**Value**	**Units**
Compressor Motor Capacity	74.57	kW
Full Load Current	96	A
Maximum Discharge Pressure	13	bar
Air Dryer Compressor	1.12	kW
Air Dryer Fan	0.124	kW

Overall, the system is composed of: a 100 HP rotary screw compressor, a filter, an air dryer, and an air receiver. Figure 2.4 shows the described system. The control logic is to maintain the line pressure by loading and unloading the compressor

Fig. 2.4. 100 HP Air Compressor System. From Left to Right: Air Dryer, Air Receiver and Air Compressor.

Table 2.4.
Measured parameters and their uncertainty on 100 HP air compressor.

Parameter	**Instrument**	**Uncertainty**
Temperature	Thermocouple	$\pm 0.25°C$
Current	Split-core 100 Amp AC current Sensor	$\pm 5\%$
Current	Split-core 600 Amp AC current Sensor	$\pm 1\%$

between 8.27 bar (120 psi) and 6.89 bar (100 psi). The compressor connection to the motor is through a shaft. An Auto/Dual control is utilized to implement this logic. The Compressor Unloads the air compressor via inlet modulation valve. Our data acquisition system consists of a 600 AMP Split-core AC current transformer Sensor from ONSET to measure the compressor power source, 100 Amp split-core AC current sensor from ONSET connected to the air dryer power source and a temperature

sensor with the range of $-40°C$ $(-40°F)$ to $50°C$ $(122°F)$ from ONSET to measure intake air temperature.Table 2.3 presents the specifications of the studied system. Table 2.4 provides information about the sensors used to monitor the operation of the air compressor system. This table also includes the uncertainty for each sensor. Minutely data were collected for 59 days under normal plant operating conditions to later analyze the compressor load forecast using ANNs.

2.5.3 1 HP 1 Stage Reciprocating Start/Stop Air Compressor

The third air compressor for our case study is located in a $45,758 ft^2$ museum. Compressed air in this facility is mainly used for driving pneumatic actuators and pneumatic solenoid valves for the process systems.

Fig. 2.5. 1 HP Air Compressor System. Top Right: Air Dryer Bottom: Air Receiver.

Table 2.5.
1 HP air compressor System specifications.

Parameter	**Value**	**Units**
Compressor Motor Capacity	0.745	kW
Full Load Current	1.6	A
Maximum Discharge Pressure	6.2	bar
Air Dryer Compressor	0.093	kW

Table 2.6.
Measured parameters and their uncertainty on 1 HP air compressor.

Parameter	**Instrument**	**Uncertainty**
Temperature	Thermocouple	$\pm 0.25^{\circ}C$
Current	Split-core 100 Amp AC current Sensor	$\pm 5\%$
Pressure	Pressure transducers	$\pm 1\%$

All in all, the system is composed of: a 1 HP reciprocating compressor, an air dryer, and an air receiver. Figure 2.5 shows the described system. The control logic is to maintain the line pressure by turning on and off the compressor between 4.82 bar (70 psi) and 3.79 bar (55 psi). The compressor connection to the motor is through a belt. There are two compressors with motors for redundancy. A Start/Stop control is utilized to implement this logic. The air Compressor starts and stops via two pressure switches, one for high level and the other one for low level. Our data acquisition system consist of a 100 AMP Split-core AC current transformer Sensor from ONSET to measure the compressor power source, 200-psi gauge pressure sensor from ONSET connected to the compressed air pipe before air dryer and after air receiver tank and a temperature sensor with the range of $-40^{\circ}C$ ($-40^{\circ}F$) to $50^{\circ}C$ ($122^{\circ}F$) from ONSET to measure intake air temperature. Table 2.5 presents the specifications of the

studied system. Table 2.6 provides information about the sensors used to monitor the operation of the air compressor system. This table also includes the uncertainty for each sensor. Data were collected for 56 days under normal plant operating conditions to later analyze the compressor load forecast using ANNs.

2.6 Data Analysis and Preprocessing

It is not uncommon to have outliers and erroneous values in data collected by different types of sensor; therefore it is important to preprocess the inputs before the neural network can be built [55]. The following descriptive analysis is done using SPSS Statistics Software for finding the mean, minimum and maximum values, as well as the outliers of electric power. Table 2.7 shows that Compressor 1 and Compressor 2 have high variances, signaling a high deviation from the expected value (mean). Shown in Figure 2.6, Compressors 1 and 3 have several the outliers greater than three standard deviations from their respective means.

Table 2.7.
Descriptive statistics of raw power consumption data obtained by the power loggers of each air compressor.

Parameter	**Compressor 1 (50 HP)**	**Compressor 2 (100 HP)**	**Compressor 3 (1 HP)**
N	3603	2892	5379
Min	13.81	0.01	0.05
Max	54.35	85.90	8.83
Mean	26.05	28.55	0.83
Std. Dev.	6.97	23.97	0.63

From the data analysis, we decide to eliminate the outliers from the power consumption dataset by applying the Hampel filter since the outliers are the simply the noises in our logged data. 50 HP (37 kW) air compressor with the full load current of

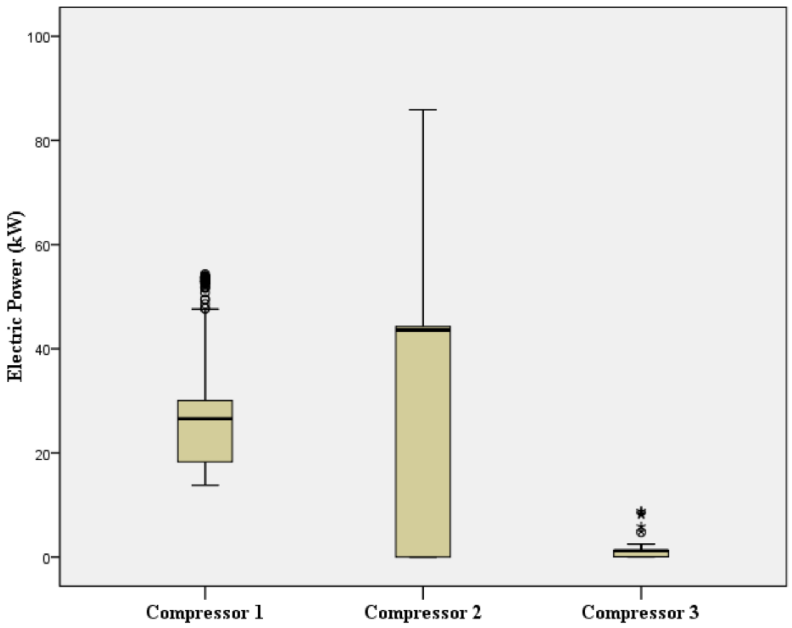

Fig. 2.6. Boxplot of measured power consumption of three compressors.

71 A cannot consume 54 kW at full load and 13.8 kW at zero load based on the specifications. Similarly 1 HP (0.74 kW) air compressor cannot consume 8.83 kW. This is a common problem among sensors and data loggers. Hampel filter is a variation of the three-sigma rule of statistics that is robust against outliers [56]. The Hampel filter replaces the outliers with a local median, keeping the length of the dataset array constant, which makes the machine learning algorithm feasible. A brief explanation of the Hampel filter is shown as the following:

Given a sequence from the entire dataset $x_1, x_2, x_3, ..., x_n$ with n number of data points and a sliding window half-width K, we can define Equation 2.2 and 2.3.

$$W_i^K = x_{i-K}, ..., x_i, ..., x_{i+K} \quad \begin{cases} n = Odd \rightarrow K = (n-1)/2 \\ n = Even \rightarrow K = n/2 \end{cases} \tag{2.2}$$

Where W_i^K is a set of numbers within a moving window and i is the index for that moving window.

$$m_i = median(x_{i-K}, ..., x_i, ..., x_{i+K}) \tag{2.3}$$

Where m_i is the median value from the moving window. After applying the Hampel filter to the sequence, a new dataset of responses is given by 2.4.

$$y_i = \begin{cases} x_i, |x_i - m_i| \leq n_\sigma S_i \\ m_i, |x_i - m_i| > n_\sigma S_i \end{cases} \tag{2.4}$$

Where n_σ is a positive integer called as threshold parameter and S_i is the median absolute deviation (MAD) defined as below [57].

$$n_\sigma \geq \frac{\max_i |x_i - m_i|}{\min_i S_i} \tag{2.5}$$

$$S_i = 1.4826 \times median(x_{i-K}, ..., x_i, ..., x_{i+K}) \tag{2.6}$$

Based on the study conducted on [57], n_σ is chosen as 3 since it will make the filter aggressive enough to remove all of the impulsive noise spikes but forgiving enough to pass the low-level noise and sinusoidal components without distortion. A more detailed description on Hampel filter can be found in [58]. After applying the filter, the statistics of the results can be seen in the Table 2.8. It is clear that the maximum and minimum power consumptions became realistic.

Table 2.8.
Descriptive statistics of power consumption after applying the Hampel filter to the data obtained by the power loggers of each air compressor.

Parameter	**Compressor 1 (50 HP)**	**Compressor 2 (100 HP)**	**Compressor 3 (1 HP)**
N	3603	2892	5379
Min	18.53	0.01	0.05
Max	50.89	85.90	1.37
Mean	30.39	33.14	0.82
Std. Dev.	3.32	22.87	0.58

Moreover, energy consumption of compressors is greatly affected by the production schedule. The temporal variation caused by weekdays and holidays affects the outcomes of the models.

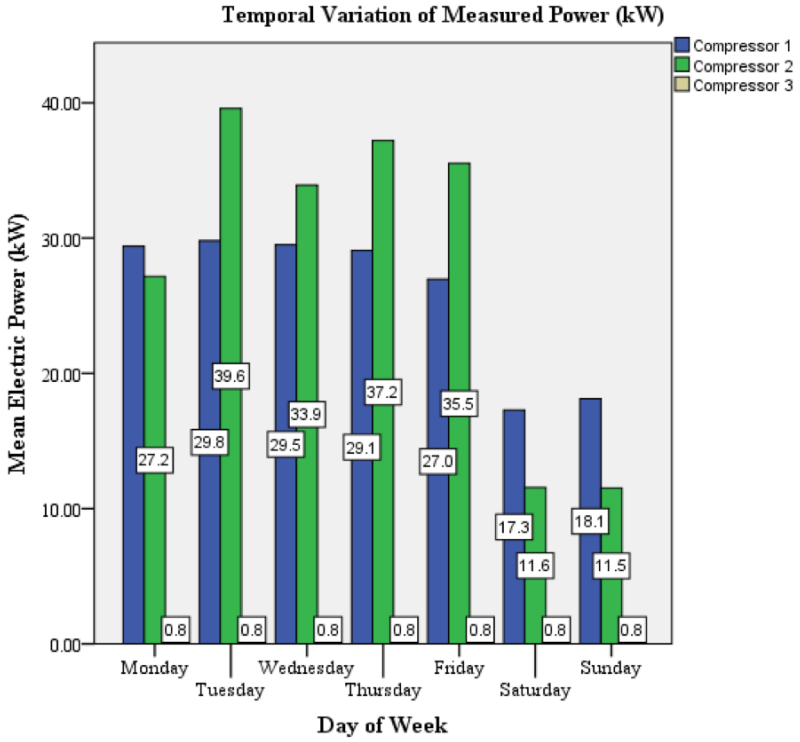

Fig. 2.7. Temporal variation of the measured power consumption of all compressors.

Figure 2.7 shows the average power drawn by each compressor in different days of a week. As can be seen in Figure 2.7, Compressor 1 and Compressor 2 has a main working schedule from Monday to Friday. Compressor 2 has a constant working pattern during the week, and therefore it is not affected by the difference in days. Consequently, it is reasonable to divide electric power consumption data of Compressor 1 and 2 into two categories: 1) working days, 2) non-working days. Figure 2.8 shows the average power drawn by compressor 3 in different days of a week. As can be seen in Figure 2.8, Compressor 3 has a constant working schedule from Monday to Sunday. Thus, it is not required to divide electric power consumption data.

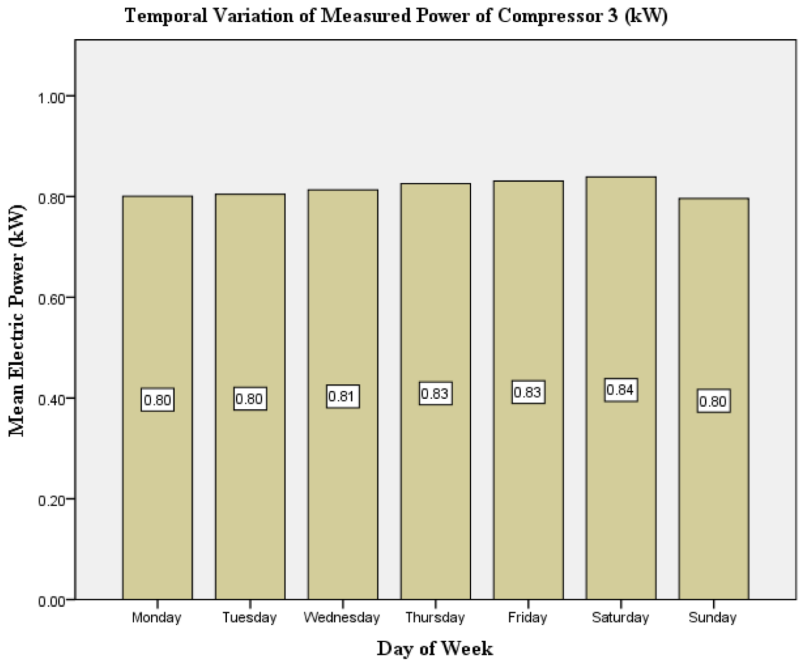

Fig. 2.8. Temporal variation of the measured power consumption of compressor 3.

After the data analysis, we decided to divide data into two scenarios representing either the working days or non-working days. Outliers are replaced by moving medians by choosing the Hampel filter with $K = 2$ and $n_\sigma = 3$ and , representing a 30-minute sliding window and three standard deviations. Consequently, after preprocessing the data, we have the following summary shown in Table 2.9.

2.7 Neural Network Deployment

We selected two types of ANN to construct the models. One is Two-Layer Feed-Forward Neural Network (FFNN) with time delays, and the other one is Long Short-Term Memory (LSTM) recurrent neural network. Data are segmented into two sets for training, testing. Each set consists of 90% and 10% of the overall dataset, respectively. For FFNN each output is predicted by a vector of inputs including the time of day, the day of the week, the pressure in the compressed air line, the temperature of the intake air, and the historical kW data in the 15-minutes interval. For LSTM recurrent

Table 2.9.
Descriptive statistics of raw power consumption data obtained by the power loggers of each air compressor.

Parameter	**Compressor 1 (50 HP)**		**Compressor 2 (100 HP)**		**Compressor 3 (1 HP)**
	Working	Nonworking	Working	Nonworking	Working
	5 $\frac{days}{week}$	2 $\frac{days}{week}$	5 $\frac{days}{week}$	2 $\frac{days}{week}$	7 $\frac{days}{week}$
N	2654	949	2124	768	5379
Min	20.5	18.53	0.01	0.01	0.05
Max	50.89	22.7	85.90	85.19	1.37
Mean	33.96	21.48	28.55	11.47	0.82
Std. Dev.	4.53	0.32	23.97	20.13	0.58

neural network, due to many hidden layers, only the power consumption data is used to predict the target output. Both models yield a single target output of electric power in kW. Table 2.10 presents the summary of the ANNs design parameters and inputs.

To prevent neural networks from overfitting, the model requires a large dataset [59]. We will utilize all the data we have for the measurement period, leaving only 96 time-steps (1 day) for future robustness testing. According to [47], the number of hidden layer neurons is recommended by the following relationship as $m = 2n + 1$, where m is the number of hidden layer neurons and n is the number of input neurons.

The results were obtained by using MATLAB machine learning toolbox, which is designed for solving time-series problems with nonlinear input-output. To perform STLF, we will forecast the power consumption of each compressor 1 time-step (15 minutes) into the future. It is widely accepted that a neural network with the same architecture will make similar predictions with among training trials, but not give

exactly the same outputs [60]. As a result, to achieve better outcomes, each model was run 5 times, the best performances were recorded and given in Table 2.11.

Table 2.10.
Summary of ANN design parameters and inputs.

Network Type	**FFNN**	**LSTM**
Inputs	minute, hour, day of week, pressure (bar), temperature (°C), power (kW)	power (kW)
Targets	power (kW)	power (kW)
Number of Layers	2	200
Number of Hidden Neurons	13	-
Training Algorithm/Solver	Bayesian Regularization	Adam
Number of Delays	2	-
Performance	MSE	RMSE

2.8 Performance Evaluation

We used two standard metrics to evaluate the performance of each forecasting model. First, this study tests the Coefficient of Determination, namely the R^2, between the observed values and the predictor outcomes. The R^2 was calculated by Equation 2.7.

$$R^2 = 1 - \frac{\sum_{i=1}^{n} |X_i - Y_i|^2}{\sum_{i=1}^{n} |X_i - \bar{X}|^2} \tag{2.7}$$

The R^2 describes how well the prediction model fits the observation. The second metric is the Root Mean Squared Error (RMSE). It calculates the deviation between the value predicted by the model and values observed. The RMSE is calculated by Equation 2.8.

$$RSME = \sqrt{\frac{\sum_{i=1}^{n} |Y_i - X_i|^2}{n}} \tag{2.8}$$

Where X_i represents the actual measured values; Y_i represents the predicted values by the model; $\bar{X}$ is the mean of the measured sample; and n is the number of predictions.

2.9 Results and Discussion

In this section, we presented the outcomes of the two models predictions. After the neural network has trained, we applied it to the remaining 96 time-steps. The results then evaluated by the performance metrics described in the last section.

2.9.1 Power Consumption Forecast for Compressor 1

The models were trained successfully using FFNN and LSTM. Figure 2.9 shows the training stage R^2 values between both prediction models and the measured values pertaining to the power consumption of Compressor 1 in working days. Figure 2.10 describes the same information in non-working days. The R^2 values showed that 84% variations in the measurement were explained by the FFNN prediction, and 83% variations in the measurement were explained by the LSTM prediction for working days [61].

For non-working days the numbers were 73% and 75%, respectively. The predictions of 96 time-steps for a working day are shown in Figure 2.11 for both models. As can be seen in Figure 2.11, the RMSE of the FFNN model is 1.41 kW, and that of the LSTM model is 1.91 kW for predictions for a working day. The predictions for 96 time-steps during a non-working day are shown in Figure 2.12 for both models. This time, the LSTM model yields a better prediction. Similarly, the RMSE of the LSTM model was also smaller than that of the FFNN model for non-working days.

The results demonstrated that both models have the ability to forecast the electric consumption. The FFNN model performed better when the variation of the data was higher as depicted during the working days whereas the LSTM model performed better when the fluctuation in the data was smaller. Another factor that might

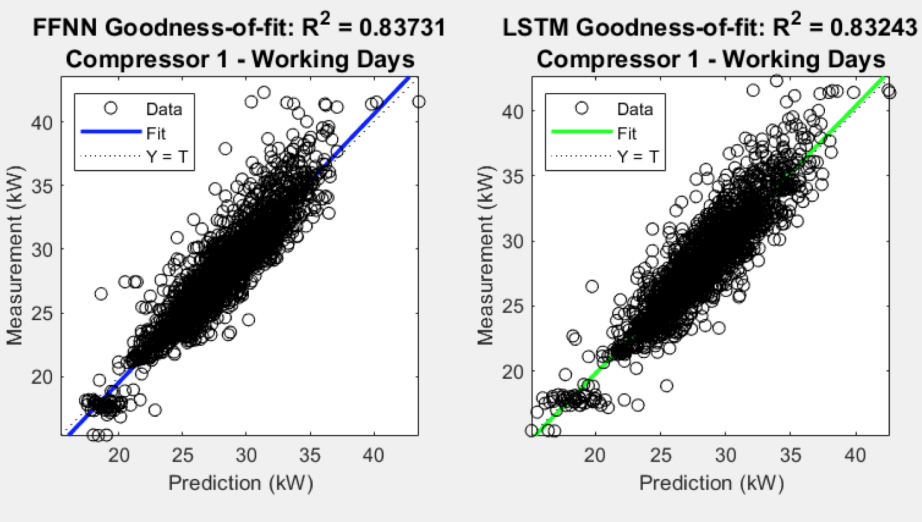

Fig. 2.9. R^2 between measured 15-minute power (kW) and predicted power by the FFNN model and the LSTM model for Compressor 1 in working days.

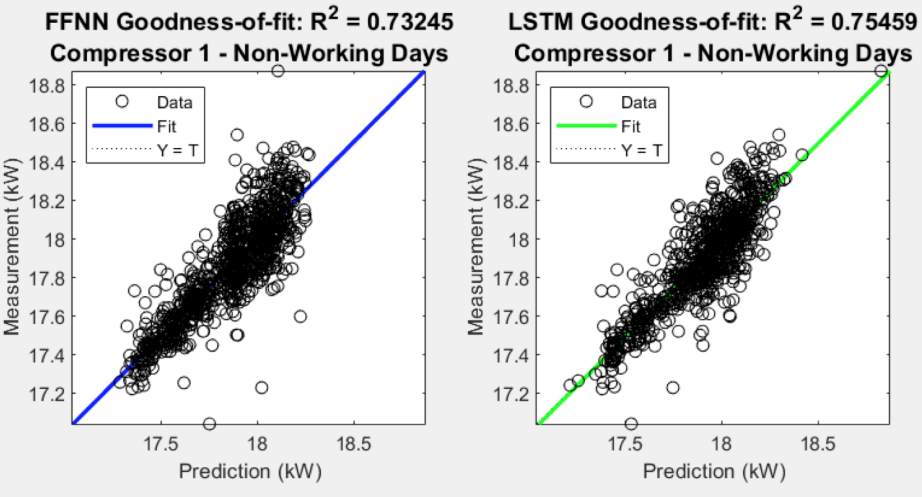

Fig. 2.10. R^2 between measured 15-minute power (kW) and predicted power by the FFNN model and the LSTM model for Compressor 1 in non-working days.

contribute to this issue could be the numbers of input. The FFNN model used more inputs related to the operating conditions and therefore yielded better prediction. However, the LSTM model could take care of more noisy data without many input

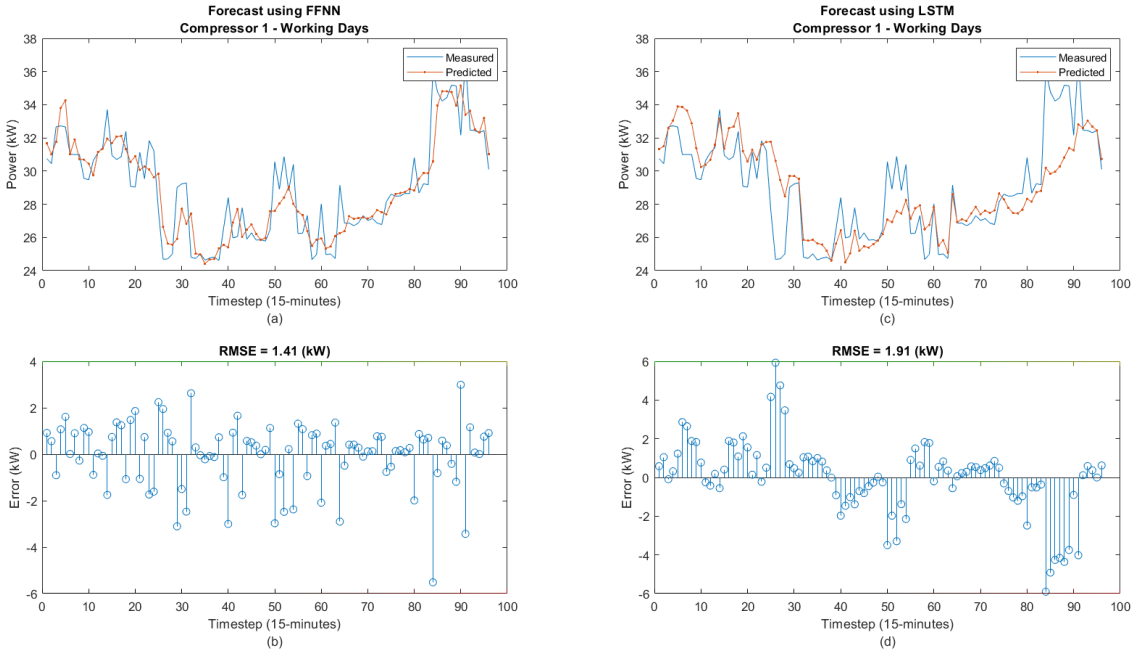

Fig. 2.11. Prediction and measurement and absolute error between them of a working day in 15 minutes interval using FFNN and LSTM for Compressor 1.

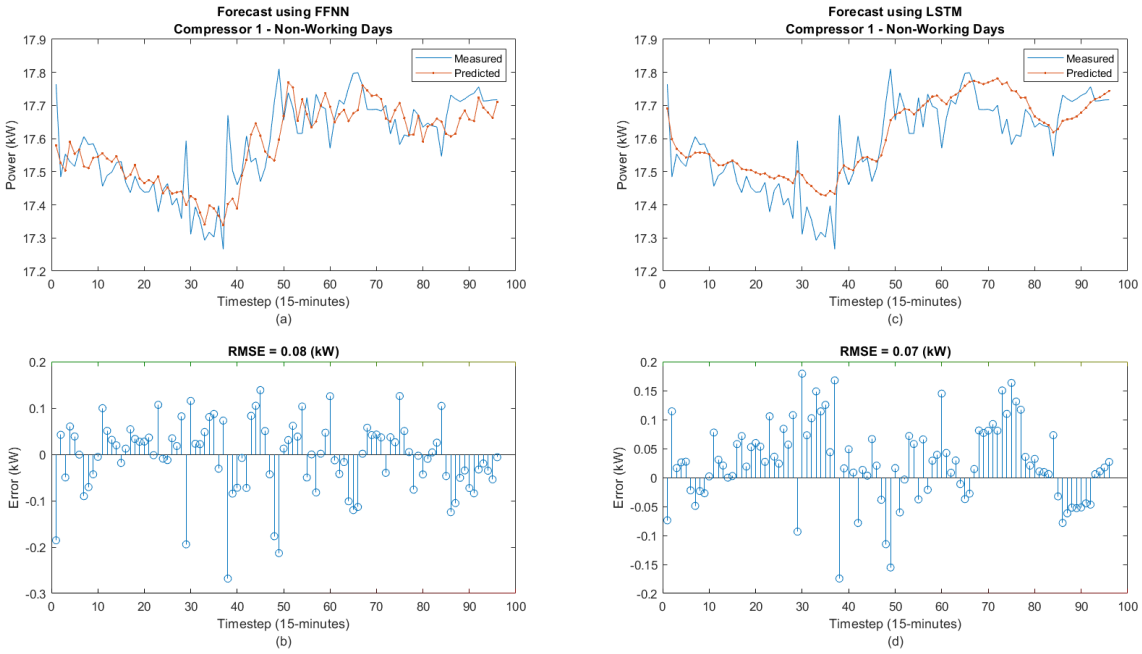

Fig. 2.12. Prediction and measurement and absolute error between them of a non-working day in 15 minutes interval using FFNN and LSTM for Compressor 1.

variables [62]. Nevertheless, both models had a difficulty to catch peak values in the measurement. It was a known issue that also exists in other ANN implementation such as wind power generation forecasting [63].

2.9.2 Power Consumption Forecast for Compressor 2

Figure 2.15 shows the prediction of 96 time-steps for a working day. The RMSE of the FFNN model was 11.25 kW, and the RMSE of the LSTM model was 10.88 kW. For non-working days the numbers are 8.88 kW and 6.65 kW respectively, as shown in Figure 2.16. As illustrated in Figure 2.13 the R^2 values at training stages are 0.87 and 0.85 for the FFNN model and the LSTM model, respectively, for working days. The R^2 values for non-working days are 0.96 for both models as shown in Figure 2.14.

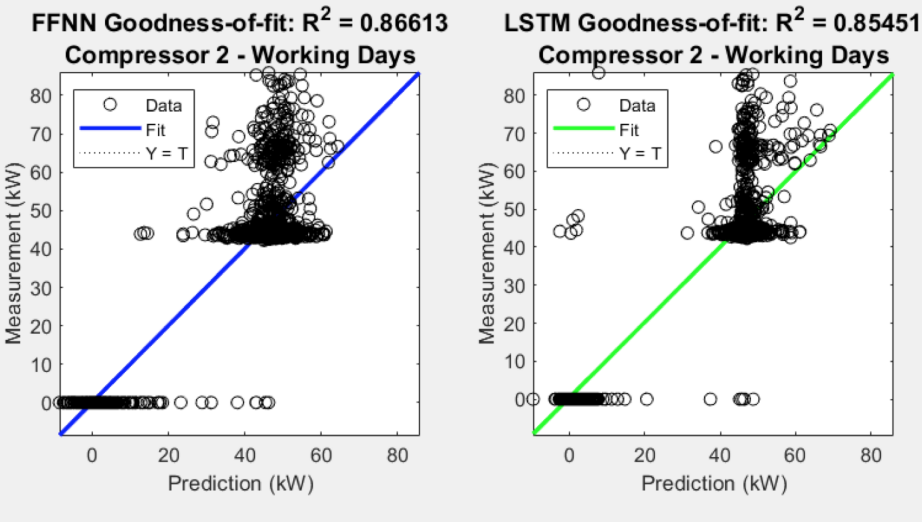

Fig. 2.13. R^2 between measured 15-minute power (kW) and predicted power by the FFNN model and the LSTM model for Compressor 2 in working days.

The results show that the FFNN model gives a better result in terms of the R^2 value at the training stage; however, the LSTM model gives a better RMSE at the prediction stage. Judging from Figure 2.15 and Figure 2.16 we believe that the LSTM

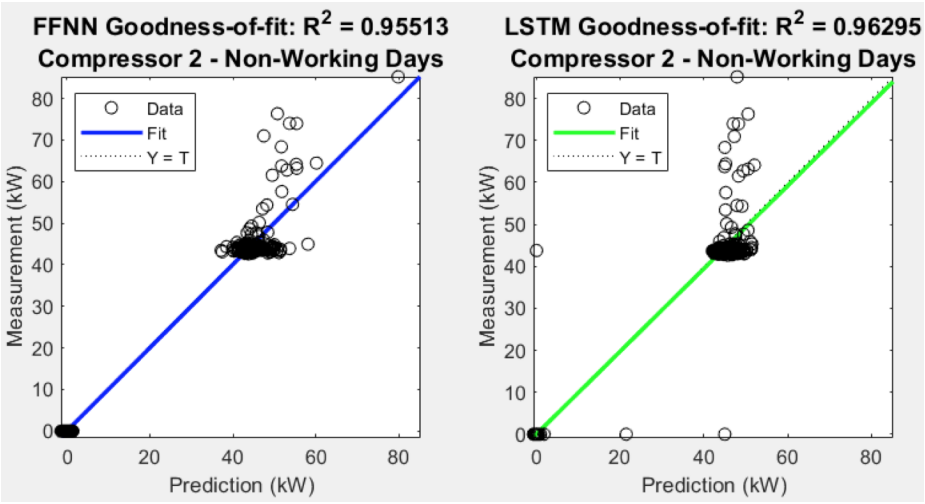

Fig. 2.14. R^2 between measured 15-minute power (kW) and predicted power by the FFNN model and the LSTM model for Compressor 2 in working days.

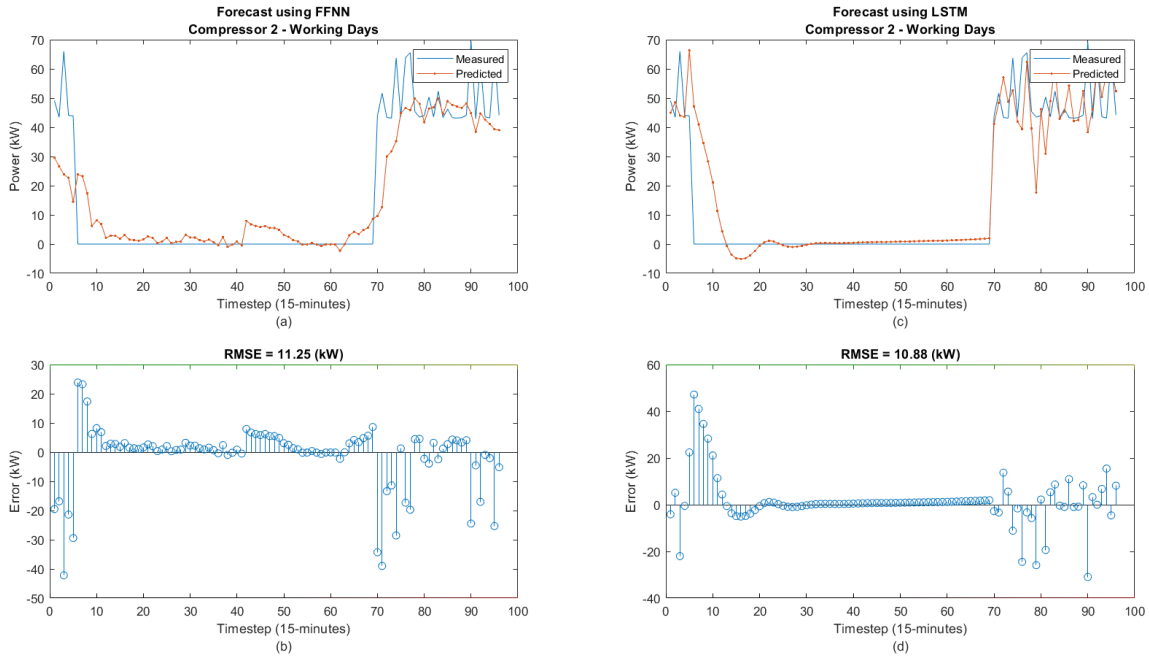

Fig. 2.15. Prediction and measurement and absolute error between them of a working day in 15 minutes interval using FFNN and LSTM for Compressor 2.

model is a better choice in forecasting the load curve of Compressor 2 as the model successfully predicts the shut-down periods as well as several load-unload operations.

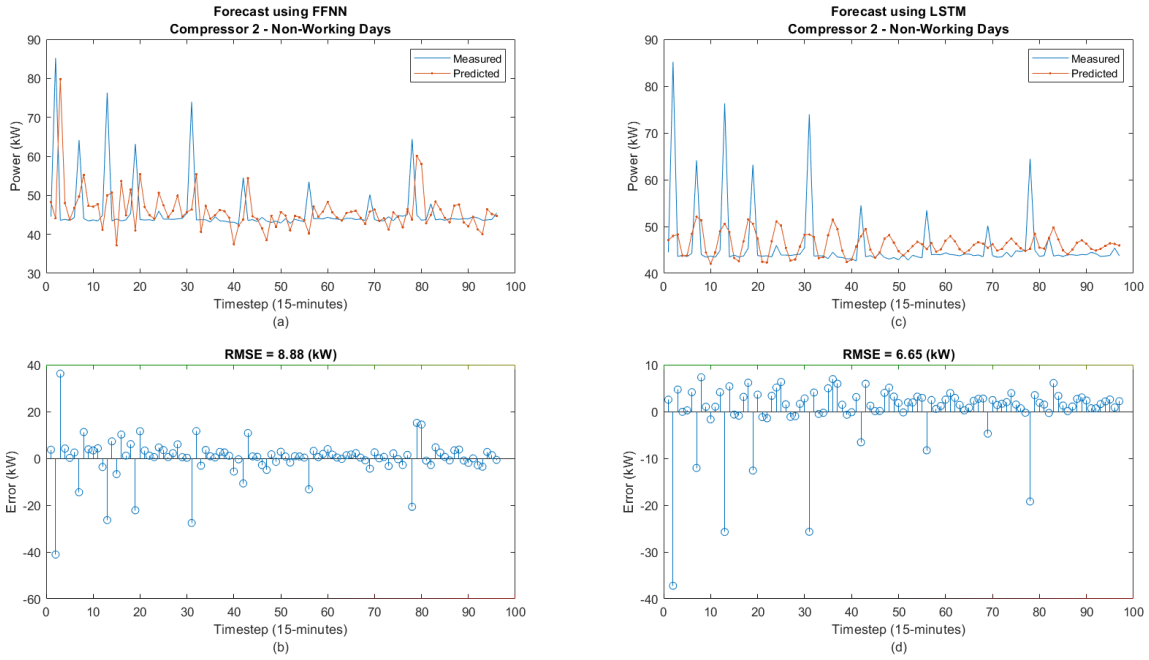

Fig. 2.16. Prediction and measurement and absolute error between them of a non-working day in 15 minutes interval using FFNN and LSTM for Compressor 2.

2.9.3 Power Consumption Forecast for Compressor 3

Because Compressor 3's schedule does not vary significantly, there is no separation between working days and non-working days. LSTM model performs better as its RMSE is 0.32 kW, compared to that of the FFNN models 0.58 kW, as shown in Figure 2.18. Figure 2.17 shows that the FFNN technique does not give a robust prediction model as the R^2 value is 0.27, whereas the LSTM model still has an R^2 value of 0.74, which represents some predictive ability.

Compressor 3 has a control type of on/off dual control, and therefore the measurement is similar to a binary categorical value. In [64] the author investigates the forecasting ability of FFNN with categorical inputs and finds out that the result is not particularly sound. This can be one of the reasons that the FFNN model does not yield an acceptable result in this case. On the other hand, the LSTM model still returns an acceptable result as it can successfully predict the peaks in the load curve.

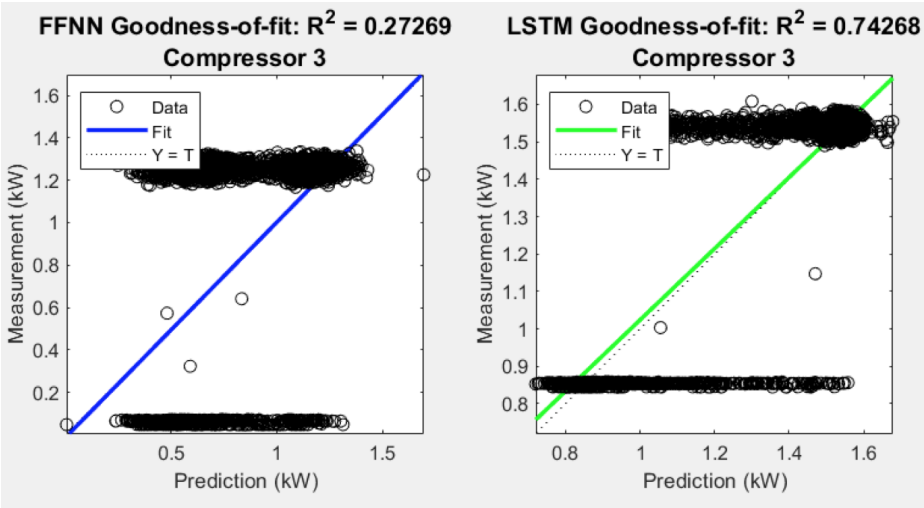

Fig. 2.17. R^2 between measured 15-minute power (kW) and predicted power by the FFNN model and the LSTM model for Compressor 3 in working days.

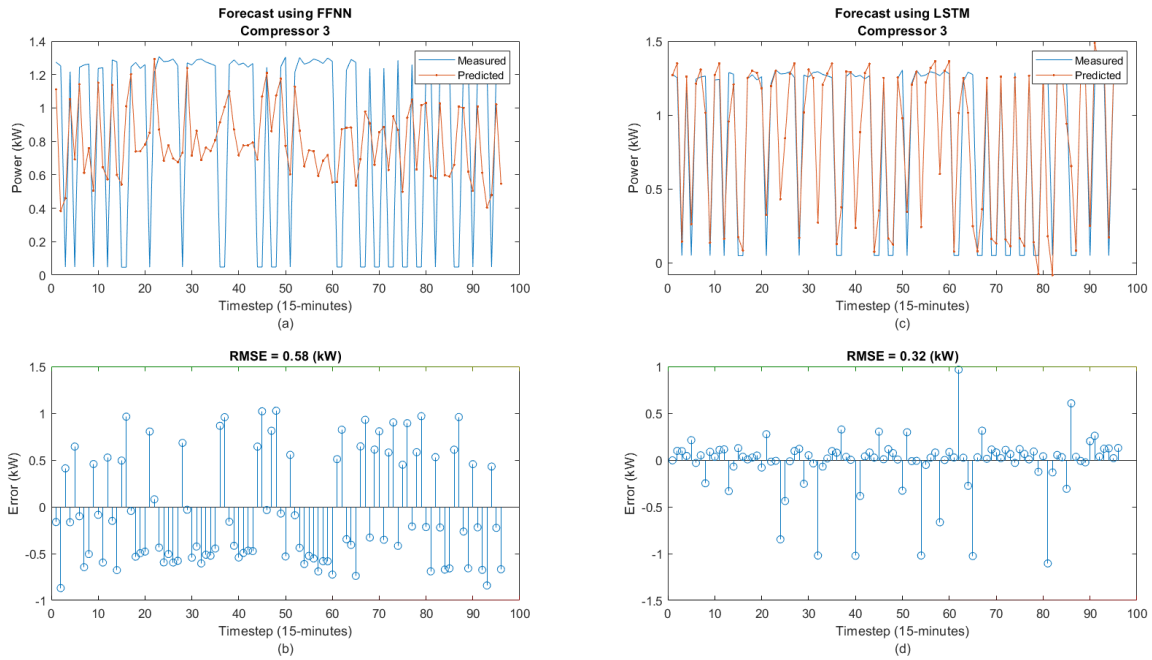

Fig. 2.18. Prediction and measurement and absolute error between them of a working day in 15 minutes interval using FFNN and LSTM for Compressor 3.

Table 2.11 shows the comparison of the RMSE and the R^2 of different types of model in working and non-working mode of the compressor. In summary, both ANN models perform well for Compressor 1 and Compressor 2. For Compressor 3 the FFNN model does not give a good result whereas the LSTM model can predict the load curve well.

Table 2.11.
Comparison of RMSE and R^2.

Model	**Mode**	R^2	**RMSE(kW)**
Compressor 1 (VFD)			
FFNN	Working	0.83	1.41
	Non Working	0.83	1.91
LSTM	Working	0.73	0.08
	Non Working	0.75	0.07
Compressor 2 (loading and unloading with auto shut-down)			
FFNN	Working	0.87	11.25
	Non Working	0.96	10.88
LSTM	Working	0.85	8.88
	Non Working	0.96	6.65
Compressor 3 (on/off dual control)			
FFNN	Working	0.27	0.58
LSTM	Working	0.74	0.32

2.10 Conclusion

There are more opportunities to become more energy efficient as new technologies provides the availability of a big data collection and data mining. In this section, we investigate the capability if an artificial neural network to predict the power consump-

tion of compressors that have different types of control. We use the time of a day, the day of week, the pressure in the compressed air line, the temperature of the air intake, and historical power consumption values to build the forecasting models. The results show that the FFNN model is generally a good technique to forecast a compressors power consumption that utilizes VFD and load-unload control. The LSTM performs better in forecasting the power consumption of a compressor with on/off dual control. Both models have the limitation to give a good prediction for peak operation. The ability to forecast electric power consumption of an air compressor is a huge step towards a successful demand response and smart manufacturing. Not only because air compressors are typical Significant Energy User (SEU) but also because they are an indispensable component in the manufacturing industry. The results of this section prove the practicality of 15 minutes ahead air compressor power consumption prediction which directly indicates that how much air compressors are loaded or their status of operation in the future. The following chapters will provide novel control algorithms to reduce the maximum electrical load for VFD driven air compressors, and more energy saving opportunities for Load/Unload controlled air compressors by using the predicted required compressed air flow rate as input. We did the prediction for power consumption since it has more broad application. The required compressed air flow rate can be calculated by using the compressor's specific power from the spec sheet. The specific power for Compressor 1 is 7.28 $kWmin/m^3$ at 8.27 bar (120 psi). The highest RMSE based on Table 2.11 for Compressor 1 is 1.91 kW which will result in 0.26 m^3/min of error. Compressor 1 full load volume rate of flow is 6.9 m^3/min based on specifications. Therefore, the accuracy of the flow rate prediction was 3.8% by dividing the error of 0.26 m^3/min to the baseline of 6.9 m^3/min. This was good enough for the proposed algorithm in chapter 3. The highest RMSE based on Table 2.11 for Compressor 2 was 11.25 kW. Compressor 2 at full load consumes around 70 kW and at unload mode consumes around 40 kW. With $\pm$11.25 kW as worth case accuracy we can still detect if the compressor is loaded or unloaded. Therefore the accuracy is good enough for the fourth chapter of this study as well.

3. AIR COMPRESSOR SYSTEM MAXIMUM ELECTRICAL LOAD REDUCTION

3.1 Introduction

Electrical peak demand and load profile have been introduced in the introduction chapter. Electrical load changes during the different times in a day. Meeting this load during the high peak is one of the most critical difficulties that utility providers are always facing [65]. In order to meet this demand utilities employ various methods such as utilizing diesel generators [66] and running their old and inefficient plants during the peak load [67]. High peak load increases the power generation cost as well as the necessary capital cost for building that infrastructure both of which can result in a higher carbon footprint [68], increase in transportation and maintenance costs and accelerate the failure of equipment [69]. Therefore peak load reduction has great importance and becoming an influential research field [70]. Peak load reduction can be accomplished both on the supply side and the demand side. On the supply side, to clip the peak load, methods such as direct load control for residential heat pumps [71], developing a behavior driven demand response program [72], Changing electricity prices over time in the wholesale markets based on the load [73] have been developed. While on the user side, to minimize the maximum load several practices namely renewable energy [74], battery energy storage system [75], thermal energy storage system [76] and using intelligent supervision, control and monitoring systems [77] have been considered. As listed below, there are three common techniques for load management which can be applied on the user side [78].

1. **Peak Clipping:** reducing the load during peak periods

2. **Valley Filling:** increasing the load during the off peak load in order to reduce the load during the peak time

3. **Load Shifting:** moving certain loads to off peak time

These practices can be incorporated in different levels. From a high-level management perspective, utilizing all the subsystems by scheduling their operation from a big picture load management point of view [17] have studied. From subsystem point of view, designing and operating subsystems themselves with a flat load curve can minimize or remove their footprint in the load fluctuations. Our approach is a combination of valley filling and load shifting. The goal of this chapter is to employ the ANN prediction from chapter 2 to design and develop a novel control algorithm to reduce the maximum load by a real-time load shifting and valley filling method in the compressed air systems with VFD control. The following section will discuss the basics of the design for the proposed method.

3.2 Basics of Design

The objective of this section is to present comprehensive design details to reduce air compressors maximum load. This algorithm ran the VFD driven air compressors smoothly and prevented compressed air shortage during the peak air demand. This method can be implemented through the primary air compressor control system or by utilizing a central smart factory management system which is shown in Figure 3.1 in order to reduce the load during the peak electrical demands. Smart factory benefits from a central control system which tries to manage the energy usage and optimize the process to maximize the efficiency of each subsystem and the entire factory. Relatively small compressed air demand fluctuations on the user side can initiate other air compressors to kick in and cause higher demand and energy usage. High air demand fluctuation for a single unit air compressor system can cause compressed air shortage and potential failures for the user side.

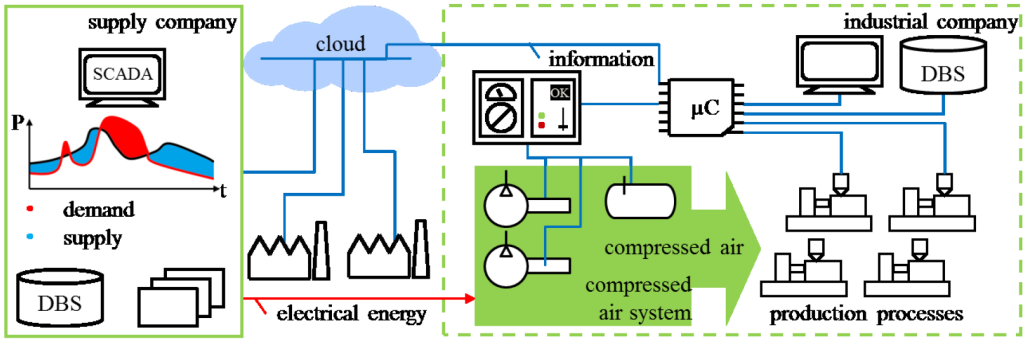

Fig. 3.1. Smart factory [1].

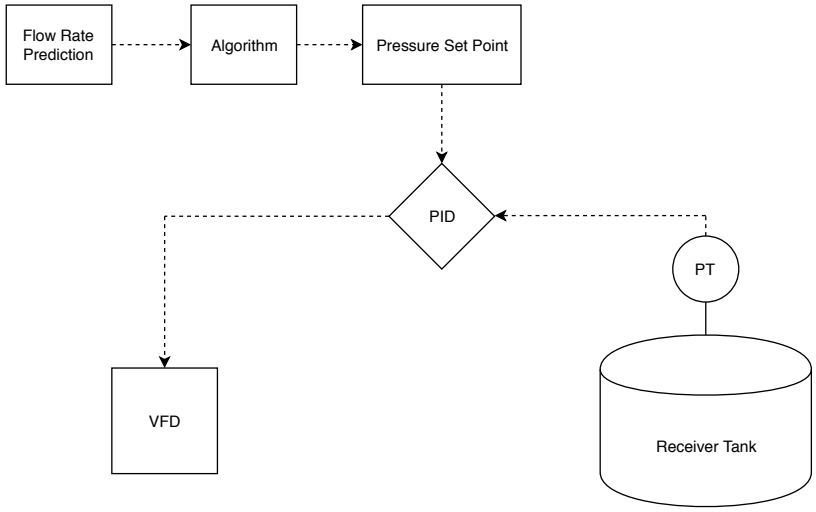

Fig. 3.2. Proposed control schematics.

Figure 3.2 presents the proposed control method. Predicted air compressor behavior is used as an input to the algorithm. Prediction data can be obtained with various methods such as utilizing the historical data to predict the future behavior similar to the second chapter of this study or by modeling the operation and predicting the compressed air flow requirement through a central management scheme for the factory [79]. Furthermore, in a fully automated production line, the pneumatic tools operation schedule is always constant. Therefore the flow rate usage pattern can be used as a feed for the algorithm without any further need for an actual prediction. As mentioned earlier, the VFD is controlled by a PID controller to follow the

pressure set point in the air receiver tank. Most of the air compressors are designed to operate in a wide pressure range, but they always operate at the minimum required line pressure in order to have the minimum energy usage without any respect to the maximum load. This algorithm optimized the set point based on the peak and running situation intelligently in order to reduce the maximum load. This goal was achieved primarily by optimizing the compressed air production with respect to the air compressors specifications and the air receiver tank size.

3.3 Modeling the Air Compressor with Air Receiver Tank

The model shown in this work was generalized in order to be applicable for studying a broad variety of actual systems. We utilized an idealized mathematical method, allowing us to formulate a clear optimization problem. The system includes an energy source which can be electricity or diesel fuel, a compressed air required load, an air reservoir, and a power management system. The power management system controls the flow of compressed air generated by the source. Produced compressed air can be either directly used by the load or saved in the air receiver for later use. The air compressor transforms the fuels energy into the compressed air which is defined by an energy consumption function depending on the generated compressed air $F(Q_g)$, and as a result efficiency to energy usage, both described by equations below.

$$Fuel = F(Q_g(t)) \tag{3.1}$$

$$Efficiency = \eta(t) = \frac{Q_g(t)}{F(Q_g(t))} \tag{3.2}$$

$Q_g(t)$ is the flow rate generated by the compressor at the time t which can be measured in units of cfm or m^3/min. $F(Q_g(t))$ is the fuel consumption function representing the dependency of fuel consumption on the compressed air production rate. This can be a function of various parameters such as compressed air production rate, inlet air temperature, compressor efficiency, motor efficiency and other components

efficiency in the system. The fuel consumption is a function of the compressed air production rate by the source. Higher compressed air production rate requires increased fuel consumption. Therefore, this function is monotonically rising $F'(Q_g(t)) > 0$ and is convex $F''(Q_g(t)) > 0$. The generated air volume at the required pressure is annotated as $V_g(t)$ with a unit of ft^3 or m^3 and can be calculated as below.

$$V_g(t) = \int_0^T Q_g(t)dt \tag{3.3}$$

The total fuel consumed by the air compressor is given by 3.4.

$$F_{total} = \int_0^T F(Q_g(t))dt \tag{3.4}$$

The air compressor load is described only by the flow rate required for users' proper operation. The flow rate profile is defined by $Q_L(t)$ measured in cfm or m^3/min. We assume that the air flow rate consumption is known at any given time in order to avoid the complicated statistical models' effect as presented in the second chapter of this study. The overall generated air volume at the required pressure consumed by the load is given by 3.5.

$$V_L(t) = \int_0^T Q_L(t)dt \tag{3.5}$$

The air receiver is used to store compressed air for later use. Compressed air supplied to the air receiver or discharged from it is indicated by $Q_S(t)$. $Q_S(t)$ is considered positive while compressed air is going into the air receiver, and negative during the time air receiver supplies stored compressed air to the users. The amount of compressed air stored in the air receiver is expressed with $V_S(t)$ measured in ft^3 or m^3 at the required line pressure. We assume that there is no leak or air loss in the air receiver tank therefore the stored air in the air receiver tank can be totally used later. We assume that there is no leak or air loss in the air receiver tank. The amount of stored air can be calculated by 3.6.

$$V_S(t) = \int_0^T Q_S(t)dt \tag{3.6}$$

The air receiver stored air is limited by the air receiver size and the air compressor operating range capabilities which defined as V_{max}. The constraint on air receiver storage is shown by 3.7.

$$0 \leq V_S(t) \leq V_{max} \tag{3.7}$$

In order to calculate V_{max} we assume that air is an ideal gas and we utilize the ideal gas law as expressed below. P is the absolute pressure measured in $Psia$ or Pa, V is the air receiver volume measured in ft^3 or m^3, m is the air mass expressed in lbm or kg, R is the gas constant equal to $1,716\frac{ft.lb}{^\circ R.slug}$ or $287\frac{J}{kgK}$ and T is the temperature measured in $^\circ R$ or K.

$$PV = mRT \tag{3.8}$$

Without manipulating the pressure in the air receiver tank, the amount of mass saved in the air receiver tank can be calculated as below which is the minimum amount of mass for proper operation.

$$m_{min} = \frac{P_{Line}V_{AirReceiver}}{RT} \tag{3.9}$$

By manipulating the pressure in the air receiver tank, the maximum amount of mass saved in the air receiver tank can be calculated as below.

$$m_{max} = \frac{P_{max}V_{AirReceiver}}{RT} \tag{3.10}$$

The temperature is assumed to be constant since the air stored in the air receiver tank is coming form the air dryer. The volume of tank is constant as well. The amount of the stored mass in the tank can be changed only by changing the pressure. Available volume or V_{max} is the volumetric amount of stored mass at the line pressure which can be used for the user side.

$$V_{max} = \frac{(m_{max} - m_{min})RT}{P_{line}} \tag{3.11}$$

3.4 Problem Definition

The goal of this control algorithm is to minimize the electrical peak load to operate the air compressor by utilizing the air receiver tank as a buffer as well as satisfying the required compressed air flow rate for the users. Higher flow rate requires higher electrical energy usage. Therefore, decreasing the maximum required flow rate will directly decrease the maximum electrical load. The air receiver tank capacity with the air compressor operational pressure range constrain the magnitude of the electrical peak load. By utilizing the definitions from the previous sections, the optimization problem can be expressed as below.

$$Minimize \quad (max \quad Q_g(t)) \tag{3.12}$$

$$V_L(t) \leq V_g(t) \leq V_L(t) + V_{max} \tag{3.13}$$

$$Q_g(t) = \frac{d}{dt} V_g(t) \tag{3.14}$$

According to 3.13 the generated compressed air volume should be kept between the bonds. The upper bond is $V_L(t) + V_{max}$ and the lower bond is $V_L(t)$. Equation 3.14 represents that the derivative of the volumetric produced air with respect to the time is equal to the produced compressed air flow rate.

3.5 Analytical Solution

A detailed mathematical solution for the optimization problem above has been studied and solved by Levron et al [80,81]. Based on their results, the created flow rate peak which makes the power peak, is minimized if the produced air at line pressure, $V_g(t)$, takes the smallest route within the generated compressed air volume bound diagram. The curve of the optimal amount of generated compressed air at the line pressure must tangent its bounding limitations. Figure 3.3 presents the statements visually. As it can be seen $V_g(t)$ has taken the smallest distance between point A and B. The optimal solution for the generated flow rate reduction does not depend on the fuel cost function $F(Q_g(t))$. However, the fuel cost function can reduce or increase

the total energy consumption with this algorithm depending on the driving method of the compressor. Majority of air compressors are either driven by diesel engines or electric motors. Diesel engines are more energy efficient at lower RPMs. Therefore, the proposed algorithm will consume less fuel. Electrical motors are more energy efficient at higher RPMs. Therefore, the proposed algorithm will consume slightly higher electricity.

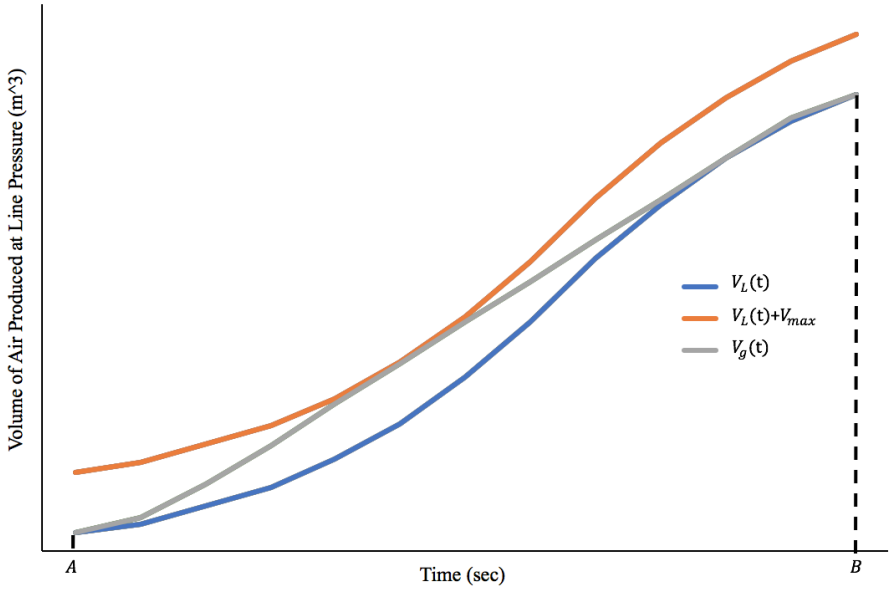

Fig. 3.3. Optimal generated compressed air path [80].

Levron et al have solved this optimization problem mathematically. In order to do this optimization in real time, we need to solve it numerically. The following section will solve the optimization problem numerically and will compare the results with the analytical solution presented in this section to prove the credibility of the outcome.

3.6 Numerical Solution

Figure 3.4 provides an overview of the numerical algorithm flowchart that has been utilized to solve the optimization problem. This algorithm first receives the flow rate data for 15 data points which are the future predicted flow rate load for the air

compressor ($Q_L(t)$) and calculated V_{max} from Equation 3.11 as an input. Then it calculates the generated compressed air volume by using the Equation 3.15. Needless to say $Q_L(t)$ units should be chosen carefully in order to use Equation 3.15. For instance, if the algorithm is used on a minute basis, the chosen unit should be per minute such as m^3/min.

$$V_L(t) = \sum_{t=1}^{t} Q_L(t) \tag{3.15}$$

Then we will fit a degree 8 polynomial equation in a least-square sense. We chose degree 8 since it fitted the best to our data points. Eight is achieved merely by trial and error process. One can follow the same process with different polynomial degrees. The criteria is having the best-fitted line. The outcome will represent the $V_L(t)$ as an equation to feed into our optimization iteration process. We chose 15 data points as input by assuming 15 minutes ahead prediction. Therefore, we will have the following relations for the curve fitting outcome.

$$t = \Big[1 : 15\Big] \tag{3.16}$$

$$V_L(t) = a_1 t^8 + a_2 t^7 + a_3 t^6 + a_4 t^5 + a_5 t^4 + a_6 t^3 + a_7 t^2 + a_8 t + a_9 \tag{3.17}$$

$$\text{coefficient values} = \Big[a_1 \quad a_2 \quad a_3 \quad a_4 \quad a_5 \quad a_6 \quad a_7 \quad a_8 \quad a_9\Big] \tag{3.18}$$

The aforementioned optimization problem can be categorized as a minimax problem since the goal is to minimize the maximum $Q_g(t)$. The whole algorithm has developed in MATLAB therefore we used fminimax function in order to solve this problem. The procedure for fminimax is using Newtons method [82] in order to minimize the possible loss for a worst case (maximum loss) which in our case is the maximum $Q_g(t)$ [83]. The detailed general fminimax function is as below.

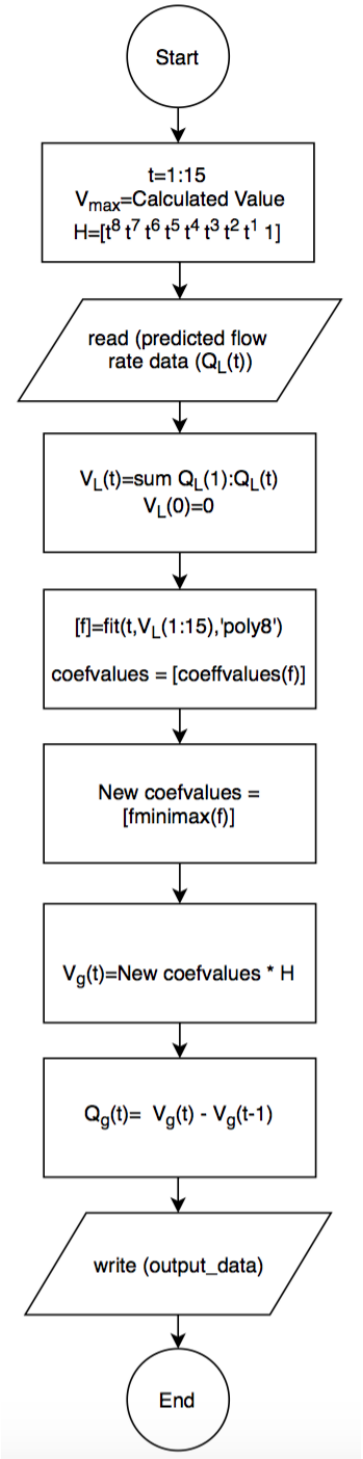

Fig. 3.4. Optimal generated compressed air path algorithm.

$$\min_{x} \max_{i} \quad F_i(x) \quad \text{such that} \quad \begin{matrix} c(x) \leq 0 \\ ceq(x) = 0 \\ A.x \leq b \\ Aeq.x = beq \\ lb \leq x \leq ub \end{matrix} \tag{3.19}$$

Where b, A, Aeq, beq, lb and ub are defining the boundary, $c(x)$ and $ceq(x)$ are functions that define desired $F_i(x)$ value [84]. This general function needs to be modified in order to solve our problem. The goal is to find the optimum coefficient values in order to formulate the $V_g(t)$ curve on Figure 3.3 by using an equation similar to Equation 3.17. The modified fminimax is formulated as below.

$$A = \begin{bmatrix} 1^8 & 1^7 & 1^6 & 1^5 & 1^4 & 1^3 & 1^2 & 1^1 & 1 \\ 2^8 & 2^7 & 2^6 & 2^5 & 2^4 & 2^3 & 2^2 & 2^1 & 1 \\ 3^8 & 3^7 & 3^6 & 3^5 & 3^4 & 3^3 & 3^2 & 3^1 & 1 \\ \vdots & \vdots & \vdots & \vdots & \vdots & \vdots & \vdots & \vdots & \vdots \\ 14^8 & 14^7 & 14^6 & 14^5 & 14^4 & 14^3 & 14^2 & 14^1 & 1 \\ 15^8 & 15^7 & 15^6 & 15^5 & 15^4 & 15^3 & 15^2 & 15^1 & 1 \end{bmatrix} \tag{3.20}$$

$$b = \begin{bmatrix} V_L(1) & V_L(2) + V_{max} & V_L(3) + V_{max} & \cdots & V_L(14) + V_{max} & V_L(15) \end{bmatrix} \tag{3.21}$$

$$x = \begin{bmatrix} a_1 \\ a_2 \\ a_3 \\ a_4 \\ a_5 \\ a_6 \\ a_7 \\ a_8 \\ a_9 \end{bmatrix} \tag{3.22}$$

$$\min_{x} \max_{t} \quad (Q_g)_t(x) \quad \text{such that} \quad \begin{matrix} V_L(t) - V_g(t) \leq 0 \\ V_g(t-1) - V_g(t) < 0 \\ V_g(t) = A.x \\ A.x \leq b \end{matrix} \tag{3.23}$$

Where $Ax \leq b$ is defining the upper boundary. In the b matrix the first and last element is kept as $V_L(1)$ and $V_L(15)$ since the generated compressed air volume needs to be same as the required load. $V_L(t) - V_g(t) \leq 0$ assures that the generated air is always equal or above the required compressed air volume. $V_g(t-1) - V_g(t) < 0$ guarantees that the $\frac{dV_g(t)}{dt} > 0$ considering it is impossible for the system to produce negative $Q_g(t)$. The whole algorithm has been coded in MATLAB. The written algorithm is generic and can be adopted for similar applications. Figure 3.4 presents the flowchart for the algorithm. We used a set of random data in order to evaluate what would be this numerical solution outcome and compare it with the mathematical solution as our proved reference. Figure 3.5 and 3.6 show the results. The storage is chosen $7m^3$ for the sake of demonstration. Figure 3.5 follows the exact optimum route given in the mathematical solution section and Figure 3.3. The created flow rate peak which makes the power peak is minimized in Figure 3.6 by taking the smallest route within the generated compressed air volume band in Figure 3.5. The curve of the optimal amount of generated compressed air at the line pressure is tangent to its bounding limitations in Figure 3.5.

After calculating the optimum compressed air generation rate for each minute, the system setpoint needs to be calculated in order to feed the PID controller to take action and run the system. The following section will provide the detailed calculation.

3.7 Setpoint Calculation

Calculating the setpoint at each minute and modifying method plays a pivotal role in the success of this algorithm. A simple mathematical method is adopted to obtain the setpoint based on the calculated optimum generated flow rate. $V_L(t)$ is the

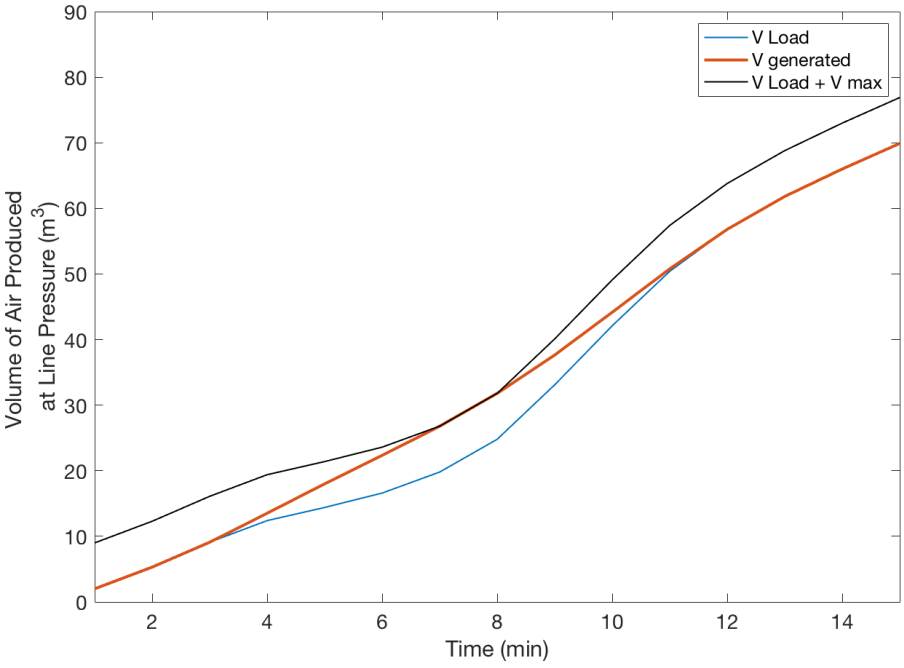

Fig. 3.5. Optimal generated volumetric compressed air path.

generated compressed air at the line pressure meaning that if we operate the system at the constant setpoint P_{line} (required line pressure), blue line on the Figure 3.5 will be the consequence. $V_L(t)+V_{max}$ is the generated compressed air at the maximum air compressor system operatable pressure P_{max} which is higher than the line pressure meaning that if we operate the system at the maximum setpoint, black line on the Figure 3.5 will be the outcome. Nevertheless operating at the maximum pressure does not mean increasing the line pressure since there is a pressure regulator valve after the air receiver tank setting at the line pressure. As Figure 3.7 shows, the additional V_{max} is stored in the air receiver tank causing the pressure inside of the tank to be higher than the line pressure. By using Equation 3.9-3.11 and considering $R, T, V_{AirReceiver}$ constant, it is clear that $V_{max} = \alpha(P_{max} - P_{line})$ where α is a constant. Similarly we can say $V_g(t) - V_L(t) = \alpha(P_g(t) - P_{line})$. Hence, the following equation can be achieved.

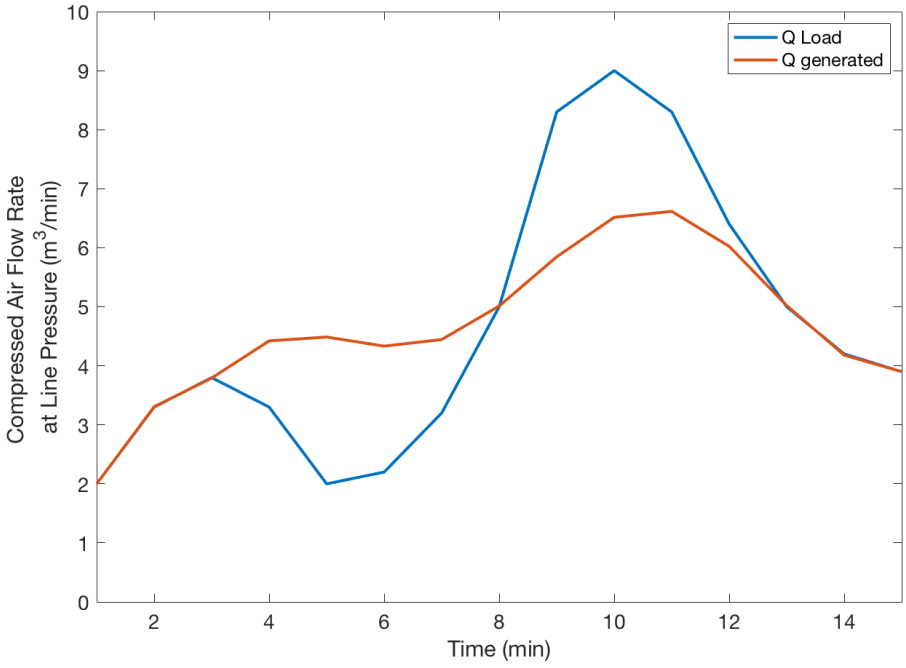

Fig. 3.6. Optimal generated compressed air flow rate path.

$$\frac{P_g(t) - P_{line}}{P_{max} - P_{line}} = \frac{V_g(t) - V_L(t)}{V_{max}} \tag{3.24}$$

Where $P_g(t)$ is the setpoint for $V_g(t)$. Therefore, $P_g(t)$ can be calculated as below.

$$P_g(t) = P_{line} + \frac{V_g(t) - V_L(t)}{V_{max}}(P_{max} - P_{line}) \tag{3.25}$$

It worth mentioning that the setpoint increase should be applied each minute slowly in order to prevent any overshoot in the PID control. The proposed algorithm has been studied in a real case scenario. The following section will present the results of this study as well as calculating the system power consumption and showing the cost-saving opportunities.

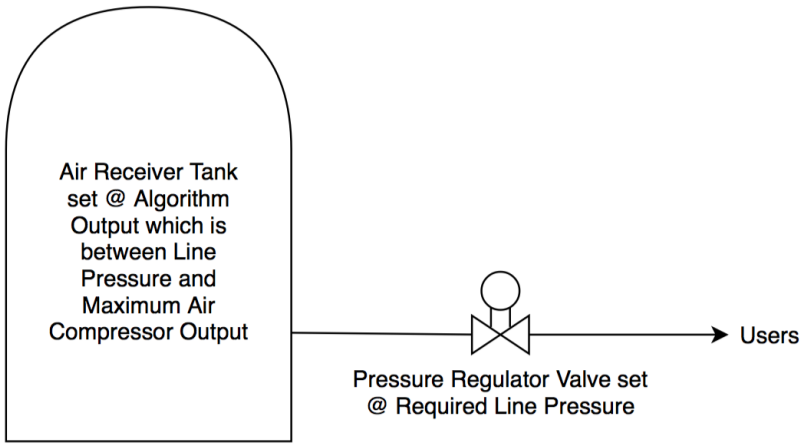

Fig. 3.7. Air receiver and pressure regulator valve.

3.8 Case Study

Our case study is located in a $50,000 ft^2$ facility which does electroplating and surface finishing for different products as presented in section 2.4.1. Overall, the system is composed of: a 50 HP rotary screw compressor, a filter, an air dryer, and an air receiver. The control logic is to maintain the air receiver tank pressure at 8.27 bar (120 psi) which is considered as the line pressure. A PID controller is utilized to implement this logic by driving the VFD. Figure 2.3 shows the described system. Another 50 HP lubricated rotary screw compressor with capacity control is installed as a backup. Figure 3.8 shows the backup air compressor system. This system system automatically starts running during the high air demand if the main compressor cannot keep the line pressure. Flow rate data and line pressure have been obtained through the human-machine interface (HMI). In this case study, the proposed algorithm was applied to this system. The case study is divided into two sections. The first section discusses the maximum electrical load reduction by using this algorithm. The second section introduces how this algorithm can be utilized to save operation cost.

Fig. 3.8. 50 HP backup air compressor.

3.8.1 Maximum Electrical Load Reduction

The effect of the algorithm on the maximum electrical load was studied in this section. In order to utilize the algorithm, V_{max} was calculated 1.76 m^3 by using the data presented in Table 3.1 and Equation 3.11. P_{max} is from the air compressor spec sheets. T is the measured temperature after the air dryer. R is the specific R value from thermodynamic tables for dry air. m_{min} and m_{max} are calculated by Equation 3.9 and 3.10.

The algorithm has been implemented on the real data logged from the air compressor. Figure 3.9 and 3.13 shows the algorithm effect on the flow rate for two different logged data in different time frames. The air compressor power consumption was calculated by using the Compressed Air and Gas Institute (CAGI) [85] measured performance data. Table 3.2 presents this data. A line with R^2 of 0.9963 is fitted to this data in order to use the interpolation technique to calculated the power consumption for the points in between. It is crystal clear that the algorithm output completely depends on the input. For data set I the algorithm flow rate output can be seen in Figure 3.10. Figure 3.11 represents the manipulated setpoint. The air compressor

Table 3.1.
50 HP air compressor system specifications.

Parameter	**Value**	**Units**
m_{max}	49.65	kg
m_{min}	31.36	kg
P_{max}	13.1	bar
P_{line}	8.27	bar
$V_{AirReceiver}$	3.02	m^3
R	287	$\frac{J}{kgK}$
T	300	K

power consumption for for data set I can be seen in Figure 3.12. Overall for data set I the maximum flow rate has been reduced 0.88 m^3/min causing maximum electrical load reduction of 2 kW and energy usage increase of 0.93 kWh. The air compressor power consumption for for data set II can be seen in Figure 3.13. Overall for data set II the maximum flow rate has been reduced 1.63 m^3/min causing maximum electrical load reduction of 3.5 kW and energy usage increase of 0.94 kWh.

Table 3.2.
50 HP air compressor performance [85].

psig	**kW/100 cfm**	**bar(g)**	**kW min/m^3**
100	19.1	6.89	6.745
125	21	8.27	7.416
190	25.9	13.1	9.146

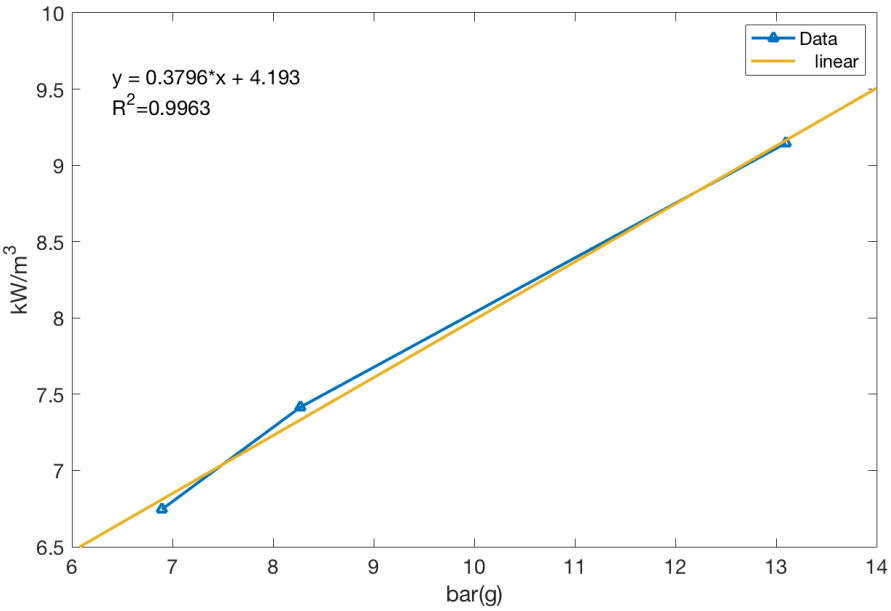

Fig. 3.9. 50 HP air compressor performance [85].

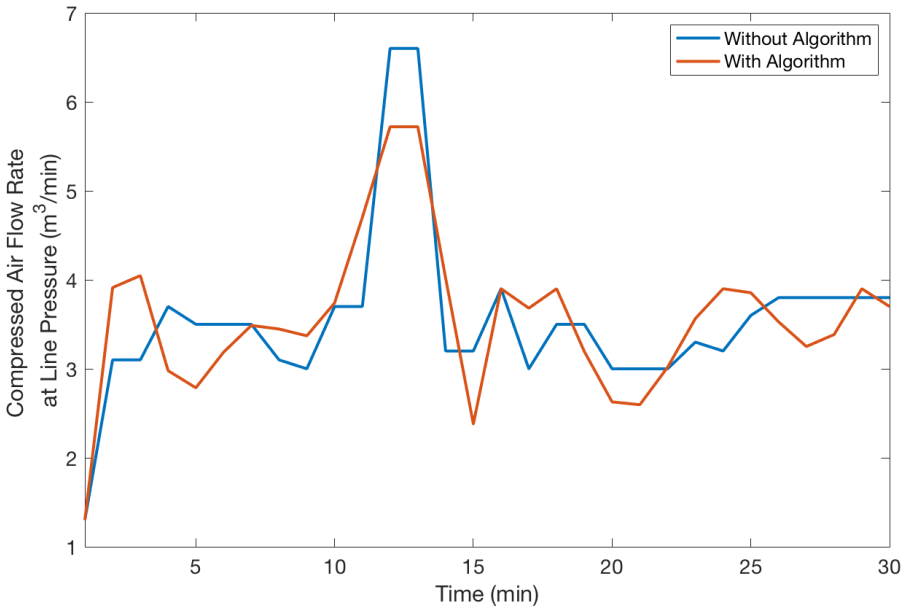

Fig. 3.10. Optimal generated volumetric compressed air flow rate (Set I).

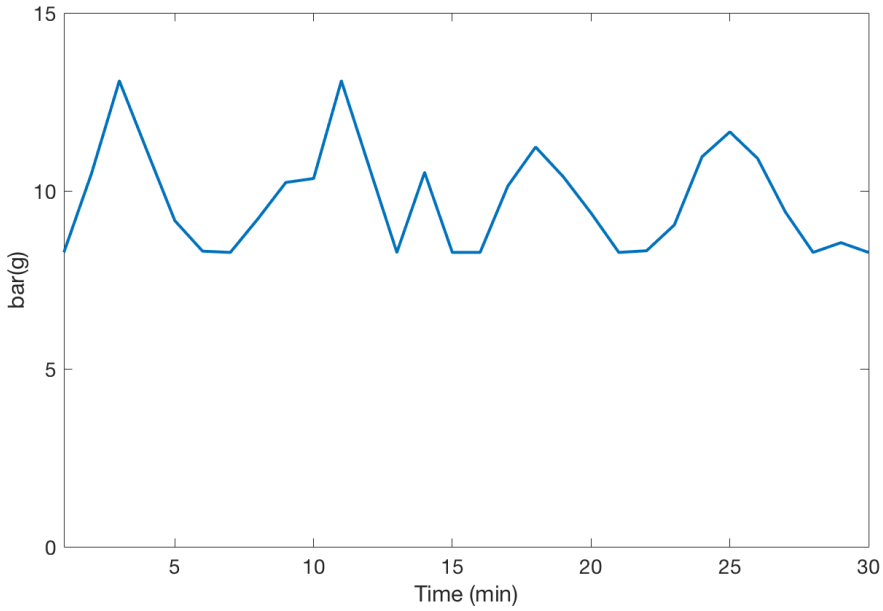

Fig. 3.11. Setpoint manipulation for optimal generated flow rate (Set I).

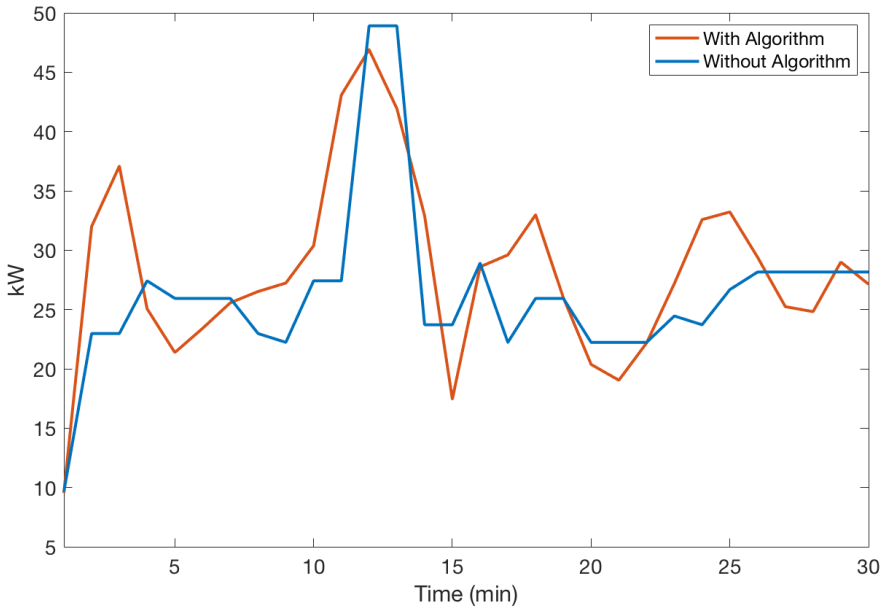

Fig. 3.12. Optimal generated compressed air flow power consumption (Set I).

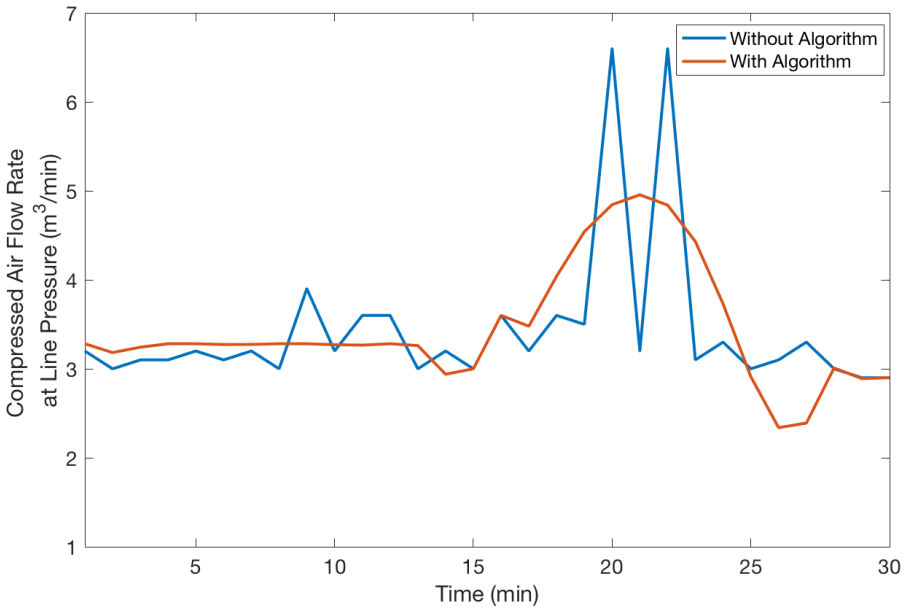

Fig. 3.13. Optimal generated volumetric compressed air flow rate (Set II).

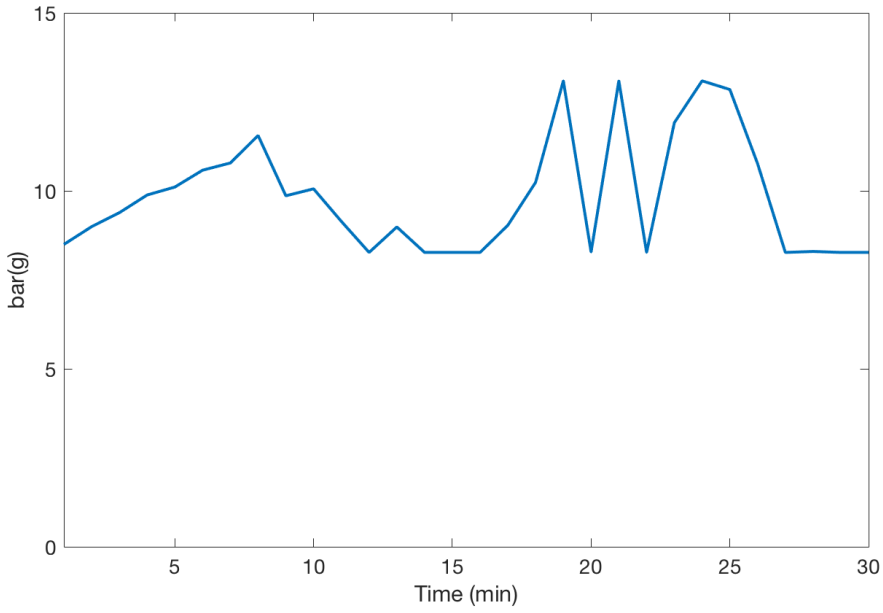

Fig. 3.14. Setpoint manipulation for optimal generated flow rate (Set II).

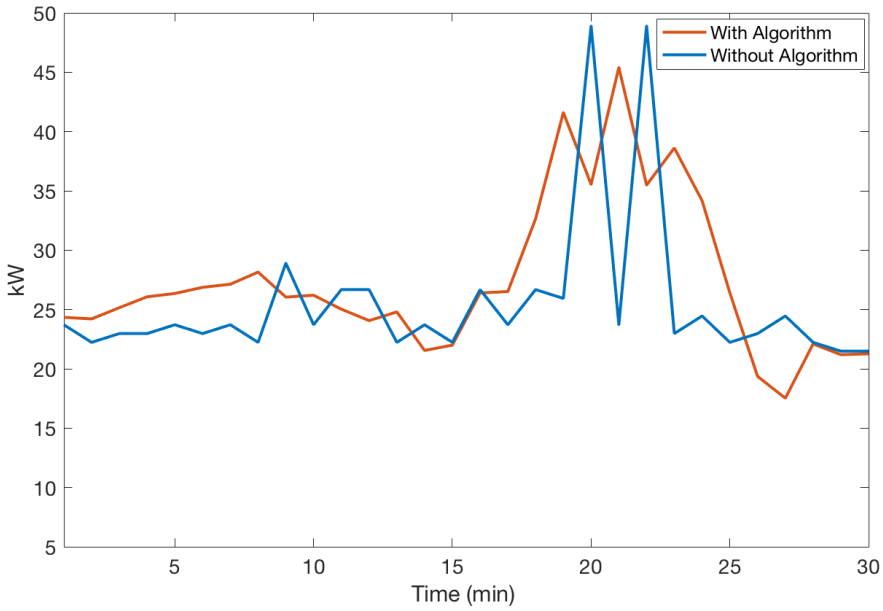

Fig. 3.15. Optimal generated compressed air flow power consumption (Set II).

3.8.2 Operation Cost Reduction

It is very common among manufacturing facilities to use backup air compressor during the peak air demand. In most of the cases, it is due to the expanding the factory or changing the equipment after the air compressor system designed. There are a handful of cases that this demand is slightly higher than main air compressor maximum output. In these cases, the proposed algorithm can prevent the backup compressor from kicking in and save energy and reduce electrical load. As mentioned previously, the studied facility is one of these cases. Based on the logged data, there are time periods that the required air flow rate is 6.864 m^3/min which is 0.064 m^3/min higher than the maximum air compressor output. This slightly high demand is causing the air receiver pressure to drop to 7.33 bar. After this point, the backup 50 HP air compressor will start running at the minimum output which is 0.264 m^3/min.

By utilizing this algorithm, the primary air compressor system can store more air in the air receiver tank and prevent the backup air compressor running by using this

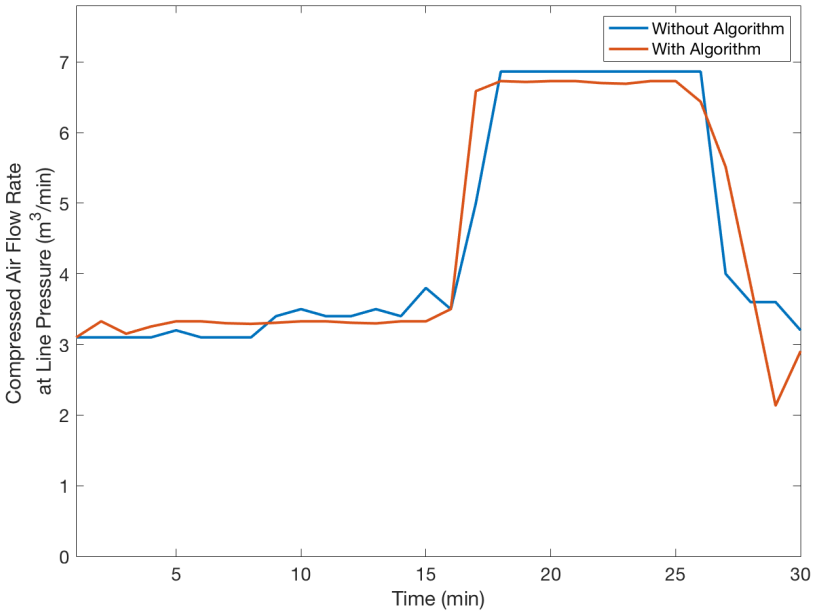

Fig. 3.16. Optimal generated volumetric compressed air flow rate (Set III).

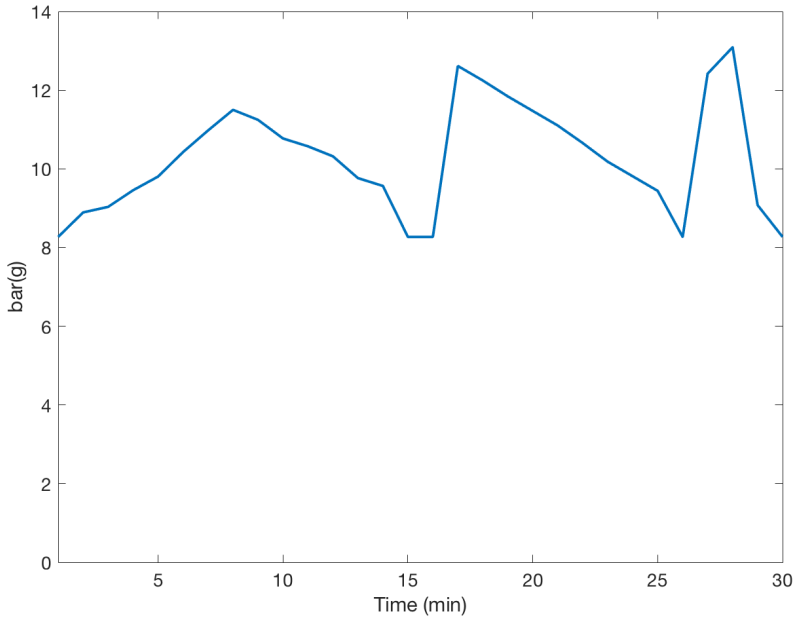

Fig. 3.17. Setpoint manipulation for optimal generated flow rate (Set III).

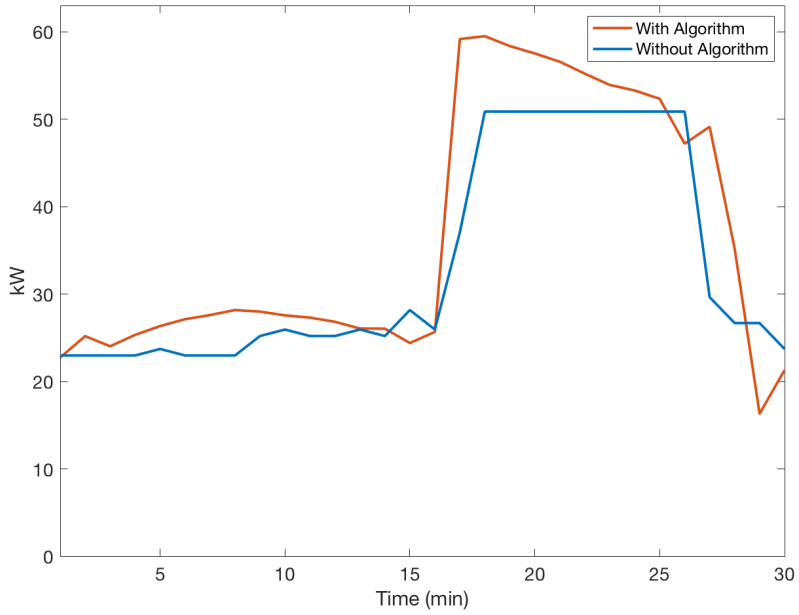

Fig. 3.18. Optimal generated compressed air flow power consumption (Set III).

stored air. Figures 3.16-18 represent one of these scenarios. Based on the specifications the minimum required power for the backup air compressor is 15.6 kW. The power consumption increase by this algorithm for the main air compressor was 8.23 kW. Therefore, the maximum load decreased 7.37 kW by preventing the backup air compressor from kicking in. Regarding energy consumption, the main air compressor consumed 1.67 kWh more while the backup system without this algorithm consumed 2.34 kWh. Consequently, this method decreased the energy usage for this 30 *minute* period by 0.67 kWh.

3.9 Conclusion and Discussion

Maximum load reduction is one of design improvement goals for every system. Moving forward to the off-grid manufacturing factories by using renewable energy these studies become more valuable. A novel control method for VFD driven air compressor system introduced. The input for this method can be from the predicted

data by using the statistical and machine learning algorithms or from a perfect model for the factory. The optimization algorithm validated numerically and mathematically. By applying this algorithm to the data and performance measured from a real air compressor system, the maximum peak load is successfully reduced. The amount of the reduction depends on the air compressor demand curve at the line pressure and air compressor specifications. This method assures that the production line will not starve during the peak compressed air demand by running the system smoothly as well as reducing the maximum electrical peak load. Figure 3.13 represents this difference. This method can also prevent secondary or backup air compressors from kicking in during slightly higher loads than running air compressor's output resulting in more maximum load reduction and energy saving. Table 3.3 presents the summary of the results of applying the proposed algorithm to the different datasets. The maximum electrical load has decreased in all the data sets. Energy is consumed slightly higher for dataset I and II due to setpoint increase. For dataset III we had energy saving by preventing the backup system from running during the peak compressed air demand.

Table 3.3.
Summary of the results after applying the algorithm.

Dataset	**Maximum Flow Rate Reduction** m^3/min	**Maximum Electrical Load Reduction** kW	**Energy Usage Increase** kWh
I	0.88	2	0.93
II	1.63	3.5	0.94
III	0.264	7.36	-0.67

4. NOVEL LOAD UNLOAD CONTROL METHOD FOR MAXIMIZING ENERGY SAVING

4.1 Introduction

Compressed air is one of the most costly utilities in industrial plants. In the United States and the European Union, air compressor system is responsible for around 10% of the electricity consumed in industry [86, 87]. Life cycle cost analysis on this system shows that the capital investment and maintenance costs account for a small portion in comparison with energy costs for operation. In many studies, the operation cost is more than 500% of the capital cost [88, 89]. Air compressor control method as well as appropriate system sizing play pivotal roles in annual pumping costs [13,90]. Therefore, this study is focused on developing a novel control method in order to reduce the energy consumption of the air compressor systems controlled with load/unload method. Chapter 1 described the air compressor system and conventional control methods that are utilized in the industry worldwide. This chapter will start with a comprehensive review of the methods and practices which have been identified to make these systems more energy efficient. Later it will introduce the issue with current load/unload control methods with proposing a new method in order to solve it. In the end, the results of applying this novel method in a real case study will be presented.

4.2 Energy Saving Practices for Air Compressor System

Compressed air systems can reach 20% to 50% energy savings by improving the system [91]. The current improvements are listed as below with a brief description [91–93].

- Eliminating inappropriate uses of compressed air: Using more economical energy sources for possible applications to minimize compressed air usage.
- Minimizing compressed air system leaks: Air leaks can be considered as a significant energy waste for this system. Leak detection practices can save energy and operation cost.
- Utilizing outside air for air intake: Reducing the inlet air temperature reduces energy used by the compressor since compressor has to do less work.
- Minimizing pressure drop and controlling system pressure: Performing regular maintenance and controlling system pressure, as well as proper system design, can prevent additional pressure drops which can increase the unnecessary load on the air compressor.
- Utilizing pressure/flow controller after air receiver: As air receiver pressure rises, the intermediate control throttles the outflow of air and prevents downstream pressure increase. Therefore, artificial demand is prevented.
- Using more efficient compressed air users: This practice can save more by reducing the air compressor load. utilizing more efficient nozzles is a common type of this practice.
- Heat recovery: More than 80% of the energy used in air compressor systems is converted to heat. A proper heat recovery practice can use this energy for useful works such as space heating, industrial process heating, water heating, makeup, air heating, and boiler makeup water preheating [10].
- Keeping the compressor and intercooling surfaces clean: This practice can prevent corrosion of the piping system, controls, instruments and tools which can reduce the maintenance cost and energy usage.

In addition to the items above, optimizing compressed air system control strategy can save a considerable amount of energy. Controls serve to regulate the amount

of compressed air being produced. Depending on the load profile various control methods have been developed. Variable speed drive (VSD) and fixed speed drive (FSD) or load/unload control methods are the most common type of control systems. VSD is recommended for a dynamic load with high fluctuations. On the other hand, FSD is more efficient for a full load operation. Figure 4.1 presents the efficiency comparison between VSD and FSD [94].

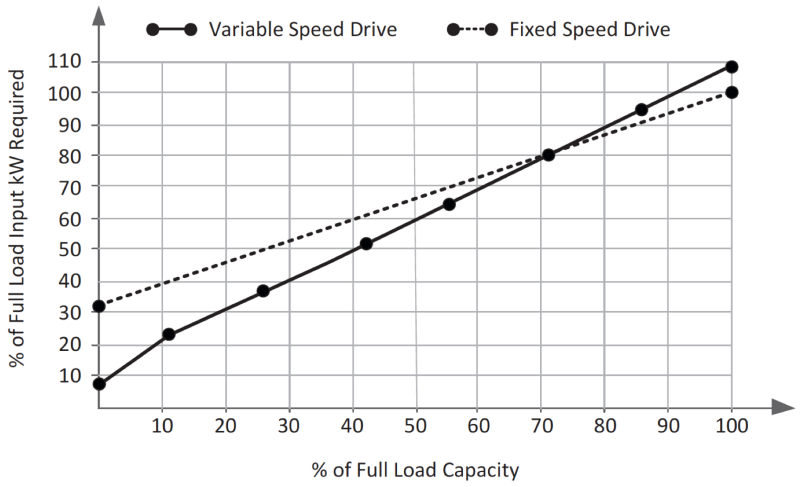

Fig. 4.1. Energy efficiency comparison of VSD and FSD compressors [94].

The type of compressor control and the relationship between the compressors output capacity and the compressed air demand in the plant can determine the drawn power characteristics. Different type of control methods and their power characteristics have been studied in [95]. Figure 4.2 provides a general comparison between different air compressor control types. Where FP(Fraction Full-Load Power) is actual compressor power) over full-load compressor power and FC(Fraction Rated Capacity) is actual compressed air output over full-load compressor output capacity). Depending on the load profile switching from one control method to another or a combination can run the system more energy efficient. Schmidt and Kissock investigated the energy savings by switching from inlet modulation control to load/unload with and without auto shutoff control for a rotary compressor [93]. The results show signifi-

cant saving by switching to load/unload with auto shutoff. This section will propose a novel load/unload control method to maximize the energy savings.

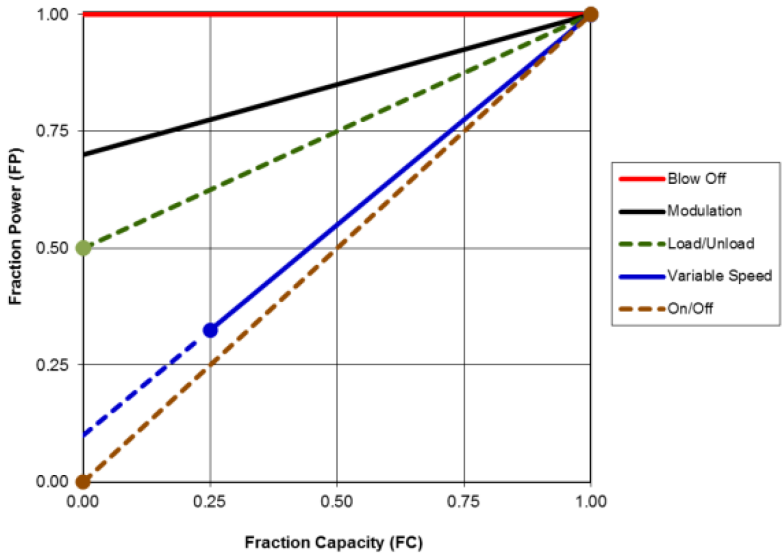

Fig. 4.2. FP vs FC for common compressor control types [96].

4.3 Problem Definition

Electrical motors are more energy efficient during the full load operation. As Figure 4.3 shows, switching from inlet modulation to load/unload with auto shutoff can have major energy reduction. The auto shutoff system basically will shut down the motor after running unloaded for more than certain period of time. Normally there are certain number of times recommended by the motor manufacturer in order to auto shutoff the system during a certain time period. There is no intelligence about when to shut down the compressor. There is a high possibility of turning the system back on after a minute for a small load and again run the system for a while unloaded till the next shutdown. As a matter of fact this can waste energy and decrease the system efficiency. This problem can be solved by introducing a novel control method. Two different control methods are introduced in order to solve this

issue. First one is more advanced level, requiring prediction algorithms resulting in more energy savings. The second method is more straightforward and doesn't require prediction. The following section will introduce the proposed design.

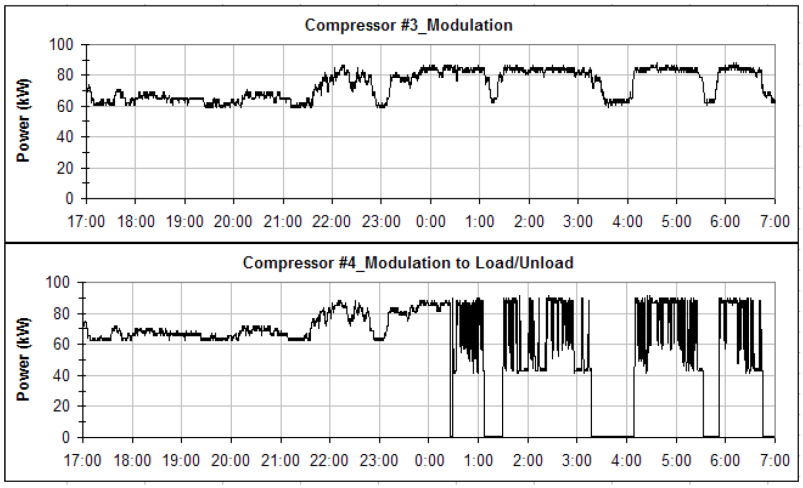

Fig. 4.3. Comparison of compressor power draw between modulation control and load/unload with auto shut-off. [93].

4.4 Basics of Design

Figure 4.4 shows the traditional load/unload control method schematics. In this method, the motor is always on. An inlet valve for the compressor controls the load on the motor. During the loaded period, the valve is open and will increase the load on the motor resulting in higher current drainage from the grid. During the unloaded period, the valve is closed and will reduce the system energy usage. The control signal to the valve is coming from pressure switches which controlling the pressure inside the air receiver by sensing the pressure with a pressure transducer. The pressure switches are set at two set pressures. The low-level pressure switch is set at the line the pressure same as the pressure regulator valve. Whenever the pressure goes below this point, the air compressor is loaded. The high-level pressure switch is set at the line plus 10 or 20 psig (0.68 bar(g) to 1.38 bar(g)) to compress more air inside the

tank for usage. Whenever the pressure goes above this point, the air compressor is unloaded.

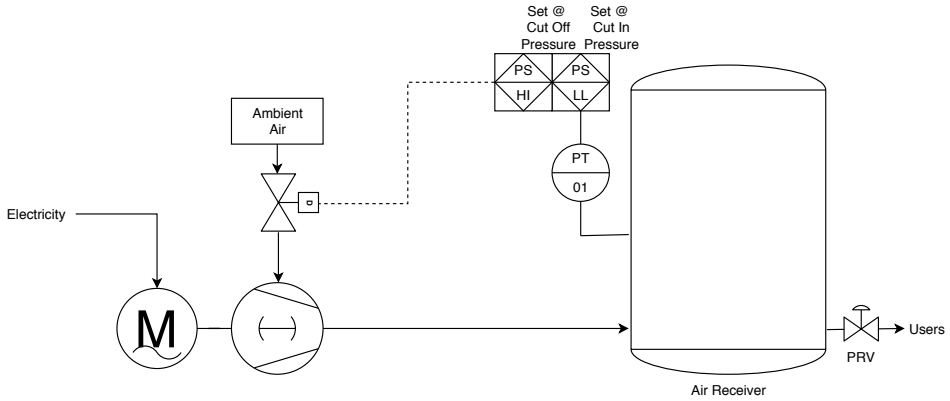

Fig. 4.4. Load/Unload control schematics without auto shutoff.

Figure 4.5 presents the control schematics for the load/unload control method with auto shutoff. Auto shutoff is introduced to the system to increase the efficiency of this method. Basically the system will turn off if it is unloaded for more than a certain period of time by taking into account the maximum allowable on/off for the electrical motor during this period.

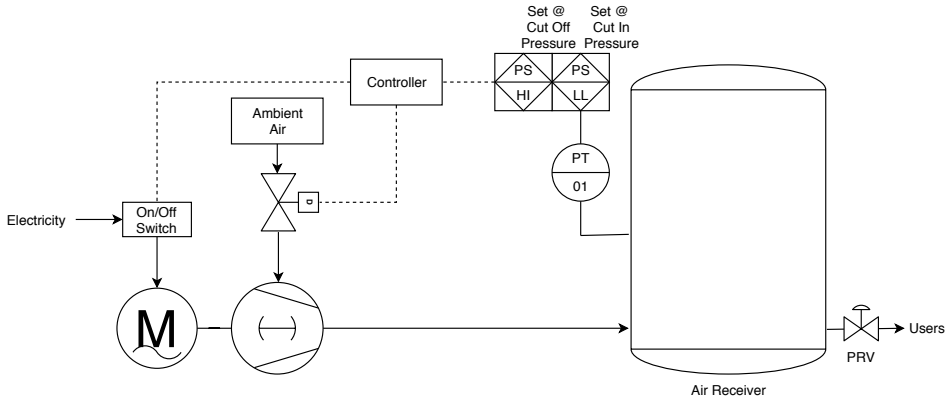

Fig. 4.5. Load/Unload control schematics with auto shutoff.

As mentioned earlier, the drawback of this method is that there is a high possibility of turning the system back on after a minute for a small load and again run the system

for a while unloaded till the next shutdown which can result in high energy usage for a small load.

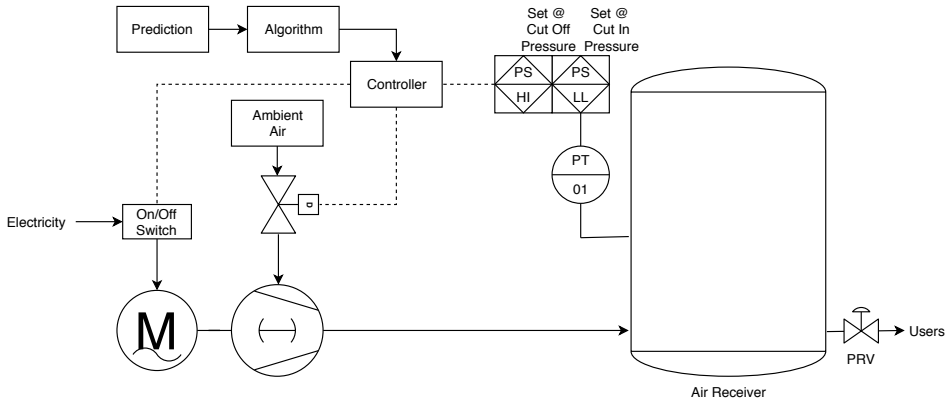

Fig. 4.6. Proposed Load/Unload control schematics with auto shutoff.

Figure 4.6 displays the novel proposed control method schematics in order to maximize the efficiency and prevent the system from running unloaded. This method will use the prediction data in order to control the system by using an algorithm. As presented earlier the prediction can come from a predictive model as developed in chapter 2 or a perfect user side model which can predict the future required air or power for an automated line. An algorithm is required in order to process this data and manage the controller. In order to prevent the system from running for a small load, more air needs to be stored to the air receiver tank, meaning higher cut-off pressure. The system cannot increase the cut-off pressure for the entire operation since it will result in a higher energy usage considering compressors requires more power to reach higher pressures. Therefore, an algorithm needs to decide when this pressure increase will result in more energy efficiency. The following section will define a perfect operation scenario and proposes an optimized algorithm in order to implement.

4.5 Proposed Solution

4.5.1 With Prediction

As shown in figure 4.6 the input for this algorithm is the prediction. The prediction data should be the required compressed air flow rate by the users to operate. The flow rate and the power consumption are related to each other at a constant operating pressure [85]. For load/unload controlled air compressor the power consumption can be calculated as below.

$$Power(kW) = \begin{cases} Loaded - Power, & Q > 0 \\ Unloaded - Power, & Q = 0 \end{cases} \tag{4.1}$$

Where Q is the required compressed air flow rate by the users with the unit of cfm or m^3/hr. For load/unload with auto shutoff controlled air compressor the power consumption can be calculated as below.

$$Power(kW) = \begin{cases} Loaded - Power, & Q > 0 \\ Unloaded - Power, & Q = 0 \quad and \quad t < T \\ 0, & Q = 0 \quad and \quad t \geq T \end{cases} \tag{4.2}$$

Where t is the time counted since unloaded, and T is the time which is set to turn off the system after running unload for more than T. By using Equation 4.1 and 4.2, the power consumption curve can be calculated from the required compressed air flow rate prediction. This power curve needs to be modified and be used to control the system. It is crystal clear that increasing the off period and minimizing the running for small loads can result into the maximum efficiency from an operation standpoint. Utilizing the prediction methods as presented in chapter 2 or modeling the system will allow us to do so. Air receiver size, maximum air compressor operating pressure, the maximum number of time a motor can be turned off during a specific time period and the recommended time between on and off are the criteria that need to be considered for this operation method. Storage size is the only parameter which

needs to be calculated, and the rest is from the specification sheets from the electric motor manufacturer. We define the storage size parameter as the loaded operating time which can be saved in the air receiver tank by reaching the highest air compressor operating pressure. Equation 3.11 can be utilized to calculate the V_{max} and storage size can be calculated as below.

$$\text{Storage size} = S = \frac{V_{max}}{Q} \tag{4.3}$$

Where V_{max} as defined in chapter 3, is the volumetric amount of stored mass at the line pressure which can be used for the user side with the unit of ft^3 or m^3. Q is the air compressor volumetric capacity running at full load at the line pressure with the unit of cfm or m^3/hr. Therefore the storage size unit is time meaning that how much time of running loaded can be saved in the air receiver tank by increasing the air receiver tank pressure or cut-off pressure.

The following criteria needs be satisfied in order to use this algorithm. The power consumption of the air compressor will increase by increasing the set pressure. The following equation can quantify the fractional power consumption increase [97].

$$FI = \frac{(\frac{P_{max}}{P_{atm}})^{0.286} - (\frac{P_{line}}{P_{atm}})^{0.286}}{(\frac{P_{max}}{P_{atm}})^{0.286} - 1} \tag{4.4}$$

Where P_{max} is the maximum operating pressure, P_{line} is the required line pressure and P_{atm} is the atmospheric pressure. The amount of the energy used by increasing the set pressure should be smaller than the energy used for the small loads in order to this method to be more energy efficient. This can be formulated as below.

$$Power_{loaded} \times S \times (1 + FI) < Power_{loaded} \times S + Power_{unloaded} \times T \tag{4.5}$$

$$Power_{loaded} \times S \times FI < Power_{unloaded} \times T \tag{4.6}$$

According to Figure 4.2 unloaded power is 50% of the loaded power and S is always less than T since it is a small load. FI is a number between 0 and 1. Therefore

Equation 4.6 is always satisfied, and the proposed method is more energy efficient than load/unload with auto shutoff method.

Identifying the points that the compressor setpoint needs to be increased in order to prevent the system from running due to small loads is the key point in this operation. A generic algorithm is developed in Python which can be used to produce the desired load profile as well as controlling the system. Figure 4.7 shows the algorithm's flowchart. Figure 4.8 and 4.9 shows the details of how the algorithm is executed by showing the details of the programming. One can produce the same output with different programming methods. As it is shown in Figure 4.7 the algorithm starts by defining the input and output as arrays. Z is set to zero and used as a counter. Max_last and zero_last is based on the last data point of the previous array. Initially, it is assumed that the system will start as loaded. Therefore the max_last is set to true and zero_last is set to false. The user needs to provide the following inputs.

- frame_size: Prediction time frame. We chose 15 due to the 15 minute ahead prediction. The user have the option to change the number.
- input_data: Input data which is the load profile.
- max_lvl: Air compressor loaded power $\times(1 + FI)$.
- avg_lvl: Average of the loaded and unloaded power.
- min_lvl: Air compressor unloaded power.
- add_lvl: Adding the number to the max_lvl to show the higher power consumption due to the set point increase or any reason that may cause energy usage increase. This option can be turned off by setting the value to zero.
- max_high_lvl: Applying restrictions to the number of times that air compressor can be set to maximum output pressure during the time frame.
- storage size: Calculated storage size by Equation 4.3.

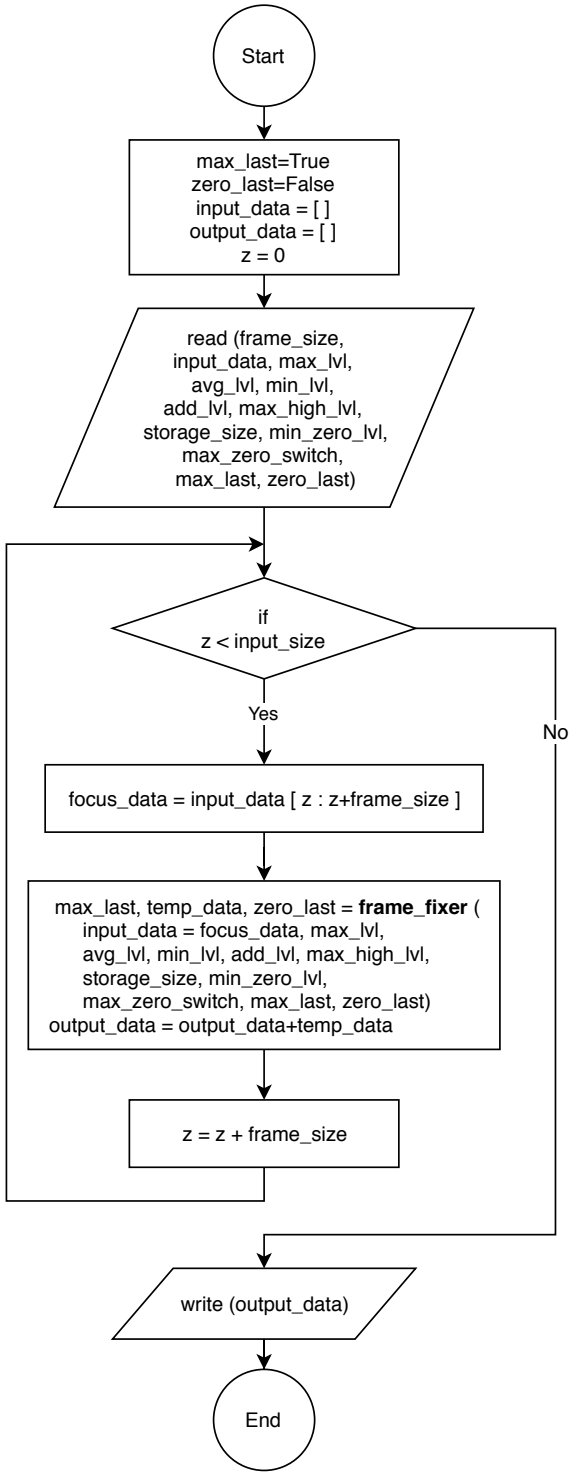

Fig. 4.7. Algorithm flowchart.

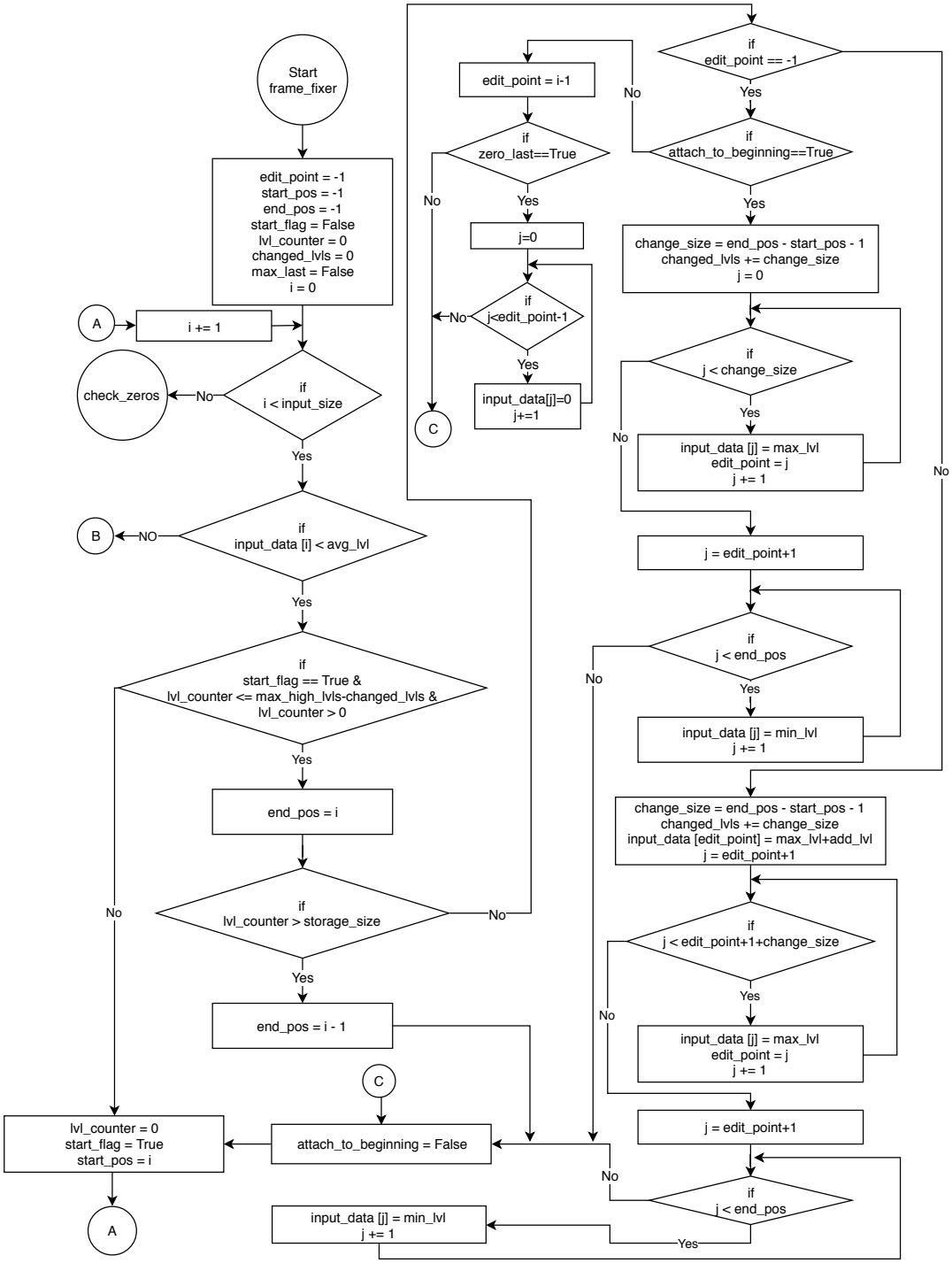

Fig. 4.8. Algorithm detailed programming flowchart 1.

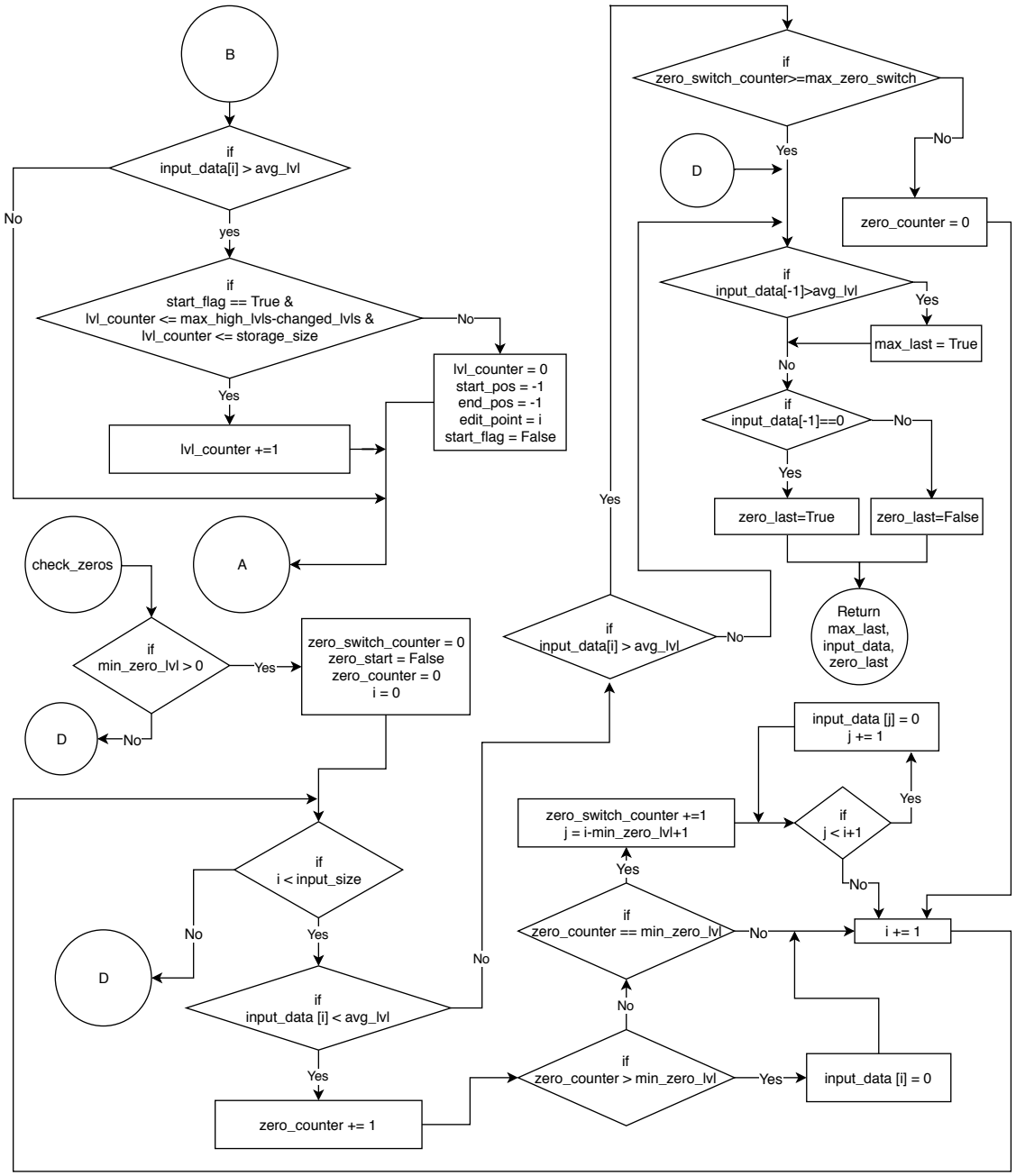

Fig. 4.9. Algorithm detailed programming flowchart 2.

- min_zero_lvl: Recommended time between on and off.
- max_zero_switch: Maximum number of time a motor can be turned off during the time frame.

Then the algorithm will utilize this information to process the data. The code will check all the criteria at each point in the time frame and modify the points with respect to the criteria. The goal is to increase the off period as much as possible by moving the small loads. In order to demonstrate the code and explain the proposed operation a set of data as shown in Figure 4.10 is used. The output can be seen in Figure 4.11. Input data is set as follow.

frame_size = 15 minute, max_lvl = 420 kW, avg_lvl = 325 kW, min_lvl = 250 kW, add_lvl = 50 kW, max_high_lvl = 15 (meaning no restriction), min_zero_lvl = 3 minute, max_zero_switch = 3

We assume there is no air stored in the air receiver tank. Consequently, the air compressor should be at the loaded mode at the first minute. Therefore the first 3 data point is moved to the beginning. This feature can be turned off by the user by changing the max_last to False. As mentioned earlier, this code can be used to control the system as well as demonstrating the proposed load profile. Therefore, we defined the add_lvl to increase the point before moved point to show the increased consumption due to the compressor setpoint increase as well as showing the point which setpoint needs to be increased to maximum. Figure 4.10 and 4.11 show point 6 and 7 are moved to point 4 and 5 and caused point 3 to be raised to 470 in order to show the more energy usage due to the set point increase. Same has happened to point 35,52 and 100. Point 60 hasn't changed since it is the last data point of the 4th time frame (45 to 60). At the 45th point, the algorithm does not know what will happen at point 61st. Whenever the system has been unloaded for more than 3 minutes the value is turned into zero meaning the motor is turned off with making sure that there is no switching to off more than 3 times. As a matter of fact, by increasing

the unloaded time periods and being able to turn the system off during these periods, energy will be consumed less, and the system will operate more efficiently.

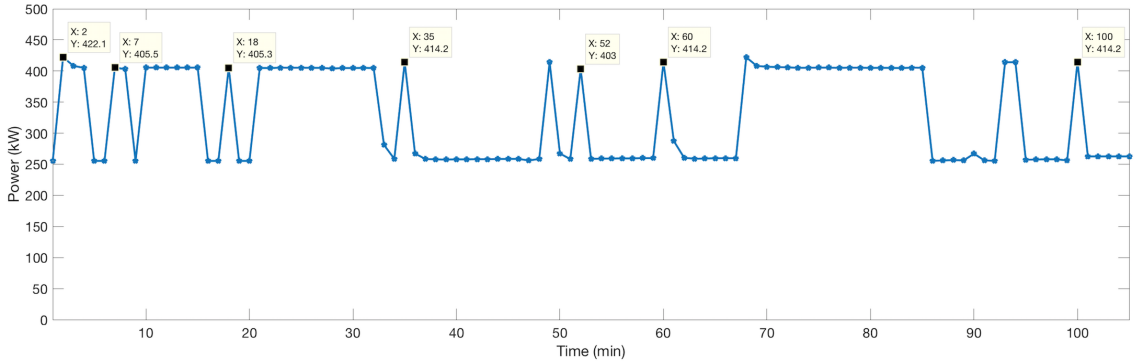

Fig. 4.10. Load/Unload control load curve.

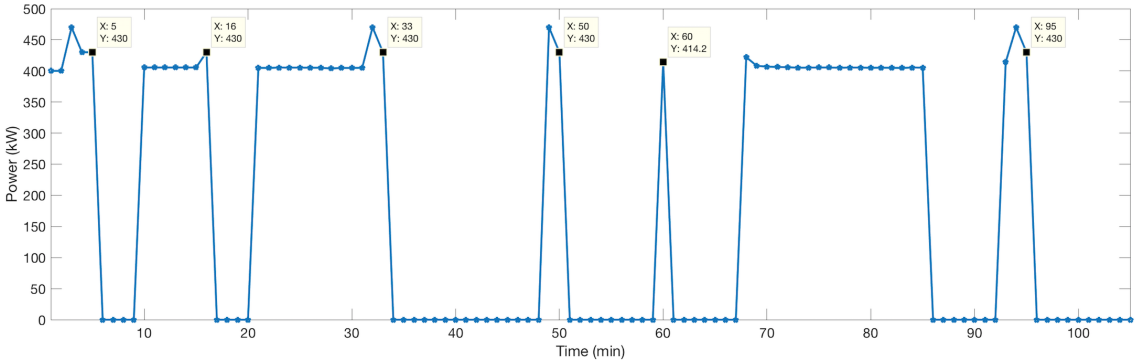

Fig. 4.11. Proposed Load/Unload control with auto shutoff load curve.

Figure 4.12 shows the load profile with only auto shutoff feature. This will shut down the compressor after running unload for 3 minutes. The area under the curve is the lowest in Figure 4.11 proving that it is the most efficient operation method. The proposed load profile can also be used to control the system by simply modifying the set pressure using the equation below.

$$\text{Set point} = \begin{cases} \text{Required Line Pressure}, & Power \leq Loaded_{Power} \\ \text{Maximum Operatable Pressure}, & Power > Loaded_{Power} \end{cases} \tag{4.7}$$

The following section will present another method without prediction.

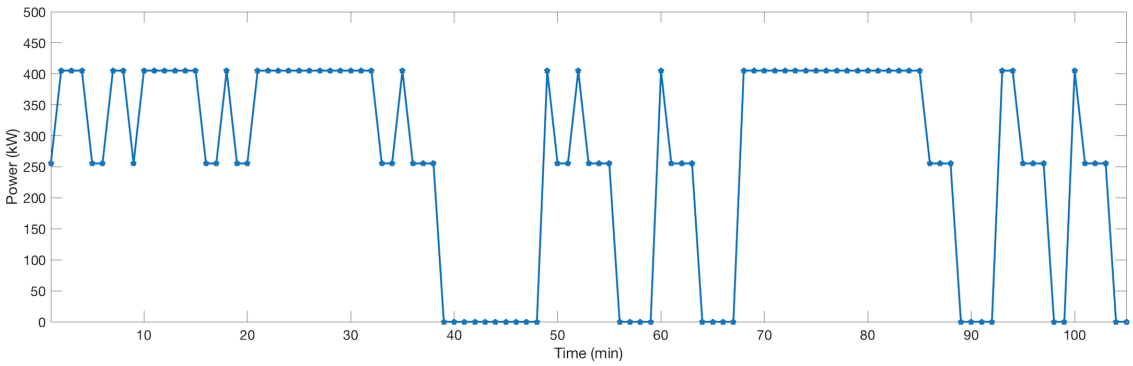

Fig. 4.12. Load/Unload control with auto shutoff load curve.

4.5.2 Without Prediction

Similar logic to the auto shutoff method can be developed in order to utilize this method without using prediction. The logic is formulated as bellow.

$$\text{Set point} = \begin{cases} \text{Required Line Pressure}, & T' > T_{loaded} \\ \text{Maximum Operatable Pressure}, & T' \leq T_{loaded} \end{cases} \tag{4.8}$$

T' is the time that if the compressor is loaded. For more than that the set point should be changed to the maximum before turning the system off. A comprehensive compressor load profile study must be conducted in order to calculate T' by using trial and error to make sure that by doing so the system will become more efficient by increasing the off period. Generally load profiles similar to the Figure 4.13 can be benefited from this method. The following section will show the results of these methods on a real case study.

4.6 Case Study

The air compressor for our case study is located in a waste water treatment plant. Compressed air in this facility is mainly used for driving pneumatic actuators and pneumatic solenoid valves as well as aeration processes. Overall, the system is com-

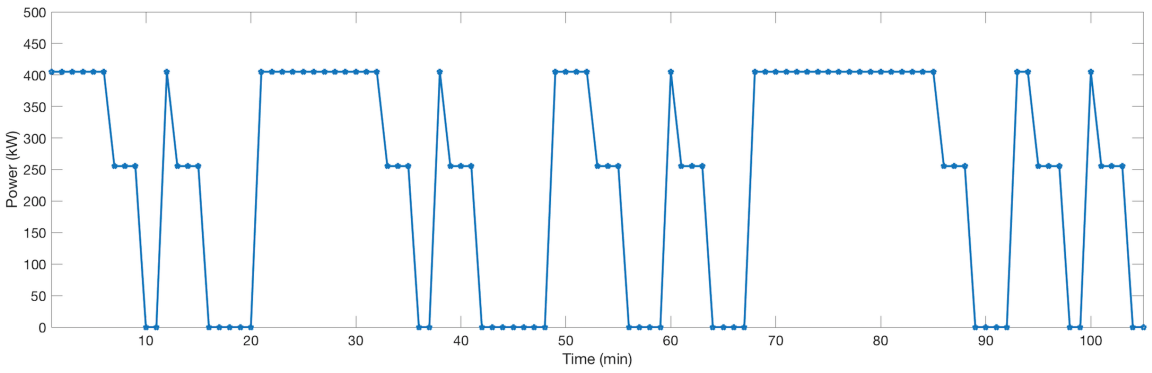

Fig. 4.13. Load/Unload control with auto shutoff load curve.

posed of: a 100 HP rotary screw compressor, a filter, an air dryer, 800 gallon (3 m^3) air receiver and an air receiver. The control logic is to maintain the line pressure by loading and unloading the compressor between 8.27 bar(g) (120 psig) and 6.89 bar(g) (100 psig). The required line pressure is 6.89 bar(g) (100 psig). An Auto/Dual control is utilized to implement this logic. The Compressor unloads the air compressor via inlet modulation valve. The maximum operating pressure is 13 bar(g) (190 psig) for this system. 43,384 minutes (30 days) of data has been logged. Figure 4.14 displays the sample power logged from this system. The system will consume around 38 kW

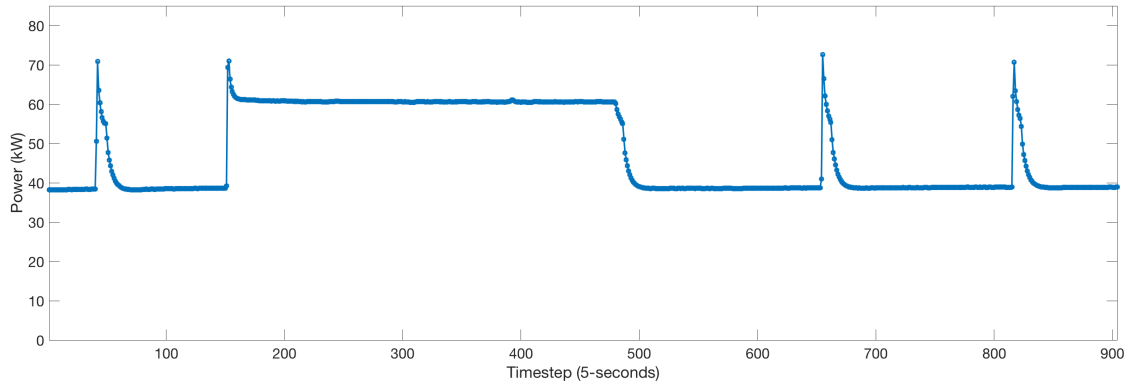

Fig. 4.14. Sample logged power from the air compressor.

for the unloaded mode and 63 kW for the loaded mode. When the system switches from unloaded to the loaded mode the power consumption goes as high as 70 kW for a few seconds due to the inrush current. By using the Equation 3.11, V_{max} is calculated as 1.84 m^3 of air at the line pressure (6.89 bar(g) (100 psig)) considering m_{max} is calculated at 13 bar(g) (190 psig) and m_{min} is calculated at cut-off pressure 8.27 bar(g) (120 psig). According to Figure 4.14 for the small loads, the loaded time is 10 seconds. Provided data sheets by the manufacturer indicate that the air compressor production capacity is 595.8 m^3/hr (350 $acfm$). Consequently by using Equation 4.3 the storage size is 11.1 seconds which is slightly higher than 10 seconds. Fractional increase (FI) due to the air receiver tank pressure increase to 13 bar(g) (190 psig) can be calculated as 0.213. By using 3 minutes unloaded time with 3 allowable shut down over 15 minutes period, the following results can be obtained for different control methods. Developed control algorithm and Excel software are used to demonstrate the power consumptions. Figures below show the results for 105 minutes of the logged data with cut-on and cut-off pressures during the operation. The following section will discuss the results.

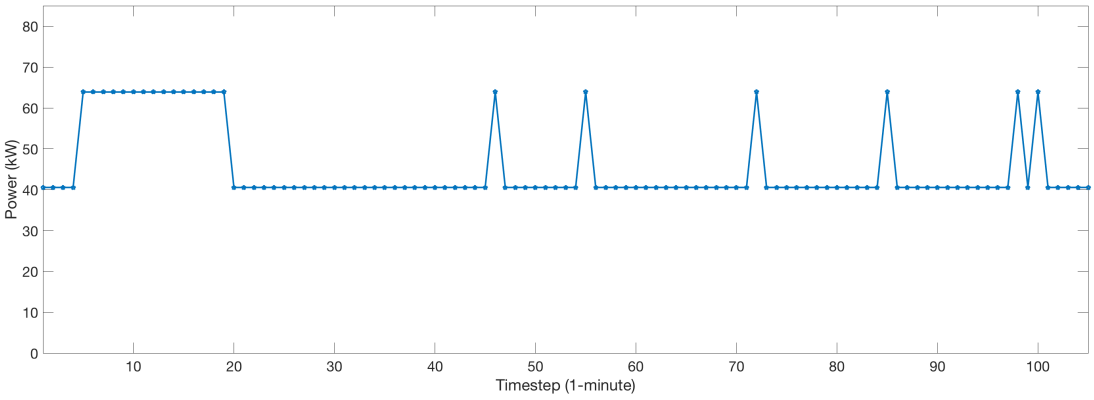

Fig. 4.15. Sample power consumption with load/unload control.

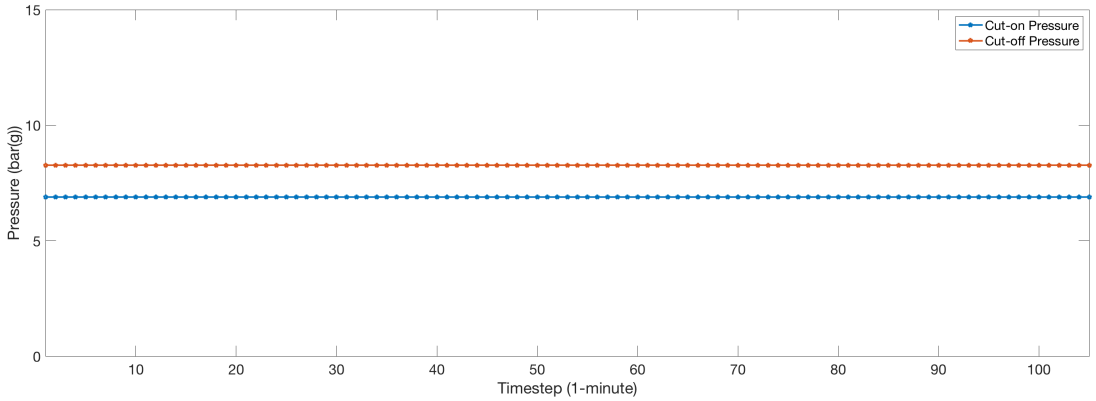

Fig. 4.16. Pressure setpoints for load/unload control without auto shutoff.

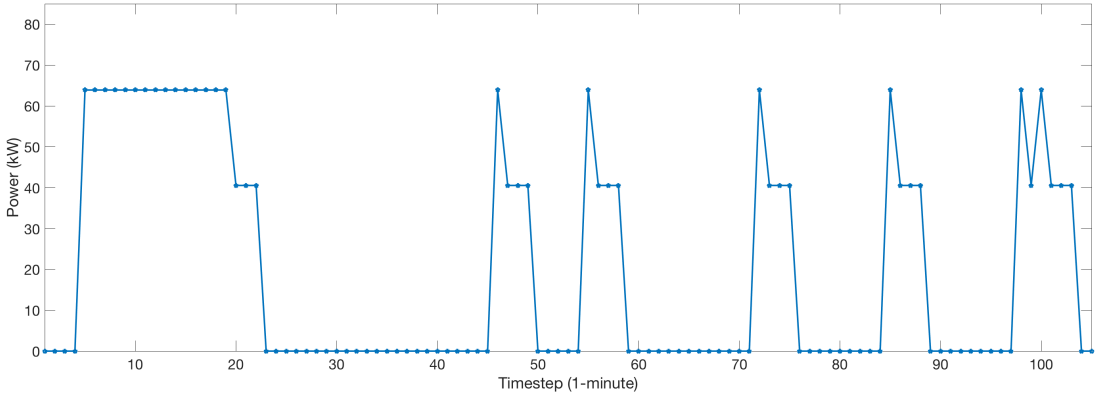

Fig. 4.17. Sample power consumption with load/unload with auto shutoff control.

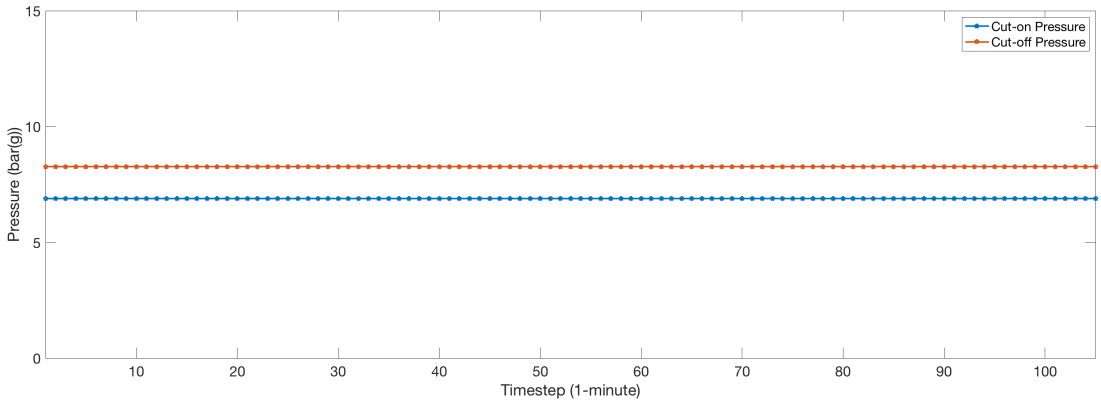

Fig. 4.18. Pressure setpoints for load/unload control with auto shutoff.

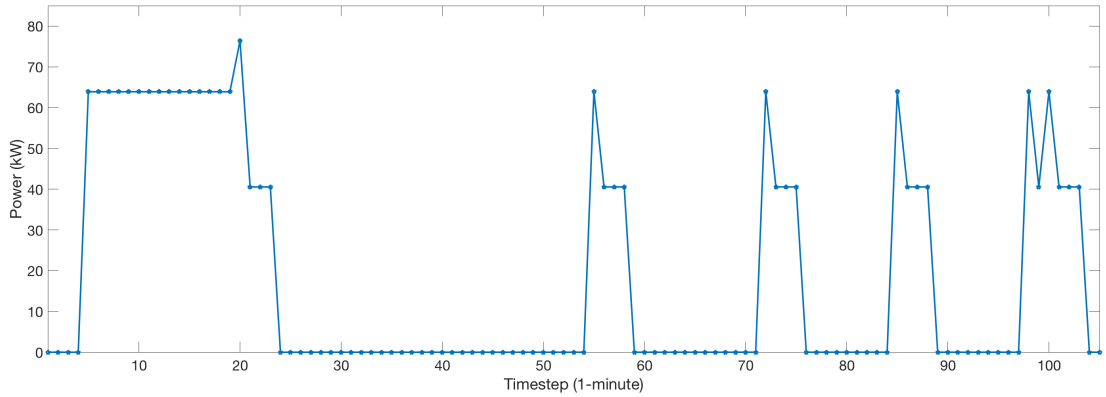

Fig. 4.19. Sample power consumption with proposed load/unload control without prediction.

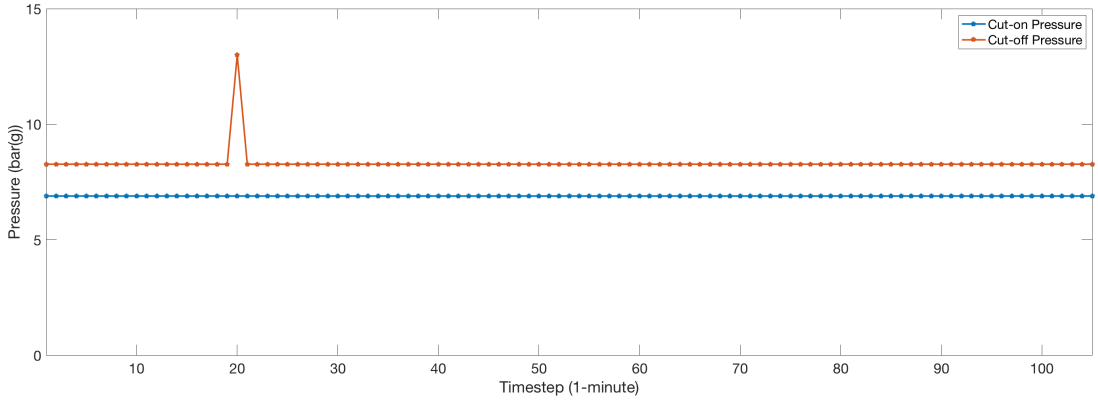

Fig. 4.20. Pressure setpoints for proposed load/unload control without prediction.

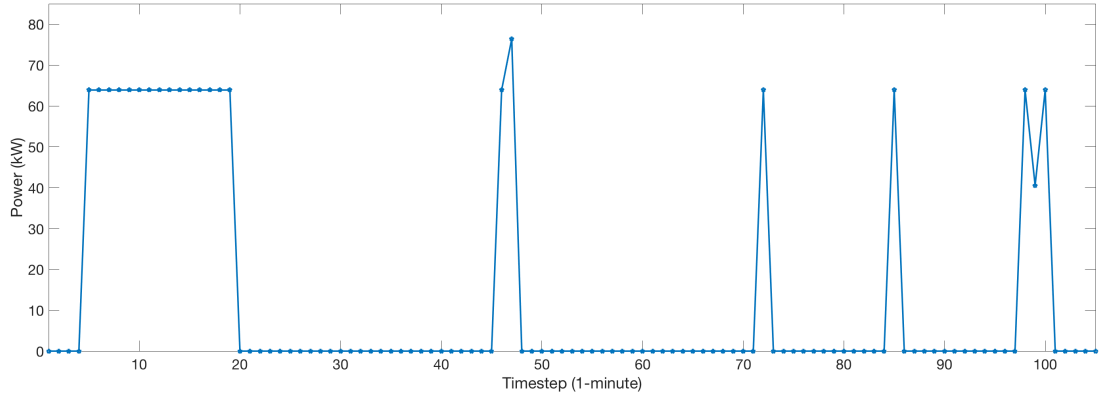

Fig. 4.21. Sample power consumption with proposed load/unload control with 15 minutes ahead prediction.

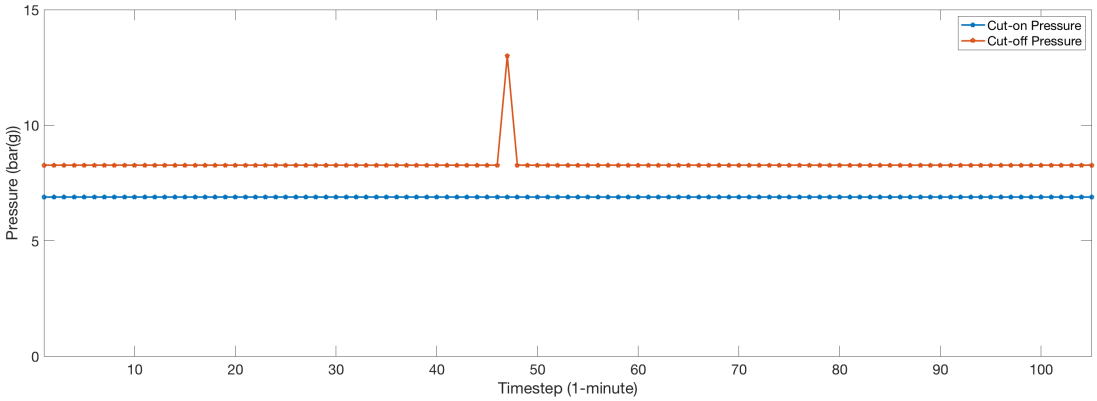

Fig. 4.22. Pressure setpoints for proposed load/unload control with prediction.

4.7 Results and Discussion

Four different control methods have been studied. Table 4.1 displays the energy consumption during a month for each method. As it can be seen from the results the auto shutoff can result in a significant energy saving by reducing 78.6% of load/unload control method. Proposed algorithm without prediction can reduce 2.5% of the energy consumed by load/unload with auto shutoff. Proposed algorithm with prediction can reduce 48.2% of the energy consumed by load/unload with auto shutoff.

Table 4.1.
100 HP air compressor system energy consumption for a month with different control methods.

Control Method	**Energy Consumption**
Load/Unload	18359 kWh
Load/Unload with Auto Shutoff	3934 kWh
Proposed Algorithm without Prediction	3836 kWh
Proposed Algorithm with Prediction	2039 kWh

The results of this section prove than compressed air storage can serve to improve system performance and efficiency by introducing novel load/unload control methods. It also proves the fact that having a perfect prediction of the system behavior can result in more energy efficient air compressor systems. Therefore, developing time series prediction tools and real-time modeling of the compressed air usage can make these systems more energy efficient.

5. CONCLUSION

This study accomplished the goal of proposing novel control and operation methods for the next generation of air compressor systems. This study proved the predictability of the air compressors operation in real time. By the passage of time, the availability of a big data collection and data mining is increasing and moving forward the technologies are being developed to use this opportunity to operate systems more energy efficient. This can also lead to more energy efficiency in overall energy consumption in a factory level by using smart manufacturing methods. The capability of an artificial neural network has been studied to predict the power consumption of compressors with various types of control. The time of a day, the day of week, the pressure in the compressed air line, the temperature of the air intake, and historical power consumption values have been utilized to build the forecasting models. The results were shown that the FFNN model is a good technique to forecast both VFD and load/unload controlled compressors power consumption. The LSTM performs better in forecasting the power consumption of a compressor with load/unload control. Both models have the limitation to give a good prediction for peak operation. Predicting electric power consumption of an air compressor can result in developing new demand response and smart manufacturing programs. The results proved the practicality of 15 minutes ahead air compressor power consumption which directly indicates that how much air compressors are loaded or their status of operation in the future. Two novel control methods have been developed to answer the question of how this prediction can help air compressors operation in system level control. Maximum load reduction is one of design improvement goals for every system. The off-grid manufacturing factories by using renewable energy these studies become more valuable. A novel control method for VFD driven air compressor system introduced. The written algorithm verified numerically and mathematically. By applying this algorithm to the data and per-

formance measured from a real air compressor system, the maximum peak load is successfully reduced. The value of the reduction depends on the air compressor demand curve at the line pressure and air compressor specs. Despite the load reduction energy consumption increased slightly. This method guarantees that the production line will not starve during the peak compressed air demand by running the system smoothly as well as reducing the maximum electrical peak load. This method can also prevent secondary or backup air compressors from kicking in during somewhat higher loads than running air compressor's output ensuing in more maximum load reduction and energy saving.

The second method aims to decrease the energy consumed with the load/unload control method to make the operation more energy efficient. Four different control methods have been studied. Auto shutoff can result in a significant energy saving. Proposed algorithms with and without prediction can reduce the energy consumed even more. The results of these methods prove than compressed air storage can be used to improve system performance and efficiency. It also demonstrates how we can benefit from having a perfect system behavior prediction system. Based on the performed case studies the following results have been obtained.

- FFNN performs a good prediction for VFD and load/unload driven air compressors. For FFNN the R^2 value of 0.83 with $RSME$ value of 1.41 kW to 1.91 kW for VFD driven have been achieved. The R^2 value of 0.85 to 0.87 with $RSME$ value of 10.88 kW to 11.25 kW for load/unload driven case study have been achieved.

- LSTM performs better for load/unload controlled air compressors with R^2 value of 0.96 with $RSME$ value of 6.65 kW to 8.88 kW have been achieved in the studied case.

- Both FFNN and LSTM did not perform very well for on/off controlled air compressor. FFNN have achieved R^2 value of 0.27 while LSTM performed better by achieving R^2 value of 0.74.

- Maximum electrical load reduction algorithm has been developed and validated. The amount of the reduced load depends on the required compressed air load profile. Two data sets have been studied. For the first one, the maximum flow rate has been reduced by 0.88 m^3/min causing maximum electrical load reduction of 2 kW and energy usage increase of 0.93 kWh. For the second data set the maximum flow rate has been reduced by 1.63 m^3/min causing maximum electrical load reduction of 3.5 kW and energy usage increase of 0.94 kWh.

- The maximum electrical load reduction method can also result in preventing the secondary or backup air compressors from kicking in during slightly higher loads than running air compressor's output resulting in more real-time demand reduction and energy saving. In the studied case, the maximum load decreased 7.37 kW and the energy usage reduced by 0.67 kWh during the 30 $minute$ period by preventing the backup air compressor from kicking in.

- Two methods have been developed to maximize the energy efficiency for load/unload controlled air compressors. The control method has been designed, and a Python code has been written which can be used for both studying the energy saving as well as controlling the system.

- Based on the conducted case study. Auto shutoff can result in a significant energy saving by reducing 78.6% of load/unload control method. Proposed algorithm without prediction can reduce 2.5% of the energy consumed with load/unload auto shutoff. The proposed algorithm with prediction can reduce 48.2% of the energy consumed by load/unload with auto shutoff.

Future Work

The following works can be recommended to continue this research.

- Investigation on improving and developing a better peak demand forecasting methods.

- FFNN model improvement for on/off dual control compressor using different inputs, network architecture, or different processing.
- Integration of the ANN with other learning technique such as the support vector machine (SVM) to further improve the forecasting ability.
- Developing software to model air compressor users in order to predict the compressed air usage in the future. This software can use cycle time of each load, users status, sequence and load amount to predict the required compressed air in the future.
- Investigating the new control methods for a group of air compressor systems which cooperate to meet the load for large facilities by using the required load prediction to maximize the efficiency of the overall system.

REFERENCES

REFERENCES

[1] R. Boehm, J. Buerner, and J. Franke, "Smart factory meets smart grid: cyber-physical compressed air systems enable demand side management in industrial environments," vol. 805, pp. 25–31, 2015.

[2] U.S. Energy Information Administration (EIA), *U.S. Energy Information Administration (EIA) Glossary*, 2018 (accessed November 2, 2018), https://www.eia.gov/tools/glossary/index.php?id=E.

[3] A. V. Meier, *Electric power systems: a conceptual introduction*. John Wiley and Sons, 2006.

[4] T. A. Short, *Electric power distribution handbook*. CRC press, 2014.

[5] Shenzhen CLOU Electronics Co., Ltd., *What is Maximum Demand Measurement?*, 2018 (accessed November 2, 2018), http://metering.clouglobal.com/2017/08/what-is-maximum-demand/.

[6] Indianapolis Power and Light Company, *Large Commercial and Industrial Rates*, 2018 (accessed November 2, 2018), https://www.iplpower.com.

[7] F. Stern and J. Spencer, *Chapter 10: Peak Demand and Time-Differentiated Energy Savings Cross-Cutting Protocol. The Uniform Methods Project: Methods for Determining Energy-Efficiency Savings for Specific Measures*. NREL/SR-7A40-68566: Golden, CO; National Renewable Energy Laboratory, 2017.

[8] Compressed air and gas institute (CAGI), "Air compressor selection and application 1/4 through 30 hp," *Compressed air and gas institute (CAGI)*, 2016.

[9] Compressed Air Challenge, "Fundamentals of compressed air systems," *US Department of Energy*, 2002.

[10] F. D. Cunha Ivor, "Compressed air energy efficiency reference guide (ceati)," *Customer energy solutions interest group (CESIG)*, 2007.

[11] C. Beals, J. Ghislain, H. Kemp *et al.*, "Improving compressed air system performance," *US Department of Energy*, 2003.

[12] Atlas Copco, *Atlas Copco Compressed air manual*. 8th edition: Atlas Copco Airpower NV, 2015.

[13] D. Wright, "Air filtration and efficiency: Cutting the cost of compressed air," *Filtration & Separation*, vol. 45, no. 9, pp. 32–34, 2008.

[14] Ingersoll-Rand Company and A. Loomis, *Compressed air and gas data*. The Company, 1980.

[15] M. Schulze, H. Nehler, M. Ottosson, and P. Thollander, "Energy management in industry–a systematic review of previous findings and an integrative conceptual framework," *Journal of Cleaner Production*, vol. 112, pp. 3692–3708, 2016.

[16] US Department of Energy, *Green Button-Open Energy Data*, (accessed September 4, 2018). [Online]. Available: https://www.energy.gov/data/green-button

[17] Q. Zhang and I. E. Grossmann, "Planning and scheduling for industrial demand side management: advances and challenges," in *Alternative Energy Sources and Technologies*. Springer, 2016, pp. 383–414.

[18] N. Kamel and Z. Baharudin, "Short term load forecast using burg autoregressive technique," in *Intelligent and Advanced Systems, 2007. ICIAS 2007. International Conference on*. IEEE, 2007, pp. 912–916.

[19] E. Gonzalez-Romera, M. A. Jaramillo-Moran, and D. Carmona-Fernandez, "Monthly electric energy demand forecasting based on trend extraction," *IEEE Transactions on power systems*, vol. 21, no. 4, pp. 1946–1953, 2006.

[20] R. Platon, V. R. Dehkordi, and J. Martel, "Hourly prediction of a building's electricity consumption using case-based reasoning, artificial neural networks and principal component analysis," *Energy and Buildings*, vol. 92, pp. 10–18, 2015.

[21] K. Methaprayoon, W. Lee, P. Didsayabutra, J. Liao, and R. Ross, "Neural network-based short term load forecasting for unit commitment scheduling," in *Industrial and Commercial Power Systems, 2003. 2003 IEEE Technical Conference*. IEEE, 2003, pp. 138–143.

[22] M. De Felice, A. Alessandri, and F. Catalano, "Seasonal climate forecasts for medium-term electricity demand forecasting," *Applied Energy*, vol. 137, pp. 435–444, 2015.

[23] M. Kandil, S. M. El-Debeiky, and N. Hasanien, "Long-term load forecasting for fast developing utility using a knowledge-based expert system," *IEEE transactions on Power Systems*, vol. 17, no. 2, pp. 491–496, 2002.

[24] D. H. Vu, K. M. Muttaqi, and A. Agalgaonkar, "A variance inflation factor and backward elimination based robust regression model for forecasting monthly electricity demand using climatic variables," *Applied Energy*, vol. 140, pp. 385–394, 2015.

[25] C. Fan, F. Xiao, and S. Wang, "Development of prediction models for next-day building energy consumption and peak power demand using data mining techniques," *Applied Energy*, vol. 127, pp. 1–10, 2014.

[26] S. Saab, E. Badr, and G. Nasr, "Univariate modeling and forecasting of energy consumption: the case of electricity in lebanon," *Energy*, vol. 26, no. 1, pp. 1–14, 2001.

[27] L. Yuancheng, F. Tingjian, and Y. Erkeng, "Short-term electrical load forecasting using least squares support vector machines," in *Power System Technology, 2002. Proceedings. PowerCon 2002. International Conference on*, vol. 1. IEEE, 2002, pp. 230–233.

[28] K. Yang and L. Zhao, "Application of mamdani fuzzy system amendment on load forecasting model," in *Photonics and Optoelectronics, 2009. SOPO 2009. Symposium on*. IEEE, 2009, pp. 1–4.

[29] S. Tzafestas and E. Tzafestas, "Computational intelligence techniques for short-term electric load forecasting," *Journal of Intelligent and Robotic Systems*, vol. 31, no. 1-3, pp. 7–68, 2001.

[30] S. Ling, F. H. Leung, H. Lam, and P. K. Tam, "Short-term daily load forecasting in an intelligent home with ga-based neural network," in *Neural Networks, 2002. IJCNN'02. Proceedings of the 2002 International Joint Conference on*, vol. 1. IEEE, 2002, pp. 997–1001.

[31] M. Q. Raza and A. Khosravi, "A review on artificial intelligence based load demand forecasting techniques for smart grid and buildings," *Renewable and Sustainable Energy Reviews*, vol. 50, pp. 1352–1372, 2015.

[32] R. K. Jain, K. M. Smith, P. J. Culligan, and J. E. Taylor, "Forecasting energy consumption of multi-family residential buildings using support vector regression: Investigating the impact of temporal and spatial monitoring granularity on performance accuracy," *Applied Energy*, vol. 123, pp. 168–178, 2014.

[33] H. Masuda and D. E. Claridge, "Statistical modeling of the building energy balance variable for screening of metered energy use in large commercial buildings," *Energy and Buildings*, vol. 77, pp. 292–303, 2014.

[34] K. Kavaklioglu, "Modeling and prediction of turkeys electricity consumption using support vector regression," *Applied Energy*, vol. 88, no. 1, pp. 368–375, 2011.

[35] A. Aranda, G. Ferreira, M. Mainar-Toledo, S. Scarpellini, and E. L. Sastresa, "Multiple regression models to predict the annual energy consumption in the spanish banking sector," *Energy and Buildings*, vol. 49, pp. 380–387, 2012.

[36] A. Kialashaki and J. R. Reisel, "Modeling of the energy demand of the residential sector in the united states using regression models and artificial neural networks," *Applied Energy*, vol. 108, pp. 271–280, 2013.

[37] L. V. Fausett *et al.*, *Fundamentals of neural networks: architectures, algorithms, and applications*. Prentice-Hall Englewood Cliffs, 1994, vol. 3.

[38] M. Amin and S. Shekhar, "Generalization by neural networks," in *Proc. of the 8th Intl Conf. on Data Eng*, 1992.

[39] J. Fei, N. Zhao, Y. Shi, Y. Feng, and Z. Wang, "Compressor performance prediction using a novel feed-forward neural network based on gaussian kernel function," *Advances in Mechanical Engineering*, vol. 8, no. 1, p. 1687814016628396, 2016.

[40] Y. Yu, L. Chen, F. Sun, and C. Wu, "Neural-network based analysis and prediction of a compressors characteristic performance map," *Applied energy*, vol. 84, no. 1, pp. 48–55, 2007.

[41] K. Ghorbanian and M. Gholamrezaei, "An artificial neural network approach to compressor performance prediction," *Applied Energy*, vol. 86, no. 7-8, pp. 1210–1221, 2009.

[42] Z. Tian, B. Gu, L. Yang, and Y. Lu, "Hybrid ann–pls approach to scroll compressor thermodynamic performance prediction," *Applied Thermal Engineering*, vol. 77, pp. 113–120, 2015.

[43] S. Ledesma, J. Belman-Flores, and J. Barroso-Maldonado, "Analysis and modeling of a variable speed reciprocating compressor using ann," *International Journal of Refrigeration*, vol. 59, pp. 190–197, 2015.

[44] J.-S. Jang, "Anfis: adaptive-network-based fuzzy inference system," *IEEE transactions on systems, man, and cybernetics*, vol. 23, no. 3, pp. 665–685, 1993.

[45] R. Ž. Jovanović, A. A. Sretenović, and B. D. Živković, "Ensemble of various neural networks for prediction of heating energy consumption," *Energy and Buildings*, vol. 94, pp. 189–199, 2015.

[46] H. S. Hippert, C. E. Pedreira, and R. C. Souza, "Neural networks for short-term load forecasting: A review and evaluation," *IEEE Transactions on power systems*, vol. 16, no. 1, pp. 44–55, 2001.

[47] R. Hecht-Nielsen, "Theory of the backpropagation neural network," in *Neural networks for perception*. Elsevier, 1992, pp. 65–93.

[48] K. Grolinger, A. LHeureux, M. A. Capretz, and L. Seewald, "Energy forecasting for event venues: big data and prediction accuracy," *Energy and Buildings*, vol. 112, pp. 222–233, 2016.

[49] M. Firat, M. E. Turan, and M. A. Yurdusev, "Comparative analysis of neural network techniques for predicting water consumption time series," *Journal of hydrology*, vol. 384, no. 1-2, pp. 46–51, 2010.

[50] T. Hu, K. Lam, and S. Ng, "River flow time series prediction with a range-dependent neural network," *Hydrological Sciences Journal*, vol. 46, no. 5, pp. 729–745, 2001.

[51] A. Yona, T. Senjyu, A. Y. Saber, T. Funabashi, H. Sekine, and C.-H. Kim, "Application of neural network to 24-hour-ahead generating power forecasting for pv system," in *2008 IEEE Power and Energy Society General Meeting-Conversion and Delivery of Electrical Energy in the 21st Century*. IEEE, 2008, pp. 1–6.

[52] K. Bhaskar and S. Singh, "Awnn-assisted wind power forecasting using feed-forward neural network," *IEEE transactions on sustainable energy*, vol. 3, no. 2, pp. 306–315, 2012.

[53] F. A. Gers, D. Eck, and J. Schmidhuber, "Applying lstm to time series predictable through time-window approaches," in *Neural Nets WIRN Vietri-01*. Springer, 2002, pp. 193–200.

[54] S. Xingjian, Z. Chen, H. Wang, D.-Y. Yeung, W.-K. Wong, and W.-c. Woo, "Convolutional lstm network: A machine learning approach for precipitation nowcasting," in *Advances in neural information processing systems*, 2015, pp. 802–810.

[55] A. Fawzy, H. M. Mokhtar, and O. Hegazy, "Outliers detection and classification in wireless sensor networks," *Egyptian Informatics Journal*, vol. 14, no. 2, pp. 157–164, 2013.

[56] H. Liu, S. Shah, and W. Jiang, "On-line outlier detection and data cleaning," *Computers & chemical engineering*, vol. 28, no. 9, pp. 1635–1647, 2004.

[57] R. K. Pearson, Y. Neuvo, J. Astola, and M. Gabbouj, "Generalized hampel filters," *EURASIP Journal on Advances in Signal Processing*, vol. 2016, no. 1, p. 87, 2016.

[58] R. K.Pearson, Y. Neuvo, J. Astola, and M. Gabbouj, "The class of generalized hampel filters," in *Signal Processing Conference (EUSIPCO), 2015 23rd European.* IEEE, 2015, pp. 2501–2505.

[59] N. Srivastava, G. Hinton, A. Krizhevsky, I. Sutskever, and R. Salakhutdinov, "Dropout: a simple way to prevent neural networks from overfitting," *The Journal of Machine Learning Research*, vol. 15, no. 1, pp. 1929–1958, 2014.

[60] F. Rodríguez, A. Fleetwood, A. Galarza, and L. Fontán, "Predicting solar energy generation through artificial neural networks using weather forecasts for microgrid control," *Renewable Energy*, vol. 126, pp. 855–864, 2018.

[61] G. Piñeiro, S. Perelman, J. P. Guerschman, and J. M. Paruelo, "How to evaluate models: observed vs. predicted or predicted vs. observed?" *Ecological Modelling*, vol. 216, no. 3-4, pp. 316–322, 2008.

[62] F. Weninger, H. Erdogan, S. Watanabe, E. Vincent, J. Le Roux, J. R. Hershey, and B. Schuller, "Speech enhancement with lstm recurrent neural networks and its application to noise-robust asr," in *International Conference on Latent Variable Analysis and Signal Separation.* Springer, 2015, pp. 91–99.

[63] K. Mason, J. Duggan, and E. Howley, "Forecasting energy demand, wind generation and carbon dioxide emissions in ireland using evolutionary neural networks," *Energy*, vol. 155, pp. 705–720, 2018.

[64] R. K. Brouwer, "A feed-forward network for input that is both categorical and quantitative," *Neural Networks*, vol. 15, no. 7, pp. 881–890, 2002.

[65] V. Mehta and M. Rohit, "Principles of power system: Including generation, transmission, distribution, switchgear and protection: For be/b. tech," *AMIE and Other Engineering Examinations. S. Chand*, 2005.

[66] A. Palamar, E. Pettai, and V. Beldjajev, "Control system for a diesel generator and ups based microgrid," *Scientific Journal of Riga Technical University. Power and Electrical Engineering*, vol. 26, no. 1, pp. 48–53, 2010.

[67] K. Van den Bergh and E. Delarue, "Cycling of conventional power plants: technical limits and actual costs," *Energy Conversion and Management*, vol. 97, pp. 70–77, 2015.

[68] Y. Chen, P. Xu, Y. Chu, W. Li, Y. Wu, L. Ni, Y. Bao, and K. Wang, "Short-term electrical load forecasting using the support vector regression (svr) model to calculate the demand response baseline for office buildings," *Applied Energy*, vol. 195, pp. 659–670, 2017.

[69] P. Bradley, M. Leach, and J. Torriti, "A review of the costs and benefits of demand response for electricity in the uk," *Energy Policy*, vol. 52, pp. 312–327, 2013.

[70] K. A. Joshi and N. M. Pindoriya, "Day-ahead dispatch of battery energy storage system for peak load shaving and load leveling in low voltage unbalance distribution networks," in *Power & Energy Society General Meeting, 2015 IEEE*. IEEE, 2015, pp. 1–5.

[71] E. Georges, B. Cornélusse, D. Ernst, V. Lemort, and S. Mathieu, "Residential heat pump as flexible load for direct control service with parametrized duration and rebound effect," *Applied Energy*, vol. 187, pp. 140–153, 2017.

[72] B. Zeng, G. Wu, J. Wang, J. Zhang, and M. Zeng, "Impact of behavior-driven demand response on supply adequacy in smart distribution systems," *Applied Energy*, vol. 202, pp. 125–137, 2017.

[73] N. Nezamoddini and Y. Wang, "Real-time electricity pricing for industrial customers: Survey and case studies in the united states," *Applied energy*, vol. 195, pp. 1023–1037, 2017.

[74] E. Reihani, M. Motalleb, R. Ghorbani, and L. S. Saoud, "Load peak shaving and power smoothing of a distribution grid with high renewable energy penetration," *Renewable Energy*, vol. 86, pp. 1372–1379, 2016.

[75] K. Divya and J. Østergaard, "Battery energy storage technology for power systemsan overview," *Electric Power Systems Research*, vol. 79, no. 4, pp. 511–520, 2009.

[76] C. R. Upshaw, J. D. Rhodes, and M. E. Webber, "Modeling electric load and water consumption impacts from an integrated thermal energy and rainwater storage system for residential buildings in texas," *Applied Energy*, vol. 186, pp. 492–508, 2017.

[77] S. Kucuk, F. Arslan, M. Bayrak, and G. Contreras, "Load management of industrial facilities electrical system using intelligent supervision, control and monitoring systems," in *Networks, Computers and Communications (ISNCC), 2016 International Symposium on*. IEEE, 2016, pp. 1–6.

[78] Z. J. Paracha and P. Doulai, "Load management: techniques and methods in electric power system," in *Energy Management and Power Delivery, 1998. Proceedings of EMPD'98. 1998 International Conference on*, vol. 1. IEEE, 1998, pp. 213–217.

[79] Y. M. Ding, S. H. Hong, and X. H. Li, "A demand response energy management scheme for industrial facilities in smart grid," *IEEE Transactions on Industrial Informatics*, vol. 10, no. 4, pp. 2257–2269, 2014.

[80] Y. Levron and D. Shmilovitz, "Optimal power management in fueled systems with finite storage capacity," *IEEE Transactions on Circuits and Systems I: Regular Papers*, vol. 57, no. 8, pp. 2221–2231, 2010.

[81] Y. Levron and D. shmilovitz, "Power systems optimal peak-shaving applying secondary storage," *Electric Power Systems Research*, vol. 89, pp. 80–84, 2012.

[82] B. T. Polyak, "Newtons method and its use in optimization," *European Journal of Operational Research*, vol. 181, no. 3, pp. 1086–1096, 2007.

[83] L. S. Matott, K. Leung, and J. Sim, "Application of matlab and python optimizers to two case studies involving groundwater flow and contaminant transport modeling," *Computers & Geosciences*, vol. 37, no. 11, pp. 1894–1899, 2011.

[84] T. Coleman, M. A. Branch, and A. Grace, "Optimization toolbox," *For Use with MATLAB. Users Guide for MATLAB 5, Version 2, Relaese II*, 1999.

[85] Compressed Air and Gas Institute, "Cagi rotary compressor performance verification program," *www.cagi.org/performance-verification/data-sheets.*, 2018.

[86] P. Radgen, "Efficiency through compressed air energy audits," in *Energy Audit Conference, www. audit06. fi*, 2006.

[87] A. P. Senniappan, "Baselining a compressed air system: An expert systems approach," Ph.D. dissertation, Citeseer, 2004.

[88] Y. Cengel, B. S. Prasad, R. Turner, and Y. Cerci, "Reduce compressed air costs," *Hydrocarbon Processing*, vol. 79, no. 12, pp. 57–57, 2000.

[89] E. M. Talbott, *Compressed air systems: a guidebook on energy and cost savings*. The Fairmont Press, Inc., 1993.

[90] C. Harding and D. Nutter, "Compressed air system analysis and retrofit for energy savings," 2014.

[91] A. McKane, "Improving energy efficiency of compressed air system based on system audit," 2008.

[92] R. Saidur, N. Rahim, and M. Hasanuzzaman, "A review on compressed-air energy use and energy savings," *Renewable and Sustainable Energy Reviews*, vol. 14, no. 4, pp. 1135–1153, 2010.

[93] C. Schmidt and J. K. Kissock, "Estimating energy savings in compressed air systems," 2004.

[94] S. Mousavi, S. Kara, and B. Kornfeld, "Energy efficiency of compressed air systems," *Procedia Cirp*, vol. 15, pp. 313–318, 2014.

[95] C. Schmidt and J. K. Kissock, "Power characteristics of industrial air compressors," 2003.

[96] S. Murphy and J. K. Kissock, "Simulating energy efficient control of multiple-compressor compressed air systems," 2015.

[97] K. Kissock, "Modeling and simulation of air compressor energy use," in *ACEEE Summer Study on Energy Efficiency in Industry*, vol. 1, no. 13, 2005, pp. 131–142.